Pacemaking in Mouse Locus Coeruleus Neurons: Electrophysiological Properties, Role of Mitochondria and Development

Ramatis Birnfeld de Oliveira

BSc in Pharmacy and Master in Biochemistry

Thesis submitted in fulfilment of the requirements
for obtain the degree of Doctor of Philosophy in
Human Physiology

School of Biomedical Sciences and Pharmacy

University of Newcastle

September 2010

Statement of originality

This thesis contains no material which has been accepted for the award of any other degree or diploma in any university or tertiary institution and, to the best of my knowledge and belief, contains no material previously published or written by another person, except where due reference has been made in the text. I give consent to this copy of my thesis, when deposited in the University Library, being made available for loan and photocopying subject to the provisions of the Copyright Act 1968.

_____

Ramatis Birnfeld de Oliveira

Acknowledgement of Authorship

I hereby certify that the work embodied in this thesis contains a published paper/s/scholarly work of which I am a joint author. I have included as part of my thesis a written statement, endorsed by my supervisor, attesting to my contribution to the joint publications.

_____

Ramatis Birnfeld de Oliveira

Paper	Contribution	Signature
de Oliveira, R. B.; Graham, Brett; Howlett, Marcus C.H.; Gravina, Fernanda S.; Oliveira, Max W.S.; Imtiaz, Mohammad S.; Callister, Robert J.; Lim, Rebecca; Brichta, Alan M.; van Helden, Dirk F.. Ketamine anesthesia helps preserve neuronal viability. Journal of Neuroscience Methods, v. 189, p. 230-232, 2010. DOI: 10.1016/j.jneumeth.2010.03.029	80% of the total	Dirk F. van Helden
de Oliveira, Ramatis B.; Howlett, Marcus C.H.; Gravina, Fernanda S.; Imtiaz, Mohammad S.; Callister, Robert J.; Brichta, Alan M.; van Helden, Dirk F.. Pacemaker currents in mouse Locus Coeruleus neurons. Neuroscience, 2010. DOI: 10.1016/j.neuroscience.2010.06.028	80% of the total	Dirk F. van Helden
de Oliveira, Ramatis B.; Gravina, Fernanda S.; Brichta, Alan M.; Callister, Robert J.; van Helden, Dirk F.. Effects of mitochondrial disruption on ionic currents and pacemaking in neurons of the locus coeruleus. *Manuscript under review in "Journal of Physiology".*	90% of the total	Dirk F. van Helden

Acknowledgments

I first would like to thank the “invisible mystery” that is out there somehow guiding us to amazing opportunities every day. One of these opportunities crossed my way and here I am after 4 years in the other side of the world finalizing my PhD thesis.

My beloved wife Fernanda is the first living one that I would like to thank, not only for her endeavours together with me in this journey but also for everything that she represents to me. Infinite love and affection are just words that cannot describe my feelings for this “little person”.

I also would like to thank my supervisor Dirk for having accepted us into his lab and supported us during all this time. More than a supervisor I have a good friend.

Marcus Howlett also deserves a big thank you for all the support that he gave me and for all his patience and comprehension with my “recently learned” English. Bob Callister also deserves a big thank for his help in reviewing the manuscripts.

Someone that also needs to be thanked is my good friend and past supervisor Jose Claudio, if was not for his outstanding comprehension and wisdom, I would never have been able to get here in Australia in time. In the same way I would like to thank a guy that is more than a friend, Daniel Gelain, for introducing us to Dirk and for all these years of friendship.

I also would like to thank my family (old and new members) for all their support and unconditional love. I guess if was not for the love, education and moral values received from them I would not be as happy as I am and for sure would not love so much to live.

I think they taught me the most important value in life that is that life never ends and every minute is important to do something in retribution to the things that we receive.

A big thanks also goes to my good friend Peter Dosen for all his technical support and friendship during all these 4 years.

Everybody that somehow helped me to carry on during this PhD period please also feel thanked.

Table of Contents

List of Abbreviations

ACSF - artificial cerebrospinal fluid

AHP – after hyperpolarization

AP - Action potential

CCCP - carbonyl cyanide m-chlorophenylhydrazone

CICR - Ca^{2+}-induced Ca^{2+} release

ChTx – Charybdotoxin

CNS – Central nervous system

DDT - Dichlorodiphenyltrichloroethane

DMSO - Dimethyl sulfoxide

EGTA - Ethylene glycol tetra acetic acid

FCCP - p-trifluoromethoxyphenylhydrazone

I_A - fast transient K^+ current (I_A)

I_{Cl} – chloride current

I_H - hyperpolarization-activated current

$I_{K\text{-}Ca}$ - Ca^{2+}-activated K^+ current

K_{Ca} - Ca^{2+}-activated K^+ channel

K_{IR} - K^+ inward rectifier current

LC – Locus coeruleus

MC – Membrane capacitance

MTC – Motor cortex

MMP – Mitochondrial membrane potential

NMDG - N-methyl-D-glucamine chloride

MNCE - Mitochondrial Na^+/Ca^{2+} exchanger

PBS - Physiological buffer solution

PD – Parkinson's diseases

R_{IN} – input resistance

SN – Substantia nigra

TEA – Tetraethylammonium chloride

TH – Tyrosine hydroxylase

TTX – Tetrodotoxin

Vm – membrane potential

4-AP - 4-Aminopyridine

$[Ca^{2+}]_c$ - cytosolic Ca^{2+} concentration

Ψm - Mitochondrial membrane potent

Abstract

This thesis presents studies on the electrophysiological properties of Locus coeruleus (LC), a group of noradrenergic neurons present in the brain stem pons. The specific interest in this neuronal population came from the fact that this neuronal population accounts for the largest noradrenergic nucleus present in the brain, providing noradrenaline input to virtually all cerebral regions and involved in controlling or modulating many types of behaviours. Another important feature is the recent "rediscovery" that LC neurons are involved in Parkinson's disease (PD), where loss of activity and/or decrease in the neuronal population are thought to be a fundamental step to the progression and maintenance of this pathology.

LC neurons release many different types of neurotransmitters, noradrenaline, however, being the most studied. Regardless, of the neurotransmitter involved, release is controlled by intrinsic spontaneous firing activity, which is the result of a combination of pacemaker currents in balance with each other. These currents determine membrane depolarization and action potential initiation, and are responsible for adjusting the neuronal firing rate according to system needs. Even though the electrophysiological properties of LC neurons have been studied for decades, the mechanisms controlling and generating the pacemaker process need further investigation. As this process is a key feature underlying the influence exerted by LC neurons, a better understanding of this process is fundamental to determining how the brain functions and how impairment of LC activity may lead to neurological disorders. For example, it has been demonstrated in PD that along with the massive loss of Substantia Nigra (SN) neurons, the noradrenergic signalling provided by LC neurons to

the SN also suffers a massive impairment. Recently, it was suggested that noradrenaline exerts a neuronal protective effect against oxidative stress and inflammation. This is of great significance, as oxidative stress and inflammation are thought to be significantly involved in the development and maintenance of PD. These finding led to the proposal that impairment in the noradrenergic signalling provided by LC neurons to the SN could be a trigger in the generation and progression of PD.

All these facts inspired me to undertake detailed investigations into LC neuronal function. My aim was to first establish a solid understanding of the pacemaker process and then integrate this knowledge into a broader context. By choosing the mouse model this would allow future detailed studies using targeted mutants. I began by investigating the cellular basis of spontaneous firing of LC neurons with special emphasis on understanding the underlying pacemaker mechanisms, particularly those involved in action potential generation. In addition, I studied the effect of age and the possible involvement of mitochondria as a regulator of this process.

The first research chapter (see chapter 3) presents a methodological approach that was found to significantly improve the viability of LC neurons. This facilitated our electrophysiological studies and should be of general use for all those investigating brain neurons *in vitro*. LC neurons are medium-sized cells with large dendritic arbours. As a result, achieving proper voltage control in voltage clamp experiments in slice preparations is a challenge. It was found that the ketamine-based anaesthesia improved neuronal viability by substantially increasing the membrane input resistance and rate of success in voltage clamp experiments. This was not only found to be the case for LC neurons but was also confirmed in another neuronal population, namely hypoglossal motor neurons.

The second research chapter (chapter 4) characterizes the combination of pacemaker currents responsible for establishing depolarization during the interspike interval voltage range in mouse LC neurons. By using a series of voltage clamp approaches, I demonstrated that the composition of currents included a TTX-sensitive voltage-dependent Na^+ conductance, a high TEA-sensitive K^+ conductance, but no Ca^{2+} conductance. Interestingly, this complement of currents is different to rat LC neurons, the most studied LC preparation, which exhibit an important persistent pacemaker Ca^{2+} current close to the threshold for action potential initiation. A lack of a persistent Ca^{2+} current in mice could represent a significant temporal change in all Ca^{2+}-dependent pathways giving a different perspective for cellular experiments carried out in the two species. This reminds us that direct comparisons between different animal species should be done with care.

The third research chapter (chapter 5) investigates developmental changes in LC pacemaker currents. The two basic conductances (i.e. Na^+ and K^+), responsible for controlling the membrane depolarization underwent changes during development. However, once again there was no evidence for Ca^{2+} conductance in the pacemaker-interval voltage range in LC neurons, either infant or adult mice. Changes in the basic pacemaker currents were accompanied by other changes such as differences in TTX-insensitive spiking activity and the levels of baseline voltage noise. This chapter presents the first detailed report on the way development induces electrophysiological changes in mouse LC neurons.

The fourth paper (chapter 6) of this thesis presents an investigation into the possible participation of mitochondria as an active modulator of LC pacemaking. Aspects of mitochondria were investigated for two main reasons: 1) they act as significant Ca^{2+}

stores and are involved in controlling the intracellular Ca^{2+} dynamic in many different cells, hence they may impact on the pacemaking process of LC neurons; and 2) many neuropathologies such as PD have mitochondrial dysfunction as primary cause, thus the understanding of the role played by mitochondria in the pacemaking process could pave the way to discover new clinical approaches that may be beneficial at very early stages of the disease. Specifically, it was found that disturbance of mitochondrial metabolism activated Ca^{2+} channels that, in turn, activated K^+ channels, which resulted in changes in the spontaneous firing activity of LC neurons. Two significant observations were made. The first was that Ca^{2+} channels activated by mitochondria were nifedipine sensitive, suggesting these were L-type Ca^{2+} channels. However, these voltage-dependent channels were activated at unusual hyperpolarized membrane potentials indicating an alternative pathway for their activation. The second observation was that activation of K^+ channels involved Ca^{2+} entry but was independent of intracellular Ca^{2+} release. These findings are of significant interest since they demonstrate a pathway for K^+ channel activation that is different than previously described by other investigators. Moreover, the fact that mitochondria may be involved in the pacemaker process, by not only buffering internal Ca^{2+} but also modulating ionic channels, indicates an exciting new perspective that could be applied to studies involving PD.

In summary, this thesis has characterized conductances responsible for controlling neuronal pacemaking in infant and adult mouse LC. Investigations of inhibiting mitochondrial function led to the proposal that mitochondria may serve as fine tune regulators of LC pacemaking. These results constitute a detailed description of fundamental electrophysiological properties of mouse LC neurons, which provide a foundation for future LC studies using mutant mice and thus providing new insights into mechanisms that control LC pacemaking. Going still further, the results presented here

can be applied to the study of the mechanisms underlying the progression of neurological diseases, such as PD, where there is direct involvement of LC neurons and their mitochondria.

Publications

The following publications have arisen from data presented in the present thesis:

Journal Articles

- **de Oliveira, R. B.;** Graham, Brett; Howlett, Marcus C.H.; Gravina, Fernanda S.; Oliveira, Max W.S.; Imtiaz, Mohammad S.; Callister, Robert J.; Lim, Rebecca; Brichta, Alan M.; van Helden, Dirk F.. Ketamine anesthesia helps preserve neuronal viability. Journal of Neuroscience Methods, v. 189, p. 230-232, 2010. DOI: 10.1016/j.jneumeth.2010.03.029

- **de Oliveira, Ramatis B.;** Howlett, Marcus C.H.; Gravina, Fernanda S.; Imtiaz, Mohammad S.; Callister, Robert J.; Brichta, Alan M.; van Helden, Dirk F.. Pacemaker currents in mouse Locus Coeruleus neurons. Neuroscience, 2010. DOI: 10.1016/j.neuroscience.2010.06.028

- **de Oliveira, Ramatis B.;** Gravina, Fernanda S.; Brichta, Alan M.; Callister, Robert J.; van Helden, Dirk F.. Effects of mitochondrial disruption on ionic currents and pacemaking in neurons of the locus coeruleus. *Manuscript under review in "Journal of Physiology".*

- **de Oliveira, Ramatis B.;** Gravina, Fernanda S.; Brichta, Alan M.; Callister, Robert J.; van Helden, Dirk F. Developmental changes in pacemaker currents in mouse locus coeruleus neurons. *Manuscript under construction to be sent for publication.*

Conference Abstracts

- Gravina, Fernanda S.; **de Oliveira, R. B.;** Graham, Brett; Howlett, Marcus C.H.; Oliveira, Max W.S.; Imtiaz, Mohammad S.; Callister, Robert J.; Lim, Rebecca; Brichta, Alan M.; van Helden, Dirk F.. Ketamine anaesthesia helps preserve neuronal viability. In: 28th International Australasian Winter Conference on Brain Research 2010, Wanaka, New Zealand, 2010.

- **de Oliveira, Ramatis B.;** Howlett, Marcus C.H.; Gravina, Fernanda S.; Imtiaz, Mohammad S.; Callister, Robert J.; Brichta, Alan M.; van Helden, Dirk F.. Pacemaker Calcium Currents: Difference in Locus Coeruleus Neurons of Mice and Rats. In: 28th International Australasian Winter Conference on Brain Research 2010, Wanaka, New Zealand, 2010.

- **de Oliveira, R. B.;** Howlett, M.; Gravina, F. S.; Callister, R.J.; Brichta, A.M.; van Helden, D.F. Properties of Locus coeruleus neurons in infant and adult mice. In: ANS/AuPS 2010 the 30th Annual Meeting of the Australian Neuroscience Society, in conjunction with the 50th Anniversary Meeting of the Australian Physiological Society, 2010, Sydney, 2010.

- **de Oliveira, R. B.;** Howlett, M.; Gravina, F. S.; Imtiaz, M.S.; Callister, R.J.; Brichta, A.M.; van Helden, D.F.. Effect of antioxidants in the pacemaking process of mice Locus Coeruleus neurons. In: Australian Neuroscience Society Inc. 29th Annual Meeting, Canberra, 2009.

- **de Oliveira, R. B.;** Howlett, M.; Gravina, F. S.; Imtiaz, M.S.; Callister, R.J.; Brichta, A.M.; van Helden, D.F.. Ion channel modulation by reactive species in mice Locus Coeruleus neurons. In: Proceedings of the XXXVI International Congress of

Physiological Sciences (IUPS2009) Function of Life: Elements and Integration, 2009, Kyoto. The Journal of Physiological Sciences, v.59, 2009.

- **de Oliveira, R. B.;** Howlett, M.; Gravina, F. S.; Imtiaz, M.S.; Callister, R.J.; Brichta, A.M.; van Helden, D.F.. Influence of mitochondria in the interspike interval pacemaking currents of mice Locus Coeruleus neurons. In: 2008 Annual Meeting of the Australian Physiological Society, Melbourne, 2008.

- **de Oliveira, R. B.;** Howlett, M.; Gravina, F. S.; Imtiaz, Mohammad S.; van Helden, D.F.. Pacemaking in Locus coeruleus. In: Kioloa Neuroscience Colloquium, Kioloa, 2007.

Chapter 1

General Introduction

1.1. The Locus coeruleus

The Locus coeruleus (LC) is the name given to a nucleus of tightly packed noradrenergic-containing neurons located in the rostral dorsolateral pontine tegmentum [1, 2]. In rat, the LC has approximately 1,600 neurons that extend projections to many different brain regions and the spinal cord [3] (Figure 1.1).

Behaviour in vertebrates is strongly controlled by LC activity, with the firing rate of action potentials playing a central role in this process. LC neuronal activity is regulated mainly by inhibitory inputs that arise from GABAergic neurons present in the nucleus prepositus hypoglossi and adjacent regions in the dorsomedial medulla [4]; and excitatory inputs that arise from glutamatergic neurons present in the nucleus paragigantocellularis in the ventrolateral medulla [5]. Experiments on animals have demonstrated that the LC increases its firing rate in response to many sensory stimuli, particularly noxious or stressful ones. Moreover, the firing rate of these noradrenergic neurons decreased in situations where the animals were calm and drowsy, or in certain stages of sleep. Because of these and other findings, the LC has been correlated with controlling the sleep-wake cycle [6], promoting a state of vigilance [7], monitoring environmental stimuli [8-10], increases in cognitive performance [11] and also in regulation of autonomic body functions [12].

LC neurons are able to spontaneously fire action potentials due an intrinsic pacemaker activity *in vivo* [13-15], in brain slices [16, 17] and in cellular cultures [18, 19]. Another key feature of LC action potential activity is that it is usually synchronous across multiple LC neurons; generating rhythmic outputs that produce widespread coordinated noradrenergic signalling [20]. Electrical coupling has been suggested as the

pathway by which LC neurons synchronize. Such synchronization means that LC neurons can integrate inputs from different brain areas and release noradrenaline to different regions at the same time. The specific mechanisms underlying synchronization between these electrically coupled neurons are still not well understood, but it has been suggested for young animals, where synchronization is more pronounced, that subthreshold membrane oscillations have a key role in this process [21]. Subthreshold membrane oscillations are observed in neurons from rats younger than 10 days but are not obviously present in adult animals, suggesting that a different mechanism coordinates the LC synchronicity in adult animals.

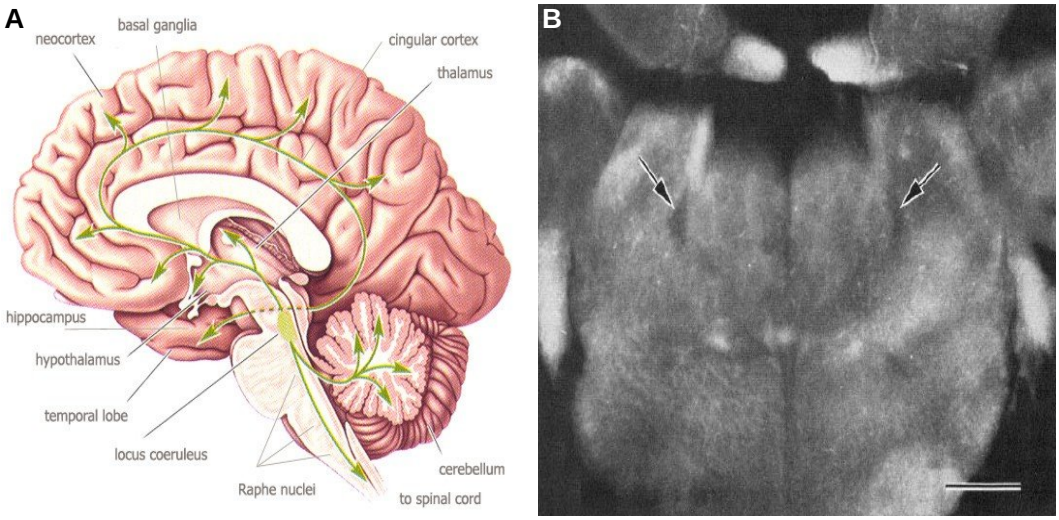

Figure 1.1: Locus coeruleus localization in the human brain (A) and in a fresh unfixed transverse mouse brain slice 100µm thick (B). Note the direction of the projections from LC to many different brain areas in the human brain (A). Scale bar 100µm (B). Adapted from [18]

One mandatory feature for electrically coupled neurons is the presence of gap-junctions, which provide the pathway for conveying current from one cell to another and resultant changes in membrane potential in the neighbouring cell. Thus in coupled cell systems such as the LC, rhythmic firing (i.e. action potentials) in a neuron will cause changes in membrane potential of adjacent neurons advancing or retarding firing of these neurons causing the neurons to synchronize their rhythmic firing. Such synchronization occurs through "coupled oscillator"-based interactions, a process first observed for coupled pendulums (e.g. coupled by springs), which when randomly stimulated influence each other's cycles leading to group entrainment (i.e. synchronization). Synchronization of rhythmical action potentials between LC neurons is gap-junction dependent and dendrites are the pathway through which electrical current flows [22]. Gap-junctions have been found between dendrites of adjacent neurons and between dendrites and axons of adjacent LC neurons but not between neurons and astrocytes or oligodendrocytes. Gap-junctions have been reported to decrease in density with age but do not completely disappear in adult animals [23]. This observation may explain why in adult animals synchronization of neuronal firing is weaker.

Going a little bit further than intrinsic features of the LC, one can find that the LC neuronal complex plays a role in many pathologies. For instance, the LC may play a very important role in the development of Parkinson's disease (PD) [24]. PD is a pathology from the movement disorders group, where a degeneration of dopaminergic neurons in the mid brain region called Substantia Nigra (SN) takes place, impairing the brain pathway responsible for control of voluntary movement [25]. In brief, this pathway is based on the exchange of information between the brain motor cortex (MC) and the basal ganglia before reaching the muscles and starts voluntary movement.

Specifically, SN neurons send excitatory signalling to the striate, which is located in the basal ganglia, structures that convey signals back the MC before the start of movement [26]. Once degeneration of SN takes place this entire pathway is impaired, resulting in a decreased excitatory signalling delivered to the MC. The causes that lead to the loss of SN neurons are still unknown; however, inflammation and oxidative stress are fundamental to the progression and development of the disease. It was suggested that all "classic" features present in the inflammation process, including increase in production and release of cytokines and phagocytises are also present in PD [27]. An involvement of oxidative stress in PD results from dopaminergic neurons presenting a systemic mitochondrial dysfunction [28], which leads to increase in free radical production and activation of intracellular pathways triggered by them.

LC involvement in PD was recently "rediscovered" and it is based on several lines of evidence. The most important connection is that there is extensive LC neuronal loss observed in PD patients [29]. PD in animal models where the LC also underwent lesions were found to have impaired recovery [30]. Other studies have shown that pharmacological stimulation of LC neurons increased resistance against the onset of PD in animal models [31]. Moreover, transgenic animals expressing a higher noradrenergic innervation appeared to be protected against neurotoxicity in the SN [32]. These data suggest that noradrenergic signals are important in preventing the development of PD, and the loss of these signals may partly sustain PD symptoms or/and worsen the DA nigrostriatal damage. Although this is a new exciting outlook about Parkinson's disease, the exact mechanism that leads to the decreased noradrenergic signalling in PD is still not known.

Another pathological condition that involves strong participation of the LC is in opiate withdrawal. In this case, the increased firing rate of LC neurons seems to be responsible for many of the signs and symptoms under these conditions [33, 34]. Acute stress also increases the firing rate of LC neurons, and this increase is sustained after the brain baseline firing rates return to normal. LC over-excitability could contribute to some of the associated behavioural changes seen under stressful [35] and physical withdrawal conditions [34, 36]. Molecular and cellular studies have shown that a complex intracellular pathway regulates LC neuron pacemaker activity in the cases cited above (Figure 1.2). One central key that regulates LC responses/adaptations, particularly during chronic perturbations, is the cAMP pathway [37-40]. This pathway regulates the expression of many proteins related with the control of the pacemaker activity and also directly activates ion channels located on the plasma membrane, playing a role in acute and chronic responses. Besides the knowledge about the cAMP pathway having a role in pacemaker activity of LC neurons, the exact mechanism by which cAMP exerts its role on the ion channels involved in LC pacemaking are still not known. Moreover, the specific ion channels involved in this process have still to be characterized, and the influence of intracellular ion stores such as endoplasmic reticulum (ER) and mitochondria, which can alter the firing frequency in these neurons, is still not known.

The pacemaker mechanism underlying rhythmical firing of LC neurons is a fundamental mechanism, which underlies LC activity and consequently its role in physiology, behaviour and brain disorders. A better understanding of LC pacemaking, the ion currents involved, what modulates each ion current, how LC neurons coordinate responses, and many other features, could impact on many different disorders. Indeed,

an improvement in knowledge about LC pacemaker activity could help to develop new approaches for treating diseases such as PD and Alzheimer.

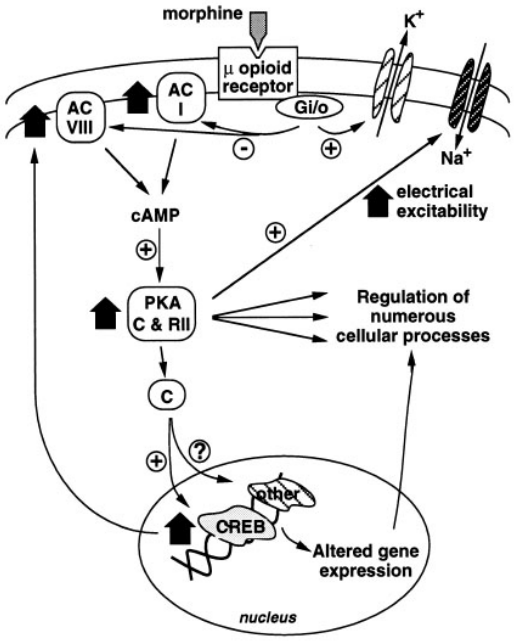

Figure 1.2: Scheme illustrating opiate actions in rat Locus Coeruleus. Note that an unspecific Sodium current is activated as part of this pathway.

Figure adapted from Nestler,1997 [41].

1.2. Pacemaker Mechanisms

1.2.1 Cardiac Pacemaker Model *(Plasmalemmal Pacemaking)*

This "classical" pacemaker model has arisen from studies on the heart pacemaker, a group of specialized cells in a region termed the sinoatrial (SA) node that rhythmically generate pacemaker action potentials that pace and trigger heart muscle action potentials and contraction [42]. SA node permeability to ionic species changes continuously in a

manner which perpetuates an automatic cycle of depolarization, action potential and repolarisation such that the membrane potential of SA node cells is always changing [43]. In this model, pacemaker currents comprised of maintained inward currents and a hyperpolarization-activated inward current depolarize the membrane potential to reach threshold to activate voltage-dependent sodium (Na_V) and calcium channels (Ca_V) [44, 45]. Once the threshold is reached, Na_V and Ca_V regeneratively open to produce an action potential that depolarizes the cells. This is only transient as Na_V channels close and the depolarization and Ca^{2+} entry respectively activate voltage-dependent and Ca^{2+} activated potassium channels (i.e. K_V and K_{Ca}). Repolarisation now occurs due to the reduction in inward Na_V current and increase in permeability to potassium ions, which carry positive current out of the pacemaker cells. During this phase, the number of open Ca_V channels and hence permeability to Ca^{2+} also continuously decrease as the membrane potential becomes repolarised. The cycle then re-starts, through the combination of sustained inward currents, hyperpolarization-activated inward currents and decreasing potassium permeability this again depolarising the membrane potential to threshold to activate Na_V and Ca_V channels. In summary, this model is a pacemaker mechanism where the action potentials, which time and trigger heart contractions, are produced by properties of voltage-dependent currents (sodium, potassium and calcium) present in the plasma membrane of pacemaker cells in the SA node.

1.2.2 Intracellular Stores Model

There is another model for cellular pacemaking and synchronization termed "Calcium Store Pacemaking". This model predicts that there is a long-range intercellular communication of depolarizations resulting from oscillatory Ca^{2+} release

from intracellular Ca^{2+} stores in the SR/ER. This mechanism depends on coupled oscillator-based entrainment of the rhythmical depolarizations produced by oscillatory store Ca^{2+} release activating inward ion current flow. Such entrainment occurs within and between gap junction-coupled cells producing pacemaker potentials that in turn activate Ca^{2+} entry into muscle cells causing contraction. The mechanism has been shown to function in a range of tissues including lymphatic [46], urethral [47] and stomach smooth muscle [48, 49].

The mechanism has more recently also been shown to function as a pacemaker mechanism in the heart where it functions symbiotically with the classical membrane pacemaker mechanism to drive heartbeats [50, 51]. According to this model, calcium (Ca^{2+}) can be released from the ER to the cytosol through two types of receptors: 1) inositol 1,4,5-triphosphate receptors (IP_3Rs) or 2) ryanodine receptors (RyRs). Both receptors can be activated by Ca^{2+} as well as their respective ligands. Ca^{2+} release from stores operated by these receptors is oscillatory, having a cycle that involves channel opening, Ca^{2+} release, channel closure and store refill. In this model pacemaker cells communicate through gap-junctions. This and the oscillatory nature of the Ca^{2+} release produce an interesting phenomenon where stores undergoing oscillatory Ca^{2+} release can entrain their release/refill cycles both within and across cells. This occurs through coupled oscillator-based interactions [52]. Transformation into an electrical rhythm occurs because the Ca^{2+} released into the cell cytosol adjacent to the cell membrane activates channels that generate inward current and consequently depolarize the cell membrane potential. This depolarization travels by current spread through gap-junctions to other cells and activates membrane IP_3Rs and voltage-dependent Ca channels that activate Ca^{2+} entry and IP_3 release into the cytosol of these cells. Once this happens, IP_3 and Ca^{2+} activate oscillatory store Ca^{2+} release, which synchronizes within and between

cells [53]. During this process a regenerative Ca^{2+} signal is produced, keeping the signal strong enough to reach all target cells. As the coupling between cells is not infinitely strong, phase delays develop between each oscillator so that the release/refill cycle of each store occurs with a delay compared to the adjacent one, resulting in a Ca phase wave [54]. Therefore, this model predicts that electrical phase waves generated by calcium release from intracellular stores are the mechanism that times and spatially coordinates activity in tissues composed from one to thousands of cells.

1.3. Brain Pacemaking

1.3.1. Pacemaking in Locus Coeruleus

LC neurons characteristically produce spontaneous action potentials due an intrinsic pacemaking activity and hence are *pacemaker neurons* [13-19]. LC neurons fire in a frequency range of 0.3 Hz to 5 Hz, with this frequency modulated by many substances including opiates [55], noradrenaline [56], substance P and muscarinic agonists [57].

Chronologically, the first characterization of currents that could control the pacemaker mechanism in LC neurons came from J.T. *Williams*' group. They reported that rat LC neurons exhibited a persistent inward calcium current, and two other types of outward potassium currents: The first one was a transient outward current that had the properties of fast voltage-activated K^+ currents (shown to be an A current); and the second was a Ca^{2+}-activated K^+ current (shown to be a SK current). They also

demonstrated that action potentials had tetrodotoxin (TTX) –sensitive and resistant components and that action potentials persisted in presence of TTX [16].

Another discovery arose relating to observations that LC neurons have an intrinsic feature of "wash out" where rhythmicity is lost when recordings are made by whole cell patch clamp techniques. Based on this finding *G.K. Aghajanian* and his group, studying opiate actions in rat LC neurons, discovered that cAMP plays an important role in controlling pacemaking of these neurons [37]. They first described that cAMP or compounds that mimic its actions, were able to produce an inward cation current carried mainly by Na^+ and this current was resistant to TTX [58, 59]. They then demonstrated that cAMP and the cAMP-dependent protein kinase (PKA) pathway had a key role in control of LC pacemaking [34-37].

Other studies have shown that opiates activate an outward potassium current [60, 61] through a pathway involving G-proteins [62]. Some controversial findings can be noted along these studies that aimed to describe pacemaking currents in LC neurons. For instance, *J.T. Williams'* group described that action potentials in LC neurons were resistant to TTX, suggesting that calcium action potentials were present in these cells, and that the pacemaking activity was probably driven by persistent inward calcium current [16]. On the other hand, other studies showed that action potentials from LC neurons were sensitive to TTX [18, 63]. Indeed the *Aghajanian,* group suggested that LC pacemaking was probably driven by non-specific sodium current [50-53]. Because of that, some authors have adopted the term "non-specific cation current" when they refer to the ionic current that drives pacemaking in the LC.

In overview, while the rat LC is known to have various Na^+, Ca^{2+} and K^+ currents the specific current or the exact combination of currents that coordinate pacemaking in

LC neurons has yet to be established. Furthermore, most studies have been carried out in rats and hence there is little knowledge about LC pacemaking in other species including that of the mouse. Table 1.1 shows a summary of the ionic currents reported in LC neurons to date.

Another important feature that needs further studies is how LC neurons coordinate their rhythmic firing. Subthreshold membrane oscillations were suggested in young animals [21], but what produces and coordinates these oscillations is still not known. Furthermore, this does not explain synchronicity in adult rat LC, which while weaker still exists [64]. A possible explanation is that pacemaking and resultant synchronicity is mediated by "Ca^{2+}store pacemaking" as LC neurons have Ca^{2+} stores and are electrically coupled by gap-junctions. Such a model could also explain the subthreshold membrane oscillations displayed by the LC in infant rats. However, unpublished findings from our group indicate that this is an unlikely hypothesis as store activators and/or inhibitors do not appropriately modulate pacemaking in these cells. Further studies are necessary to better understand how the LC pacemaker operates and how it produces synchronised rhythmic firing.

Current	Subtype of Channels present in LC	Other information	Sources *(references)*
K^+ Inward Rectifier	K_{ir} (3.1-3.3) or GIRK (1-3)	Channels coupled with G-proteins; currents are activated by opiates	[65]
Fast Transient $K^+(I_A)$	{K_v1.1 or KCNA}*	Transient current activated after membrane hyperpolarization; sensitive to 4-aminopyridine	[16, 66, 67]
Sustained K^+ Current (I_K)	{K_v3.1 or KCNC}*	Current sensitive to TEA	[66]
Calcium-Activated K^+	BK or KCNM; SK (2 and 3) or KCNN (2 and 3)	BK immunoblotting was reported but no report of ionic currents; very little expression of SK-2 and very high of SK-3	[16, 68-70]
K^+ Leak	TASK1	Activated by halothane and inhibited by pH acidification	[71]
ATP-Sensitive K^+ Conductance	ATP-sensitive K^+ Channels	Induced by hypoxia	[70, 72]
NMDA-Induced Outward Current ($I_{NMDA-out}$)	NMDA receptors	Activation increases the influx of Ca^{2+} and it activates Ca^{2+}-dependent K^+ currents	[70]
TTX-Insensitive Inward Na^+	TTX-insensitive Channels (??)	Activated by different compounds in presence of TTX	[66, 73, 74]
TTX-Sensitive Inward Na^+	Voltage–dependent TTX-sensitive channels (??)	Fast event of action potentials; Persistent Na^+ currents	[66, 75, 76]
Cobalt/Nifedipine-Sensitive	L-Type Ca^{2+}	Activated by acidosis	[75, 77]
ω-Conotoxin-Sensitive; ω-Agatoxin-Sensitive	N-Type Ca^{2+}; P-Type Ca^{2+}; Q-Type Ca^{2+};	Increased by barium and inhibited by many different compounds	[77]
Persistent Inward Ca^{2+} current	??	Active near the threshold for action potential initiation (~ -45 mV)	[16]

Table 1.1: Summary of all ionic current described in LC neurons. *Immunoblotting for specific subtype not found in the reviewed literature. ? - Indicates that no information about specific subtypes was found.

1.3.2. Pacemaking in other Brain Areas

Neurons present in the central nervous system (CNS) are split into many different brain areas; they have different functions and characteristics according to their internal constituents. The pacemaking mechanisms present in these neurons also change according to function and localization in the brain. Localization appears to be particularly relevant because different types of ion channels are expressed according to the region. Table 1.2 presents an overview of different types of neurons and the respective ionic current that is considered to primarily drive pacemaking.

Neuronal Cell Type	**Pacemaking current**
Neostriatal cholinergic interneurons	I_h
Globus pallidus neurons	I_h
Subthalamic neurons	*Persistent* Na^+
Cerebellar granule cells	*Persistent* Na^+
Suprachiasmatic nucleus neurons	*Persistent* Na^+
Dopaminergic neurons	*Persistent* Ca^{2+}
Locus coeruleus (Rats)	*Persistent* Ca^{2+} *and Persistent* Na^+

Table 1.2: Inward pacemaker currents in different types of neurons.

Different types of ionic currents may also be involved in generation of action potentials (APs) and to relay information among neurons. The majority of neurons are not able to produce action potentials by themselves; they only produce action potentials

when they receive excitatory synaptic inputs that cause super-threshold depolarization. Pacemaker neurons in general utilise up to three different pacemaker currents to generate action potentials. One of these is a current called the hyperpolarization-activated current (I_h), which as the name indicates, is an inward current activated at high negative membrane potentials. I_h, together with other currents, drive the membrane potential to reach threshold to produce an action potential [78-80].

A second pacemaker current is the "persistent sodium current" that is active in membrane voltages around -65mV to -40mV [81-83]. It was suggested that the persistent sodium current could be a feature of the normal gating behaviour of sodium channels, where they would produce this sustained/steady state current [84]. However, specialized types of sodium channels were also characterized as responsible for this persistent current [85]. The persistent sodium current seems to be present as part of the physiology of almost all neurons described so far [81, 86-91]. It contributes to creating many different firing frequencies and patterns, which helps to spread information among the neuronal networks.

There is also a third pacemaker current, which appears to be a special feature of midbrain dopamine neurons, that is a sub-threshold calcium current that is active in the interspike interval along with Na^+ currents [92, 93]. This current is responsible for driving membrane depolarization to threshold for action potential initiation. A similar current was also identified in LC neurons from rats [94]. Going a little further about dopaminergic neurons and pacemaking activity, recently it was suggested that the spontaneous electrical activity of dopaminergic neurons may be fundamental to the survival of these neurons, and hence pathologies that affect dopaminergic neuron pacemaking could lead to Parkinson's' disease [95]. In this situation, an imbalance of

ionic currents could result in membrane hyperpolarization reflecting an imminent cell death. The hyperpolarization seems to be associated with intracellular mechanisms involving alterations in the normal mitochondrial metabolism in these dopaminergic neurons, as shown in Figure 1.3.

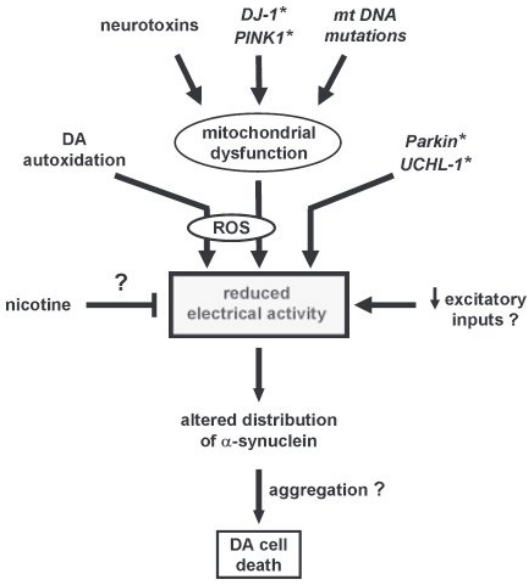

Figure 1.3: Hypothetical scenario linking the loss of dopaminergic (DA) neurons in Parkinson disease (PD) to a deficit in excitability.

1.4. Mitochondria

1.4.1. General information

Mitochondria are membrane-enclosed organelles that are virtually present in all eukaryotic cells of living organisms; they contain a large amount of internal membrane that provides a framework for an elaborate set of electron-transport processes that produce most of the ATP needed by the cells. They are usually depicted as stiff, elongated cylinders with a diameter of 0.5-1 μm. However, time-lapse micro-cinematography of living cells has shown that mitochondria are remarkably mobile and plastic organelles, constantly changing their shape and even fusing with one another and then separating again. The mitochondrial inner membrane is the location of the electron-transport chain (respiratory chain). Through a sequence of oxidation reactions mitochondria use the energy derived from electron transport to pump H^+ out of the matrix to create a trans-membrane electrochemical proton gradient. The large amount of free energy released when H^+ flows back into the matrix provides the basis for ATP production in the matrix (sections based in [96]).

Mitochondria are involved in many other cellular processes other than their "traditional" role of producing ATP. They are involved in buffering intracellular Ca^{2+} and free radical production (discussed in the next section) and also have a fundamental role in other processes such as cellular death [97-99] and cellular signalling [100], and have been linked with neurological diseases [27, 29, 32]. Mitochondrial membrane potential has also been shown to be modulated by cytoskeleton proteins having the ability to reverse free radical production induced by vitamin A treatment [101]. In neurons, disruption of the mitochondrial membrane potential has been shown to impact

on pacemaking [102, 103] and a correlation exists between mitochondrial activity and neurotransmitter release [104]. Thus mitochondria have an important role in many different cellular processes.

1.4.2. Role of Mitochondria in Cellular Pacemaking

Mitochondria play a very important role in calcium signalling participating in the regulation of many intracellular pathways; each can store huge amounts of calcium ions internally in the mitochondrial matrix with functions maintained by an electrical gradient across the inner membrane [105-107]. The mitochondrion has specialized machinery to transport Ca^{2+} across its membranes; Ca^{2+} uptake is performed by a selective ion channel termed Uniporter (MCU) [108], while Ca^{2+} release can be performed by two different structures, the first one is a mitochondrial Na^{+}/Ca^{2+} exchanger (MNCE) and the second one is the mitochondrial permeability transition pore (MPTP) [109]. Recently it was shown that compounds that block mitochondrial functions such as p-trifluoromethoxyphenylhydrazone (FCCP), ruthenium red, CGP-37157 and others, can modulate some neuronal functions including action potential firing rates, suggesting that mitochondria can modulate ionic currents [104, 110]. The mitochondrial role in calcium dynamics and related electrical activity is potentially very important in pacemaking, as it has a seminal role in Ca^{2+} homeostasis and internal Ca^{2+} signalling can activate or modulate ionic pacemaker currents.

Mitochondria provide a means of buffering cytosolic Ca^{2+} and they also participate together with the endoplasmic reticulum (ER) in the physiology of Ca^{2+} oscillations that are present in many cells as a regulatory pathway [111]. Importantly, mitochondria are the largest intracellular source of reactive species and free radicals (such as reactive

oxygen species (ROS) and reactive nitrogen species (RNS)) [112, 113]. Reactive species can modulate a great variety of ion channels and receptors [114, 115], consequently modulating ionic transport/content into the cells. For instance, large-conductance Ca^{2+}-activated potassium channels (BK), IP_3 and RyRs have their activity increased by ROS [116].

A new outlook about intracellular modulation is emerging based on the finding of "ROS microdomains". Here, local production of ROS is considered to modulate molecules confined to that space. These ROS microdomains are physiologically different from the Ca^{2+} microdomains previously suggested in the literature [117]. The greatest difference is that ROS microdomains have a sustained concentration gradient and a much longer half-life than the Ca^{2+} microdomains, which have a half-life around 20ms [116]. According to this point of view, ROS microdomains could be generated near to the plasma membrane and hence modulate ion channels and receptors. In pacemaker neurons for instance, ROS microdomains could modulate channels or stores, changing the firing frequency in these neurons. In this case, ROS produced by mitochondria would have a direct effect in controlling pacemaking. Some evidence has been presented demonstrating that mitochondria can directly modulate potassium inward rectifier channels, hence playing a role in the control of ionic currents [118, 119]. It has also been shown that mitochondria can modulate L-type Ca^{2+} channels through a pathway involving cytoskeleton proteins; in this situation, it was proposed that there was a feedback such that L-type Ca^{2+} channels modulated mitochondrial activity according to cellular demand [120]. There is also evidence that L-type Ca^{2+} channels can be modulated by reactive species, which oxidise amino acid residues (cysteine) at key positions in the protein altering channel activity [121, 122].

Thus mitochondria and associated pathways could make an important contribution to neuronal pacemaking due their ability to modulate ionic channels and consequently change neuronal firing rate.

1.5. Brain development and pacemaker mechanisms

Brain development is a non-linear process at both the structural and functional level [123-125]. Fundamental to this are processes that underlie brain adaptation to new environments and situations [126]. In development, new neuronal connections extend to reach different brain regions [127-129] accompanied by morphological changes in synapses [130-133] and neuronal electrophysiological properties [134, 135]. Brain-mapping techniques along with prospective sample studies have demonstrated that the development of brain grey matter from childhood to early adulthood is a nonlinear process, progressing in a localized, region-specific manner coinciding with the functional maturation such that, regions associated with more primary functions develop earlier compared with regions that are involved with more complex and integrative tasks [136].

As has been noted, LC neurons project widely across the brain providing a modulatory influence on many physiological processes and different types of behaviour. Importantly, given that the level of stimulus experienced by an individual has a remarkable impact on brain development [126], it is likely that LC neurons strongly contribute to this process. Furthermore, as neuronal plasticity changes in different stages of life including in the elderly [137], LC neurons are also likely to change their

properties to adapt to different phases of life. This is certainly the case for other tyrosine hydroxylase (TH)-containing neurons, as has been demonstrated for dopaminergic neurons present in the Substantia Nigra that undergo developmental/maturational changes in the pacemaker mechanism [138, 139]. Thus certain types of neurons, especially TH-containing ones such as LC neurons, could change their combination of pacemaker currents, this impacting on action potential generation and hence firing rates. In LC neurons, morphological changes involving axonal branching [140, 141] and changes in the number and direction of projections to other brain regions were reported in animals of different ages [142]. Such morphological changes will affect many functions including formation and localization of synapses and hence excitatory and inhibitory signalling generating differences in neuronal firing rate [143]. Such modulation does not necessarily depend on changes in pacemaker currents. In the case of the LC, evidence has been presented suggesting that LC neurons increase firing frequencies with development [144]. Other studies have demonstrated that general electrophysiological properties such as input resistance also change during development/maturation [94], indicating that LC neurons undergo changes during development.

At present, it is not known whether developmental changes in firing frequency in LC neurons arise as a consequence of brain-related morphological changes or are due to a rearrangement of pacemaker currents. Information comparing electrophysiological properties of LC neurons at different ages is also absent.

Chapter 2

Methods

All experiments were performed in accordance with the guidelines developed by The University of Newcastle Animal Care and Ethics Committee.

2.1. Preparation of brain slices

Brain slices containing the LC were prepared from Swiss mice (P7-12, both sexes) or adult (8-12 weeks old, only used in chapter 5) overdosed with Ketamine (100 mg/kg i.p.). In chapter 3 only, slices containing hypoglossal motor neurons were also prepared using exactly the same protocol described in this section. Mice were decapitated and the brain was rapidly removed and immersed in ice-cold "modified sucrose ringer" containing (in mM): 25 $NaHCO_3$, 11 glucose, 235 sucrose, 2.5 KCl, 1 NaH_2PO_4, 1 $MgCl_2$ and 2.5 $CaCl_2$, bubbled with 95% O_2/5% CO_2 [145]. The cerebellum and brain stem were isolated and slices (270-400μm thick for infant and 140 μm thick for adult) were obtained with a vibrating tissue slicer (Leica VT1000S). Generally only one slice contained the LC. Slices were kept in a chamber (containing artificial cerebrospinal fluid - ACSF) at room temperature and high oxygen for 1.5-2 h before experiments commenced. ACSF used in all experiments contained (in mM): 120 NaCl, 25 $NaHCO_3$, 11 glucose, 2.5 KCl, 1 NaH_2PO_4, 1 $MgCl_2$ and 2.5 $CaCl_2$, constantly bubbled with 95% O_2/5% CO_2. Individual LC neurons were visualized using infrared video microscopy with differential interference contrast and identified according to their large size and location near the ventrolateral border of the fourth ventricle. Immunohistochemistry using antibodies against Tyrosine Hydroxylase confirmed the location and identity of these neurons (see Supplementary Figure 4.1 A, B in chapter 4). Hypoglossal motor

neurons were identified by their large size and location relative to the central canal/4th ventricle [146]

2.2. Preparation of fresh dissociated LC neurons

Neurons were isolated using an adapted protocol according to Akaike, N. and A.J. Moorhouse, 2003 [147]. Brain slices were cut using the same protocol described in the "Preparation of brain slices" section. After 1.5-2 h resting, slices were placed in the ACSF-containing recording chamber and neurons were isolated using a custom made vibrating device. This device vibrates a fine glass electrode with a sealed tip just above the tissue surface causing dissociation of the cells. It generally provided about 10 healthy neurons per slice. After isolation, neurons were left 15 min to settle on the glass bottom of the recording chamber and then gentle ACSF perfusion was commenced.

2.3. Electrophysiology

After isolation, the slice containing the LC was identified and transferred to a recording bath where it was viewed with an upright microscope (Olympus BX50) and superfused with ACSF. Individual LC neurons were visualized using infrared video microscopy with differential interference contrast and identified according to their large

size and location near the ventrolateral border of the fourth ventricle. Most recordings were made from spontaneously firing LC neurons *in situ* in brain slices. Because LC neurons are large, it was difficult to maintain voltage clamp for fast rates of membrane depolarization (> 50 mV/s). This precluded us from using the interspike interval AP clamp technique to investigate pacemaking. Therefore, we developed a methodology that allowed us to achieve good voltage control over LC neurons and record fast activating Na^+ and Ca^{2+} currents when depolarizing ramps were applied. Voltage control was achieved by using a low-noise whole cell voltage clamp amplifier (Axopatch-1C), low fluid levels in the recording chamber, and low resistance electrodes (1.8 – 2 MΩ). The age of the animals was also crucial for achieving voltage control. Neurons from mice < P5 could not be voltage-clamped, however good voltage control could be achieved in 80% of neurons in P7-12 mice. Neurons were considered to be adequately voltage clamped when no unclamped spikes were observed during voltage ramps. Both voltage and current clamp recordings were low-pass filtered at 5 kHz and data were sampled at 100 kHz. I-V plots constructed from voltage clamp recordings had each individual current normalized by the corresponding cell size, with values expressed as pA/pF.

2.4. Solutions and pharmacology

To minimize problems associated with *washout* of spontaneous electrical activity when recording from LC neurons, we developed the following protocol. First, the whole cell recording mode was established in voltage clamp. After waiting 10 s, a voltage

ramp was applied and the test solution was superfused over the neuron of interest via a local-perfusion system [146] for 60 s. A second ramp was then applied. This protocol together with the rapid local solution exchange (exchange time ~ 2 s) allowed the entire experiment to be completed in < 2 min. In some cases, test solutions were applied over the slice for 8 min before beginning recording. In these experiments control recordings were not made, as cells were held in the cell attached mode (i.e. without internal access) during the 8-minute equilibration period before obtaining the whole cell recording configuration.

The internal pipette solution contained (in mM): 135 K methylsulfate, 8 NaCl, 10 HEPES, 2 Mg_2ATP, 0.3 Na_3GTP, 0.1 EGTA, pH: 7.3. This internal was used throughout all experiments except where otherwise noted. The control external solution used was ACSF. To analyse TTX-sensitive voltage-dependent Na^+ currents, 1 μM TTX was applied through the local perfusion system. In cases where TTX-insensitive currents were studied, a HEPES-ACSF bathing solution containing (in mM): 151 NaCl, 13 glucose, 10 HEPES, 2.5 KCl, 1 $MgCl_2$ and 2 $CaCl_2$ was used, where NaCl was replaced by N-methyl-D-glucamine chloride (NMDG) in the test solution. Ca^{2+} currents were also investigated using the HEPES-ACSF solution containing K^+ channel blockers (15 mM TEA+150 nM apamin) and TTX (1 μM). In these experiments $CaCl_2$ was replaced by equimolar $CoCl_2$ in the test solution. The roles of specific K^+ currents were investigated by applying different K^+ channel blockers and TTX (1 μM). Depolarizing pulse-based measurement of Na^+ currents required reducing the size of the currents so they could be voltage clamped. This was achieved by establishing the cell attached mode on a neuron (i.e. without internal access) and then perfusing the slice with ACSF plus 35 nM TTX for 5 minutes, and then with a Ca^{2+}-free high Mg^{2+} (5 mM) ACSF plus 35 nM TTX for 5 min. The whole cell recording mode was then established and a

voltage pulse protocol was applied ~ 30 s later (pulse series 1). This was followed immediately by rapid local perfusion with 1 μM TTX in the same Ca^{2+}-free high Mg^{2+} ACSF for 60 s. This abolished the Na^{+} current. The voltage protocol was then repeated (pulse series 2) and the resting differential current (pulse series 1 minus pulse series 2) was calculated to reveal the TTX-sensitive Na^{+} current.

Depolarizing pulse-based measurement of Ca^{2+} currents involved a similar approach. Neurons were held in cell attached mode and a HEPES-ACSF, containing 1 μM TTX, was applied for at least 8 minutes. The whole cell recording mode was then established and a voltage pulse protocol was applied ~ 30 s later (pulse series 1). The 1 μM TTX HEPES-ACSF solution but now with equimolar Co^{2+} substituted for Ca^{2+} (i.e. 2 mM) was then applied for 60 s and the voltage protocol repeated (pulse series 2). The resulting differential current (pulse series 1 minus pulse series 2) was calculated to reveal the underlying Ca^{2+} current. In both protocols described above the holding potential was -85 mV and a Cs^{+}-based internal pipette solution was used containing (in mM): 130 CsCl, 1 $MgCl_2$, 10 EGTA, 10 HEPES, 2 Mg_2ATP, 0.2 Na_3GTP, pH: 7.3.

In chapter 5, differential currents were obtained by subtracting the current generated by the first voltage protocol from that generated by the second (i.e. control – test), unless otherwise stated. Hyperpolarization-activated currents (I_H) were measured after perfusing 1 μM TTX into the bath for 8 min before internal cell access was gained. Depolarizing step-pulses, designed to activate these currents, were applied under voltage clamp 10 s after gaining internal cell access.

2.5. Acquisition and analysis

Data were acquired using Axograph 4.8 software (ITC-16 interface, and a Mac G4 computer), and analyzed using Axograph X 1.1.0 software. For voltage-clamp experiments the series resistance for our electrodes in whole cell mode was 5.2 ± 0.1 MΩ and no compensation was performed when applying ramp or pulse protocols. Linear leak subtraction was not used during experiments due the noise generated; it was corrected using Axograph software during data analysis. Recordings obtained by ramp protocols were normalized for leak currents by linear fit between -90 mV to -70 mV and filtered at 1 kHz using Axograph X software prior to analysis. Due to incremental artefact currents produced by cell capacitance in neurons, I-V graphs constructed from recordings obtained by pulses were normalized by removing the calculated artefact current at -78 mV from all other values (i.e. the capacitive current artefact at -78mV was extrapolated or scaled up to other values and subtracted). Input resistance, cell capacitance and series resistance were measured by the software according to the response to a -5 mV pulse delivered shortly after gaining internal cell access. Resting membrane potential was measured using Axograph software by taking the membrane potential value of the middle part of the interspike interval zone 2 (for definition of zone 2 see chapter 4). Corrections for junction potentials were calculated using the Windows version of JPCalc [148]. These corrections were -8.5 mV, -8.2 mV and -7.7 mV for the junction potentials between ACSF in the bath and K methyl sulphate, CsF or 15mM EGTA internal pipette solutions respectively. There were also -10 mV and -5.3 mV corrections for the junction potential between and the HEPES-ACSF solution and the K methyl sulfate internal pipette solution or CsCl-based internal pipette solution

respectively. All the graphs and figures presented in this thesis had the values corrected for junction potential.

In chapter 3, the criteria used to analyse the success rate of voltage clamp experiments for neurons in LC slices was "all or none", more specifically: in a "good" slice > 80% of the neurons could be successfully clamped and in a "bad" slice > 80% of neurons could not be clamped even though the neurons were functional. This criterion was used for statistical analysis of the success of voltage clamping with comparisons made between slices and hence animals, as one slice was used for each animal. A chi-square test assessed the difference in numbers of animals where LC neuronal voltage clamping was or was not successful, and an independent groups *t*-test assessed the difference in R_{IN}, between the ketamine-anesthetized and control groups.

All data are presented as mean ± SEM. GraphPad Prism 4.02 was used to prepare graphics. Statistical analyses were performed with SPSS version 17.0, using one-way ANOVA and the Bonferroni post hoc test otherwise noted. All experiments were carried out at 35 ± 2 °C. All drugs were obtained from Sigma Chemicals except TTX, which was purchased from Alomone Laboratories, Israel.

2.6. Cytosolic Ca^{2+} and Ψm measurement

Relative intracellular [Ca^{2+}] or mitochondrial membrane potential (Ψm) were measured in freshly dissociated LC neurons. After isolation (described in "*2.2. Preparation of fresh dissociated LC neurons"* section), LC neurons were incubated in

ACSF at room temperature containing either 10 μM Oregon green/AM for 45 min or 5μg/mL JC-1® for 1h [149]. The recording chamber containing these neurons was then placed on the stage of a Nikon TE200 inverted microscope connected to a BIORAD 1000 confocal scanner system with the isolated neurons viewed with a x60 water immersion objective. ACSF was perfused for at least 10 min before commencing the experiments. The Oregon green fluophore was excited using a 488 nm argon laser with intensity set to 3% and recordings made using a 522 nm emission filter. JC-1 experiments were made using the argon laser set to 1% intensity, having a filter combination of 488 nm for excitation and 522 nm for emission to record the green fluorescence, and a filter combination of 514 nm for excitation and 585 nm for emission to record the red fluorescence. Responses to application of 1 μM CCCP, delivered via rapid local-perfusion, were recorded using the BIORAD system. The Oregon green experiments involved briefly opening the shutter every 10s with fluorescence images collected for 12 min (1 min before, 6min during 1 μM CCCP application, 5 min recovery). The JC-1 experiments involved briefly opening the shutter every 30s with fluorescence images collected for 13 min (2 min before, 1 and 3 min during 1 μM CCCP application and after 8 min recovery). Relative fluorescence plots were analysed off-line using ImageJ® software.

2.7. Immunohistochemistry

Brain slices, cut using the protocol presented in the section "Preparation of brain slices", were fixed with paraformaldehyde 4% (in 0.1M phosphate buffer, pH 7.4) for 20 hours at 4°C, followed by rinsing with 80% ethanol, dimethyl sulfoxide (DMSO) in

physiological buffer solution (PBS, pH 7.4). Whole-mount immunohistochemistry was performed incubating the tissue with a rabbit anti-tyrosine hydroxylase antibody (1:100, Chemicon) overnight at room temperature and this was localized with donkey anti-rabbit IgG conjugated to FITC (1:50, Jackson Immunoresearch Laboratories). The secondary antiserum was rinsed with PBS and the tissue was examined using an Olympus BX51 microscope with appropriate filters.

2.8. Predicted net interspike interval pacemaker current

This was determined using a previously published methodology [150]. Net pacemaking current was calculated using – C x dV/dt, where C is the cell capacitance and dV/dt is the time derivative of averaged APs including the interspike interval. As cell capacitance and firing frequency for all neurons in slices was 68 ± 0.9 pF and 1.98 ± 0.44 Hz respectively, we used 68 pF for "C", and averaged APs from cells that were firing at ~ 2 Hz. Generally 10 - 20 APs were obtained from each cell and used for analysis. APs were aligned at their peaks and an epoch, 500 ms long and commencing 250 ms before the peak, was averaged. This generated a single AP cycle that was then combined with itself to generate a complete interspike interval.

Chapter 3

Ketamine anaesthesia helps preserve neuronal viability

"*Published in Journal of Neuroscience Methods, v. 189, p. 230-232, 2010. DOI: 10.1016/j.jneumeth.2010.03.029"*

3.1. Abstract

The dissociative anesthetic ketamine that acts as an N-methyl-D-aspartate (NMDA) antagonist has been reported to improve neurological damage after experimental ischemic challenges. Here we show that deep anesthesia with ketamine before euthanasia by decapitation improves the quality of neonatal mouse neuronal brain slice preparations. Specifically we found that neurons of the *locus coeruleus* (LC) and hypoglossal motor neurons had significantly higher input resistances, and LC neurons that generally are difficult to voltage control, could be more reliably voltage clamped compared to control neurons.

Keywords: ketamine, Locus Coeruleus, Hypoglossal motor neurons, electrophysiological properties, input resistance, viability.

3.2. Introduction

Ketamine is a well known dissociative anesthetic that acts as an N-methyl-D-aspartate (NMDA) antagonist [151]. It is commonly used for elective surgeries [152], as treatment for acute and chronic pain [153], and also to establish an animal model for psychosis [154]. Ketamine has also been reported to improve neurological function and reduce damage after experimental ischemic challenges [155]. The effects of acute and chronic ketamine can vary among studies due to different methodological approaches. Acute treatments seem to present a higher incidence of "positive" outcomes, such as

improvement in depressive symptoms [156], whereas chronic treatments have been associated with psychotic-like symptoms, dependence and other effects [157-159].

Electrophysiological studies have shown that direct ketamine application in neurons results in a decreased firing frequency, due to an inhibition of Na^+ and K^+ channels [160]. An increase in input resistance and inhibition of excitatory post-synaptic potentials (EPSPs) has also been associated with direct application of ketamine [161]. Such action occurs during application of ketamine with these properties returning to control levels within minutes after removal of the ketamine. The present study examined electrophysiological properties of neurons of the locus coeruleus (LC), a key mood state-associated nucleus containing noradrenergic neurons that project widely across the brain [12, 162], with the studies repeated in hypoglossal motor neurons. Our specific aim was to evaluate if ketamine anesthesia before animal sacrifice would enhance neuronal viability, as without this we found that, while we could reasonably voltage clamp hypoglossal neurons, this was not the case for LC neurons. We found ketamine anesthesia before animal sacrifice reduced the conductance (i.e. leakiness) of both neuronal preparations and hence improved whole cell voltage control of LC neurons.

3.3. Results

Ketamine improved LC neuron viability, in slice preparations from ketamine-anesthetized mice versus those that did not receive ketamine before euthanasia (hereafter termed controls). Recordings from LC neurons in ketamine-anesthetized mice exhibited better voltage control and higher input resistances (R_{IN}) compared with those from controls (Table 3.1). In voltage clamp experiments, depolarizing ramps were applied and the experiment was considered successful if unclamped action potential artifacts were not observed in the current trace (Figure 3.1). Ketamine anesthesia, led to a marked improvement ($p<0.05$) in the success rate of voltage clamp experiments in LC slices: 73% for the ketamine-anesthetized group (54 animals) versus 42% from controls (52 animals) as presented in Table 3.1. R_{IN} was significantly higher (~30%, $p<0.001$) in the neurons from the ketamine-anesthetized group compared to controls (Table 3.1), suggesting improved cell viability. The possibility that the voltage clamp was better in reducing breakthrough spikes in LC neurons under voltage clamp after euthanasia with ketamine did not occur because ketamine damaged Na^+ channels, as the excitability of treated and untreated animals was indistinguishable when measurements of neuronal firing activity were compared (data not shown). To determine whether the protective effect of ketamine generalized to other neuronal populations, we repeated the experiments on hypoglossal motor neurons. Though hypoglossal neurons are relatively large, good voltage control was always achieved during ramps; however, R_{IN} was higher (~25%) in neurons from ketamine-anesthetized animals ($p<0.05$, Table 3.1). These results on hypoglossal neurons again indicate that ketamine improves neuron viability.

	Locus Coeruleus		Hypoglossal	
	Ketamine	**Control** (No Ketamine)	**Ketamine**	**Control** (No Ketamine)
No. animals with neurons that could be voltage clamped	**39 animals (73%)** $^{+}$	22 animals (42.5%)	**5 animals (100%)**	**5 animals (100%)**
No. animals with neurons that could not be voltage clamped	15 animals (27%)	30 animals (57.5%)	0 animals	0 animals
Input Resistance (MΩ)	**256.8 ±9.8 ****	194 ±7.3	**64.9 ±4.3 ***	51.6 ±2.1
Membrane Capacitance (pF)	70 ±0.9	68.3 ±0.9	83.7 ±4.3	89.9 ±4.0
Series Resistance (MΩ)	4.9 ±0.09	4.9 ±0.1	5.1 ±0.2	4.8 ±0.2
No. of cells	129	159	38	35

Table 3.1: The effect of ketamine on the success rate of ramp voltage clamp experiments and input resistance (R_{in}). LC neurons in brain slices of mice deeply anesthetized before euthanasia by decapitation were successfully clamped in 73% of the slices, compared to 43% for non-anesthetized mice. Hypoglossal neurons did not present ramp voltage clamp control problems in the either group. R_{in} was higher in LC and hypoglossal neurons from ketamine-anesthetized mice, however, membrane capacitance (C_m) and series resistance (R_s) did not change. $^{+}$ Different from the control (i.e. no ketamine) group (Chi-square test; $P<0.05$). *, ** Different from the control (i.e. no ketamine) group (Independent groups *t*-test; * $P<0.05$, ** $P<0.001$). R_{in}, C_m and R_s values are presented as mean ± SEM.

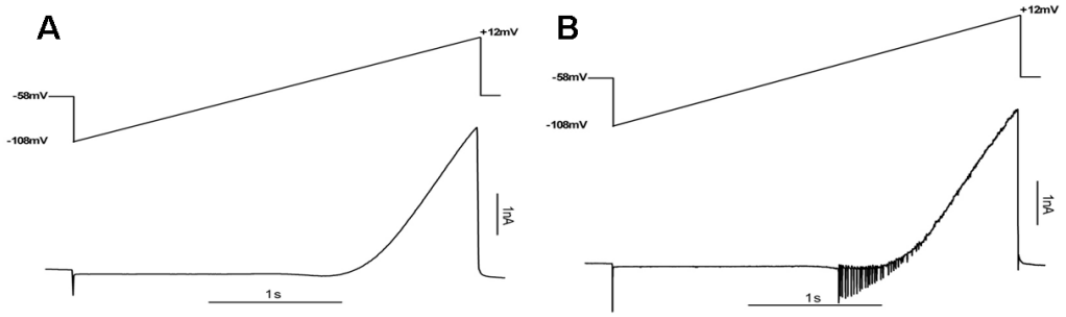

Figure 3.1: Example of successful (A) and unsuccessful (B) voltage clamp experiments. In A) voltage control was good and there were no "breakthrough" inward spikes during the depolarizing ramp-evoked current, whereas in B) voltage control was poor and many unclamped fast-activated voltage-dependent spikes occurred during the same ramp protocol. Holding potential for A and B was -58mV.

3.4. Discussion

Neuron viability is a key issue for experiments on slices of CNS tissue. The results presented here indicate ketamine-anesthesia, before euthanasia by decapitation, provides an important strategy for preserving neuron viability. Indeed, it significantly improved the success rate of our voltage clamp experiments in LC neurons. It is unlikely that the effects observed here arose through a residual ketamine effect, as it has been shown that direct application of ketamine in tissues washes out in minutes [160]. We have not evaluated if anesthesia by itself would exert similar outcomes. We chose to pre-treat

with ketamine, because of its known protective action in limiting cell damage during ischemia – reperfusion [155]. This protective action most likely arises through its well-established antagonist action of ketamine on NMDA receptors [151]. This, in combination with blockage of Na^+ and K^+ channels, probably decreases metabolic demands, caused by markedly increased neuronal firing and resultant Ca^{2+} loading, which occur during slice preparation. Such damage is likely to be reflected electrophysiologically as a decreased R_{IN}. Importantly, membrane capacitance was unchanged by ketamine (Table 3.1). This argues against a role for factors such as altered gap junction-mediated coupling between neurons. Our findings therefore provide quantitative support for using ketamine-anesthesia to improve the viability of neurons in brain slices.

3.5. Supplementary material for this chapter:

3.5.1. Results

The possibility of ketamine damaging Na^+ channels and reduces breakthrough spikes in voltage ramps was analysed by comparing action potential (AP) shapes and AP rise times from the ketamine and no ketamine group. The AP rise time were (μs) 706.4 ± 19.6 and 736.2 ± 14.4 for the ketamine and no ketamine group respectively, indicating that ketamine did not damage Na^+ channels (46 APs analysed for ketamine group and 41 APs analysed for no ketamine group; p=0.23). Supplementary Figure 3.1 further confirmed this result demonstrating no differences in the rise time of AP from both groups.

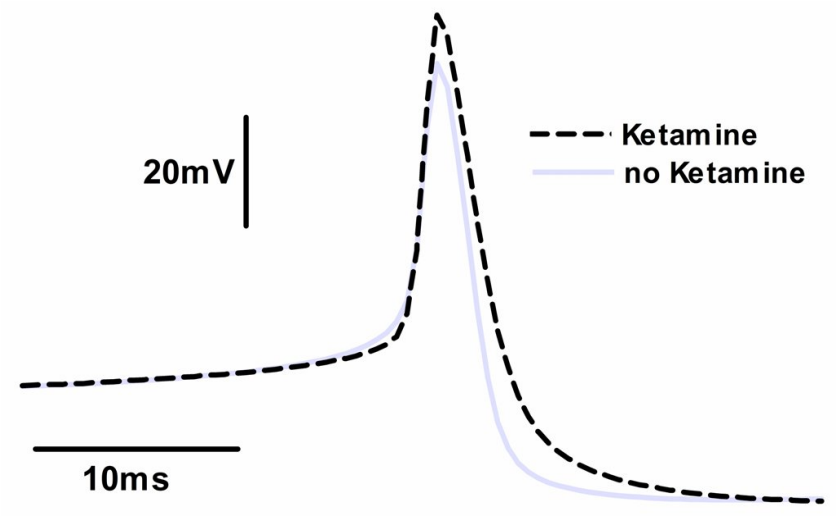

Supplementary Figure 3.1: Comparison of action potentials from Ketamine X no Ketamine group. Action potentials shown are averages of action potential sections from current clamp recordings from both groups (Ketamine = 29 and no Ketamine = 41)

Chapter 4

Pacemaker currents in mouse *Locus Coeruleus* neurons

"*Published in Neuroscience, 2010. DOI: 10.1016/j.neuroscience.2010.06.028*"

4.1. Abstract

We have characterized the currents that flow during the interspike interval in mouse LC neurons, by application of depolarizing ramps and pulses, and compared our results with information available for rats. A TTX-sensitive current was the only inward conductance active during the interspike interval; no TTX-insensitive Na^+ or oscillatory currents were detected. Ca^{2+}-free and Ba^{2+}-containing solutions failed to demonstrate a Ca^{2+} current during the interspike interval, although a Ca^{2+} current was activated at membrane potentials positive to -40 mV. A high-TEA (15 mM) sensitive current accounted for almost all the K^+ conductance during the interspike interval. Ca^{2+}-activated K^+, inward rectifier and low-TEA (10 μM) sensitive currents were not detected within the interspike interval. Comparison of these findings to those reported for neonatal rat LC neurons indicates that the pacemaker currents are similar, but not identical, in the two species with mice lacking a persistent Ca^{2+} current during the interspike interval. The net pacemaking current determined by differentiating the interspike interval from averaged action potential recordings closely matched the net ramp-induced currents obtained either under voltage clamp or after reconstructing this current from pharmacologically isolated currents. In summary, our results suggest the interspike interval pacemaker mechanism in mouse LC neurons involves a combination of a TTX-sensitive Na^+ current and a high TEA-sensitive K^+ current. In contrast with rats, a persistent Ca^{2+} current is not involved.

Key Words: electrophysiology; pacemaker currents; sodium channels; potassium channels; calcium channels; voltage clamp.

4.2. Introduction

The Locus Coeruleus (LC) is a nucleus of tightly packed spontaneously firing noradrenergic neurons located in the rostral dorsolateral pontine tegmentum [1, 2]. Behavior in animals, such as attention and behavioral flexibility [162], state of vigilance [7], environmental stimuli monitoring [8, 10], among others, are strongly controlled by LC activity, with action potential (AP) firing rate playing a central role in this process. Experiments have demonstrated that LC neurons exhibit increased firing rate in response to many stimuli, particularly those that are noxious or stressful [163-165]. In contrast, the firing rate of LC neurons is decreased in situations where animals are calm and drowsy, or in certain stages of sleep [13, 166]. The mechanisms underlying these changes have yet to be fully elucidated but a starting point is to first understand how spontaneous firing, and hence pacemaking is controlled under basal conditions.

In brainstem slices, LC neurons exhibit a complex pacemaker mechanism where different currents combine to produce slow membrane depolarization during the interspike interval. In rats the pacemaker mechanism generates spontaneous firing at frequencies ranging from 0.3-5Hz [64, 167]. Although the electrophysiological properties of LC neurons have been investigated extensively, the identity of the currents flowing during the interspike interval is still poorly understood. Early studies on rat LC indicated the interspike interval involved a combination of a persistent Ca^{2+} current, a TTX-sensitive persistent Na^{+} current and Ca^{2+}-activated K^{+} currents [94]. More recent studies now consider that pacemaking is determined, in part, by an inward non-specific cation current carried primarily by Na^{+} [37, 66, 74].

A range of channels and currents has been characterized in LC neurons, with most results obtained from rat. Inward currents involved in the interspike interval depolarization and/or AP generation include voltage-dependent fast-activating and persistent Na^+ TTX-sensitive conductances, and voltage-dependent L-, N-, P- and Q-type Ca^{2+} conductances [66, 75-77, 94]. Outward currents active during the interspike interval and/or in AP shaping include the fast transient K^+ (I_A - KCNA), sustained K^+ (I_K - KCNC), inward rectifier K^+ (GIRK 1-3), Ca^{2+}-activated K^+ (SK or KCNN 2 and 3) currents [65-67, 69, 70, 94, 168]. Labeling studies suggest other channels such as BK (i.e. KCNM) are present in LC neurons but there is no electrophysiological evidence that these channels are functional [68, 168]. The relative contribution of the above suite of channels to pacemaking is yet to be fully established, however it is clear that a number of external stimuli alter LC firing frequency by either modulating existing currents and/or recruiting others during the interspike interval [169-172].

The present study characterizes the pacemaker currents in spontaneously active mouse LC neurons under resting conditions and compares the findings to information available for the rat. Our results suggest that the currents flowing in the interspike interval of mouse and rat LC neurons have common elements, but differ in that mouse LC neurons lack a persistent Ca^{2+} current during the interspike interval.

4.3. Results

4.3.1. Electrophysiological properties of mouse LC neurons

We recorded from 138 spontaneously firing LC neurons: 118 in slices and 20 that had been mechanically isolated. The electrophysiological properties of these neurons are summarized in Table 4.1. Neurons in slices had lower input resistance and higher capacitance than isolated neurons, reflecting the loss of dendritic processes during the isolation process. In contrast, resting membrane potential, firing frequency range and AP properties did not differ in the two preparations. The isolated neurons were only used to confirm the veracity of findings made in slices under voltage clamp (see section 4.6 Supplementary Materials at the end of this chapter).

Electrophysiological Property	***LC neurons in slices (N = 118)***	***Isolated LC neurons (N = 20)***
Input resistance (MΩ)	250 ± 9.5	**374 ± 34***
Capacitance (PF)	68 ± 0.9	**40 ± 1.7***
Resting membrane potential (mV)	-54 ± 0.5	-50 ± 1.7
Firing frequency (Hz)	0.3 - 5 Hz	0.8 – 5 Hz
AP spike height (mV)	89.7 ± 1.7	84.9 ± 6
AHP amplitude (mV)	21 ± 1.3	21 ± 3.9

Table 4.1. Electrophysiological properties of fresh isolated LC neurons and neurons present in slices. * different from slice group.

Using averaged AP recordings from neurons in slices, we divided the interspike interval into three membrane potential zones (see supplementary Figure 4.1 C): *the after hyperpolarizing zone (AHP)* from -68 mV to -58 mV; *the pacemaking zone* from -58 mV to -48 mV; and *the fast channel activation zone* from -48 mV to -42 mV. Zone 1 (*AHP*) is the consequence of K^+ channel opening: including Ca^{2+}-dependent K^+ channels triggered by Ca^{2+} entry into the neuron during the repolarizing phase of the AP [173]. Zone 2 (*pacemaking zone)* is a consequence of inward and outward ionic currents, the specific combination being dependent on neuron type. Zone 3 is the threshold region where voltage-dependent channels are activated to generate an AP. The division into zones was implemented to facilitate the study of the intrinsic pacemaker currents. In the present work we focus on the second zone within the interspike interval.

4.3.2. Effect of TTX on pacemaking in LC neurons

Application of 1μM TTX abolished APs in 18 of 24 neurons tested and resulted in a depolarization of ~ 5 mV (i.e. to -48.4 ± 0.6 mV; Figure 4.1 A). The remaining 6 neurons exhibited small TTX-resistant spikes and a larger depolarization of ~ 15 mV (i.e. to -39.5 ± 3.7 mV; Figure 4.1 B). Similar TTX-resistant spikes have been reported in other CNS neurons and are thought to be generated by a mechanism that is different to the pacemaker that generates normal spontaneous neuronal firing. Their presence appears to be correlated with Ca^{2+} channels that open at more depolarized membrane potentials [174-176].

The ionic currents underlying these TTX-resistant spikes could be generated by TTX-insensitive Na^+ channels. Therefore, we recorded voltage-ramp induced membrane currents in low Na^+ solution in the presence of 1 μM TTX and found no evidence for

TTX-insensitive inward currents within the interspike interval voltage range (i.e. between zones 1 and 3; Figure 4.1 C). In contrast, the differential current (i.e. (Na^+ + TTX) – (NMDG + TTX)) exhibited a very small outward current (< 10 pA) when NaCl was replaced by NMDG (Figure 4.1 D). This small current was at the limit of our system's resolution and was not studied further. Significantly, large amplitude, long duration TTX-resistant spontaneous APs arose at depolarized potentials when ACSF containing 1 μM TTX + 15 mM TEA was rapidly applied (Figure 4.1 E, F). These APs were likely to be driven by Ca^{2+} currents, as equimolar substitution of Co^{2+} reversibly abolished this activity (Figure 4.1 E). Importantly, the pacemaker currents driving this occurred at depolarized potentials (mean: -44 ± 1 mV; n=7) and hence were unlikely to contribute to normal pacemaking (i.e. zone 2 voltage range: -58 to -48 mV).

Together, these findings demonstrate that TTX-insensitive conductances are not involved in pacemaking in the mouse LC.

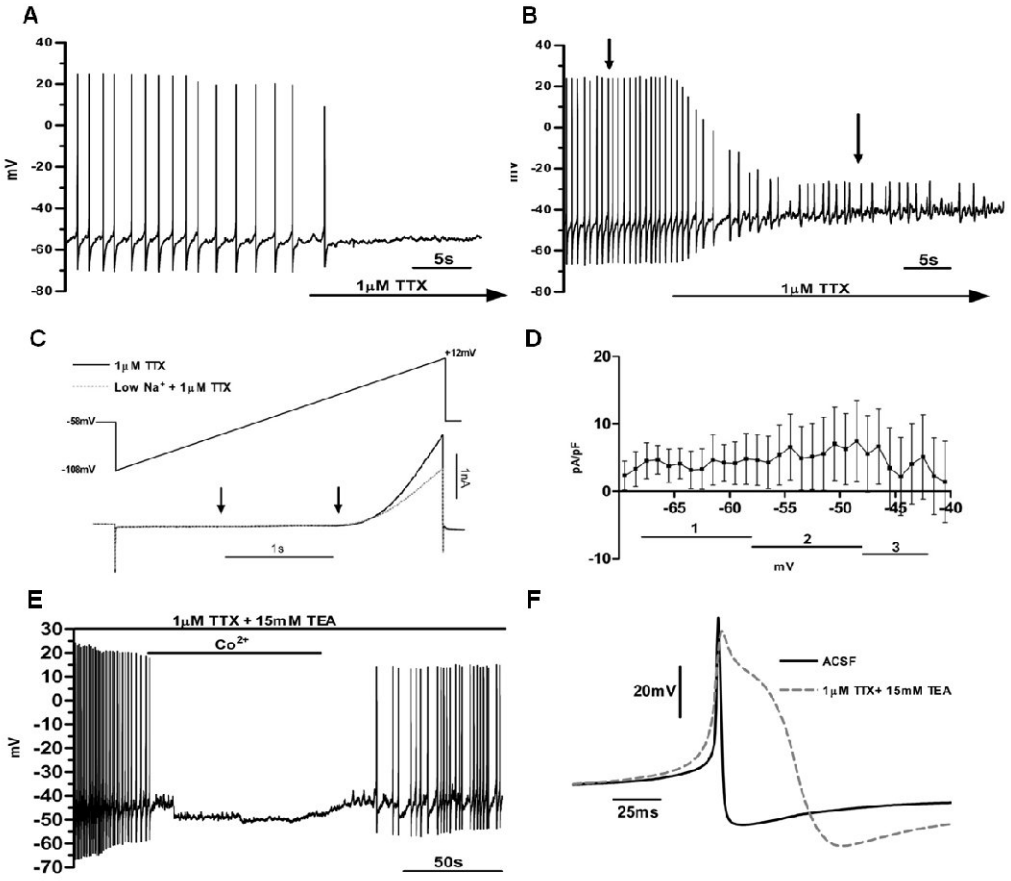

Figure 4.1. The effects of TTX. ***A***, Blockade of voltage-dependent Na^+ channels by TTX abolished APs in the majority of neurons. ***B***, A minority of neurons exhibited TTX-resistant spikes, which generated at more depolarized levels (*First arrow* Vm -48.4 ± 0.63 mV; *second arrow* Vm -39.5 ± 3.7 mV). ***C,*** Absence of TTX-insensitive currents over the interspike interval voltage range (n=14 neurons; NMDG substitution for NaCl). ***D***, Plot of differential current of *C* showing the mean ± SEM and with interspike interval zones marked. ***E***, Spontaneous TTX-insensitive APs recorded in 1 μM TTX + 15 mM TEA that were blocked in HEPES- Ca^{2+} free Co^{2+} ACSF solution and hence were Ca^{2+} channel-based APs. This pacemaker activity occurred at depolarized potentials (mean: -44 ± 1 mV; n=7), suggesting no involvement of these currents in the normal pacemaker activity occurring in zone 2. ***F***, Comparison of a Na^+

AP recorded using ACSF solutions and a Ca^{2+} AP (shown in *E*), showing the slow time course of the Ca^{2+} action potential.

4.3.3. Voltage-dependent Na^+ currents

The role of voltage-dependent Na^+ currents during the interspike interval was investigated by applying depolarizing voltage ramps in the presence of 1 μM TTX (Figure 4.2 A, B). The differential current indicates that 1 μM TTX blocked an inward Na^+ current that activated at the beginning of zone 1 (i.e. the AHP). This current increased gradually in an approximately linear fashion throughout zones 1 and 2 and then exhibited a steeper, approximately exponential, activation in zone 3 (Figure 4.2 B, E). We further investigated this TTX-sensitive Na^+ current by applying a series of depolarizing pulses over a wider voltage range. This was achieved by applying a lower concentration of TTX (35 nM), to decrease the amplitude of the Na^+ current to levels that could be adequately voltage clamped. We also used a Cs^+-based internal pipette solution in these experiments to block outward K^+ currents (see Methods). The pulse protocol and resultant differential sodium currents obtained by subtracting the currents recorded in 1 μM TTX are shown in figure 4.2 C, D at different time scales. The mean I-V plots of the differential currents obtained from voltage ramps and pulses indicates both methods reveal similar TTX-dependent Na^+ currents over the interspike interval voltage range (Figure 4.2 E, F). This voltage-dependent Na^+ current parallels the behavior of "persistent" Na^+ channels, which have been widely reported in many CNS neurons in the range -65 mV to -40 mV, and are typically activated at -55 mV [177]. These results show that an inward TTX-sensitive Na^+ current operates in the interspike interval voltage range in mouse LC neurons. Notably, the current exhibits a much steeper activation at membrane potentials positive to ~ -45 mV (zone 3).

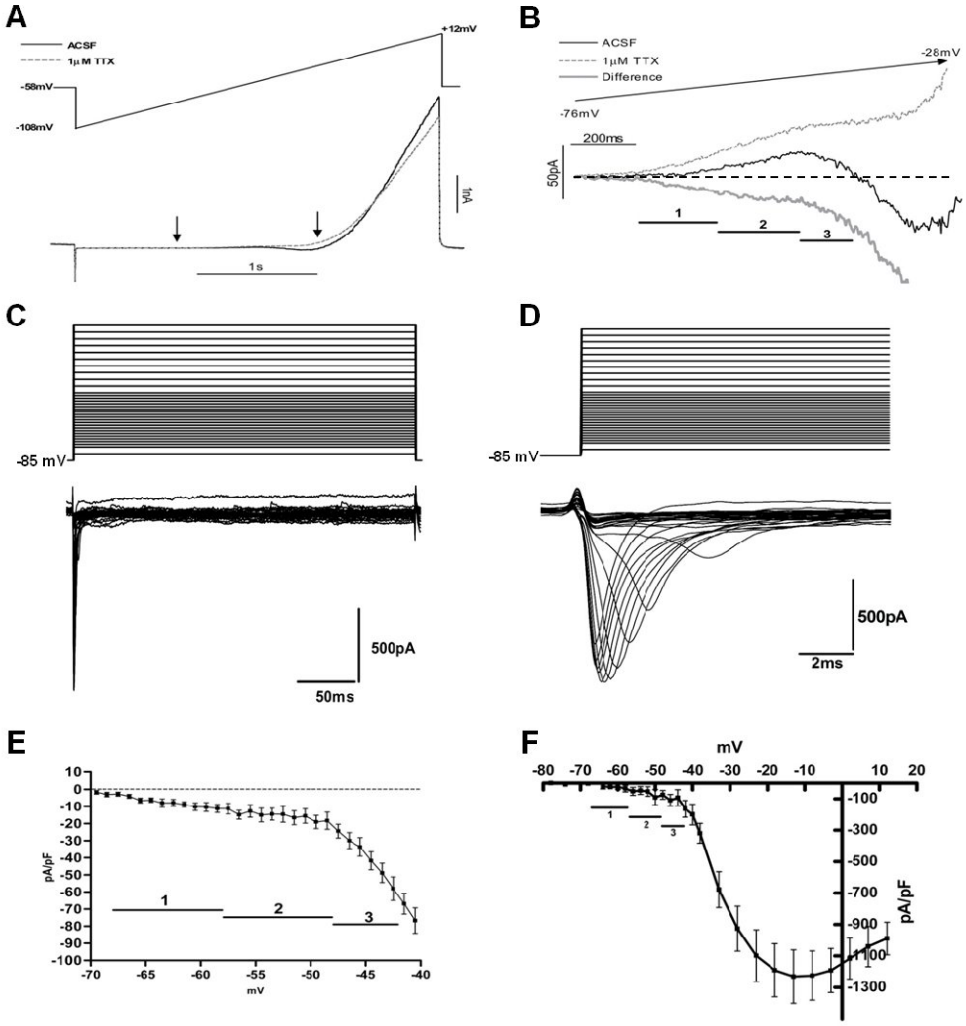

Figure 4.2. TTX-sensitive Na^+ currents evoked by depolarizing ramps and pulses. ***A,*** Average voltage ramp-evoked currents in ACSF (black line) and with ACSF + TTX (1 μM; red line; n=9; $V_{holding}$ -58 mV). ***B,*** Magnified view of the recording marked by the arrows in *A*. The grey line represents the differential Na^+ current (i.e. currents in ACSF – currents ACSF+TTX). ***C,*** Representative Na^+ currents obtained by applying depolarizing pulses from a holding potential of -85 mV using Cs^+-filled electrodes. The currents were derived by subtracting currents in Ca^{2+}-free ACSF + 35 nM TTX from currents obtained in Ca^{2+}-free ACSF + 1μM TTX for the same pulse voltages (n=6). ***D,*** Magnified view of the currents shown in ***C***. ***E*** and ***F***, I-V plots showing the differential

currents from the experiments presented in ***A*** (ramps, n=9) and ***C*** (pulses, n=6) respectively. Plots show mean ± SEM. 1, 2 and 3 represent the interspike interval zones.

4.3.4. Voltage-dependent Ca^{2+} currents

Previously, Ca^{2+} currents and Ca^{2+} channel isoforms have been characterized in rat LC neurons [75, 77] and these have been shown to be active within the interspike interval voltage range [94, 178]. Accordingly, we searched for a Ca^{2+} current in mouse LC neurons by measuring the differential current between HEPES-ACSF (+ 1 μM TTX) and HEPES-Ca^{2+}-free Co^{2+} ACSF (+ 1 μM TTX) using depolarizing ramps and pulses (Figure 4.3). Whereas, a Ca^{2+} current was elicited at membrane potentials more depolarized than ~ -40 mV, no significant Ca^{2+} current was detected over the interspike interval voltage range (i.e. -68 to -42 mV; Figure 4.3 B, E, F). The currents positive to –40 mV showed characteristics that are typical of voltage-dependent Ca^{2+} currents, exhibiting fast transient and persistent non-inactivating components (Figure 4.3 C, D). This high-threshold activated Ca^{2+} current is likely to underlie the spontaneous activity shown in figure 4.1 B and fits with reported Ca^{2+} channels in mouse LC neurons [179].

We further investigated the role that Ca^{2+} channels subserve in normal pacemaking in experiments where we added $BaCl_2$ to ACSF solution in the presence of 1 μM TTX. As barium ions generally have a higher conductance than Ca^{2+} through Ca^{2+} channels, we felt this approach might unveil a Ca^{2+} current that was not detected in the experiments outlined in Figure 4.3. These experiments provided no evidence for a Ca^{2+} current over zones 1-3 (Figure 4.4 A, B). Taken together, these results show that Ca^{2+} currents are not active in the interspike interval voltage range in mouse LC neurons. They are, however, important at more depolarized Vm where they participate in pacemaking.

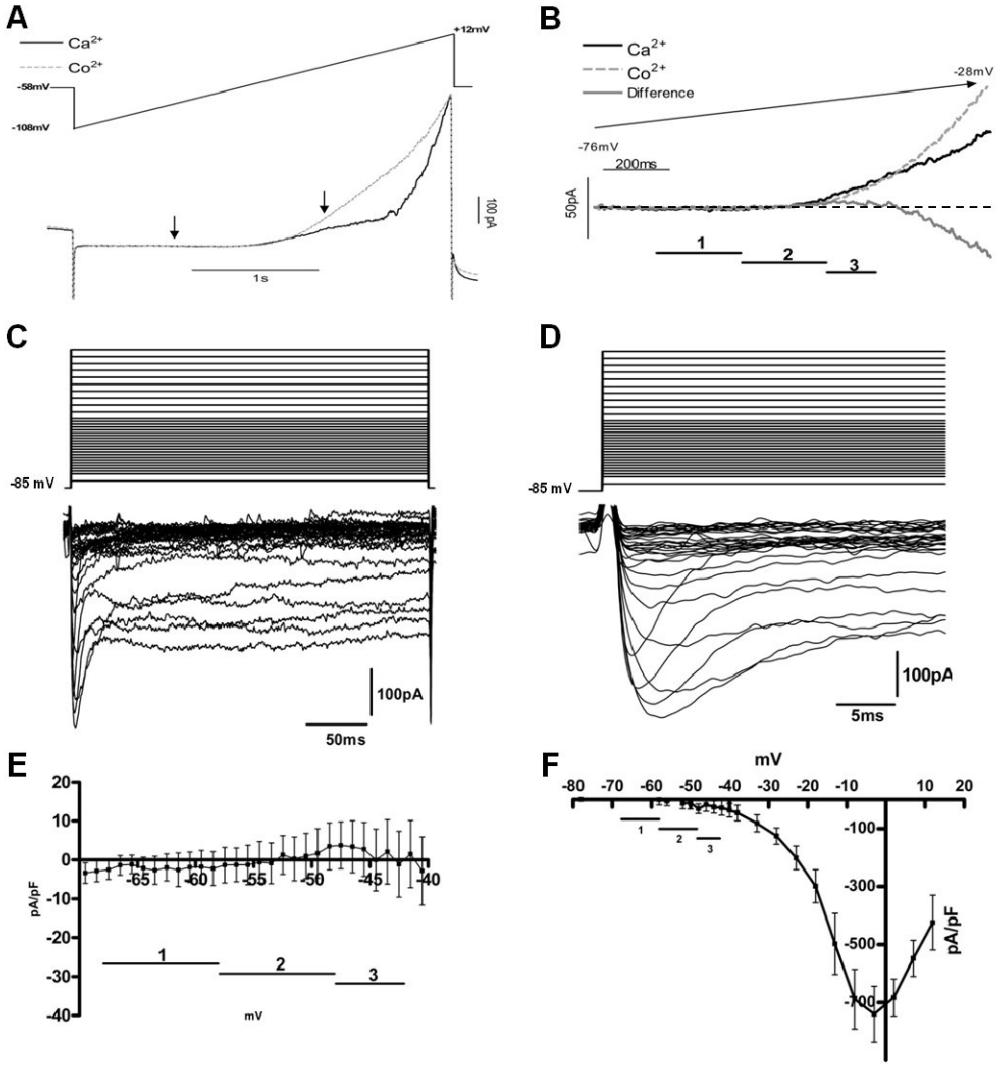

Figure 4.3. Ca^{2+} currents evoked by depolarizing ramps and pulses. ***A***, Average voltage ramp-evoked currents in Ca^{2+} solution (i.e. HEPES ACSF + 1 μM TTX + 15 mM TEA + 150 nM apamin; black line) and Co^{2+} solution (i.e. same solution except with 2 mM Co^{2+} substituted for Ca^{2+}; red line; n=11). ***B***, Magnified view of the region encompassing the interspike interval zones (marked by arrows in *A*). The difference current (Ca^{2+}– Co^{2+} solutions) plotted in grey indicates an absence of measurable Ca^{2+} current in zones 1-3; the holding potential for both experiments was -58 mV ***C,*** Representative differential Ca^{2+} current evoked by applying depolarizing pulses from a holding potential of -85 mV with recordings made using Cs^{+}-filled electrodes. The differential current was obtained by subtracting the currents recorded from pulses applied in HEPES ACSF +1 μM TTX from the corresponding currents in the same solution except that Co^{2+} is substituted for Ca^{2+} (n=9). ***D,*** Magnified view of the

currents shown in ***C***. ***E*** and ***F***, I-V plots showing the differential currents from the experiments presented in ***A*** (ramps, n=11) and ***C*** (pulses, n=9) respectively. Plots show mean ± SEM. 1, 2 and 3 represent the interspike interval zones.

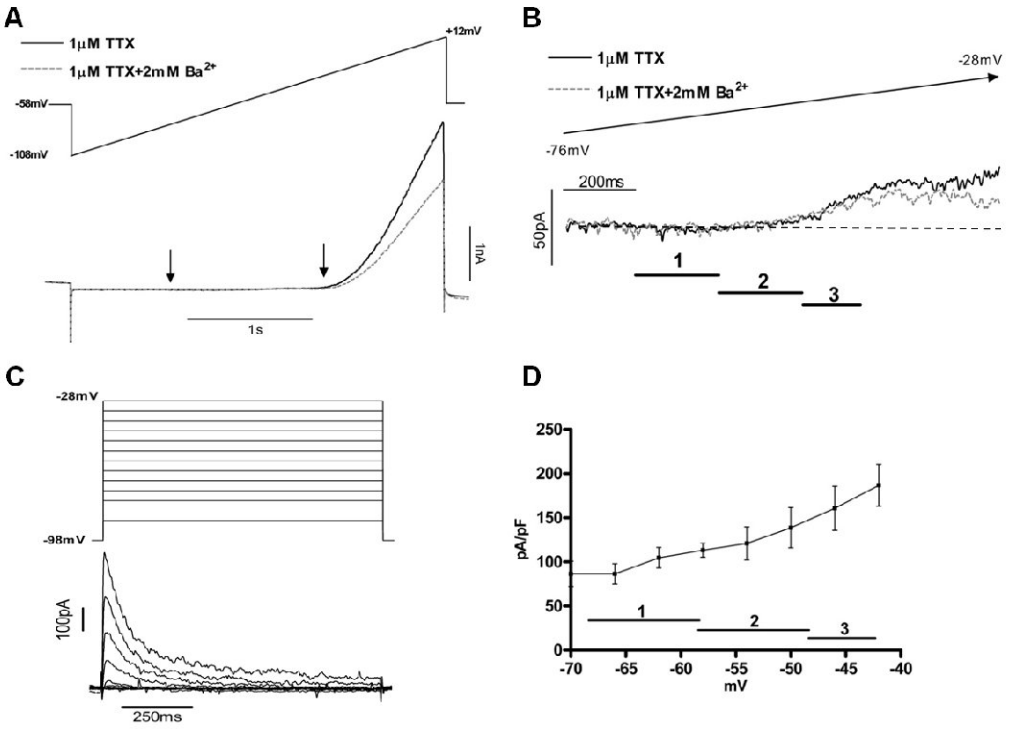

Figure 4.4. Investigation of Ca^{2+} current and a 4-AP-sensitive K^{+} current. ***A***, Average voltage ramp-evoked current in ACSF + 1 μM TTX (black line) and upon addition of 2 mM Ba^{2+} (red line) (n=10). ***B***, Magnified view of the recordings of A for the voltage range encompassing the interspike interval zones 1-3 (marked by arrows in *A*; n=10). ***C***, Effect of 1 mM 4-AP on pulse-evoked currents applied in 1 μM TTX ACSF solution – 1 μM TTX+1 mM 4-AP ACSF solution (sample record; neuron holding potential -98 mV). ***D,*** I-V graph derived from experiments of the type presented in *C* plotted over the interspike interval voltage range (n=8; mean ± SEM).

4.3.5. Voltage-dependent K^+ currents

We next investigated the effects of routinely used K^+ channel blockers on currents that were active in the interspike interval voltage range. These included 4-aminopyridine (4-AP), tetraethylammonium chloride (TEA), charybdotoxin (ChTx), apamin and Cs^+. Blockade of 4-AP-sensitive K^+ channels provided a curious result with 4-AP (1 mM) causing an apparent activation of K^+ currents during depolarizing ramps (data not shown). This phenomenon has also been reported for ramp activation in tuberomammillary nucleus neurons [180], where 4-AP increases the open time of 4-AP-sensitive K^+ channels. To avoid the contaminating effects of such channel behavior, we therefore applied depolarizing pulses when neurons were held at hyperpolarized potentials (-98 mV). This protocol revealed a large outward 4-AP-sensitive current within the interspike interval (Figure 4.4 C, D).

Due to variable sensitivity of different K^+ channels to TEA, we tested the effects of both low (10 μM) and high (15 mM) TEA concentrations (Figure 4.5). Ramp-evoked currents in ACSF and low TEA solutions did not reveal a significant differential current within the interspike interval voltage range (Figure 4.5 A, B). In contrast, application of high TEA caused a substantial inhibition of the outward current (Figure 4.5 C). Importantly, high TEA solution revealed a current within the interspike interval (Figure 4.5 D, E). Comparison of APs recorded in ACSF and high TEA solutions further demonstrated the profound impact of high TEA. AP-duration was lengthened considerably suggesting substantial participation of TEA-sensitive currents in the falling phase of the AP (Figure 4.5 F).

Cs^+, ChTx, apamin were also tested to evaluate the role of Ca^{2+}-activated K^+ channels (B_K, I_K and S_K) and inward K^+ rectifier channels, respectively, during the

interspike interval. No significant current within the interspike interval voltage range was revealed (data not shown).

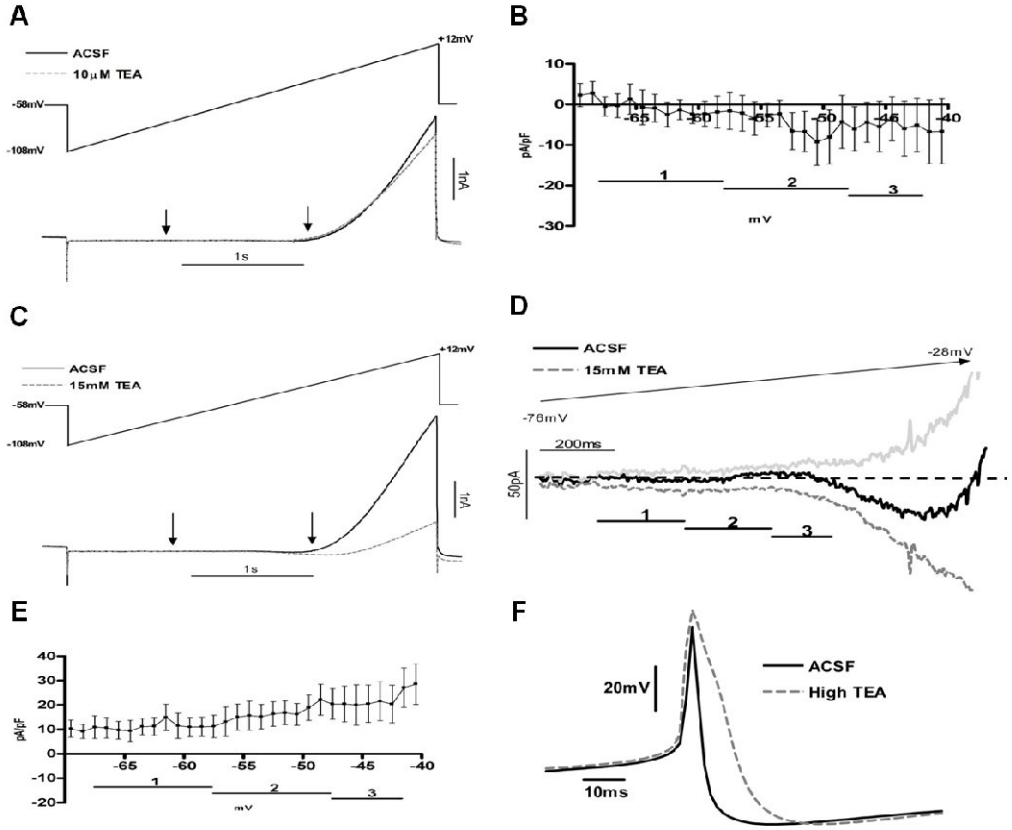

Figure 4.5. Effect of TEA on ramp-evoked currents. ***A***, Representative recording showing average ramp-evoked currents in ACSF (black line) and upon addition of 10 μM TEA (red line). ***B***, I-V plot showing the differential current obtained for the experiment presented in *A*, demonstrating an absence of low TEA sensitive currents in the interspike interval (n=8; mean ± SEM). ***C-F*****,** Effect of 15 mM TEA on ramp-evoked currents and AP shape: ***C,*** Average voltage ramp-evoked currents in ACSF (black line) and ACSF + 15 mM TEA (red line). ***D,*** Magnified view of currents during the interspike interval zones (marked by arrows in *C*). The differential current (control-(ACSF+TEA)) is included (grey line; n=9) and is also shown as in **E** as a point plot showing the means ± SEM. ***F,*** AP comparison in ACSF (black) and 15 mM TEA (red) solutions. The high TEA solution increased the AP width two-fold. APs shown represent an average of 60-70 APs.

4.3.4. Comparison of predicted and experimental voltage ramp-induced currents

The approach used here to assess net current flow during the interspike interval voltage range is based on a recent report characterizing interspike interval currents in spontaneously active neurons in the ventral tegmental area [150]. The analysis is based on averaging AP recordings to obtain a mean interspike interval (see Methods). The derivative of the mean interspike interval reflects the net pacemaker current. The average firing frequency for LC neurons in slices recorded in the present work was ~ 2 Hz. Based on this, AP recordings were averaged and differentiated (Figure 4.6 A, B). The net ionic current calculated using the mean capacitance of 68 pF (Table 4.1) was very small (i.e. < 1 pA), inward and of relatively constant amplitude during zone 2 of the interspike interval. Importantly, this current matched the voltage ramp-induced current recorded in ACSF (Figure 4.6 C) and the net current obtained by addition of the pharmacologically isolated TTX-sensitive current and the high TEA-sensitive current (Figure 4.6 D). These data confirm that pacemaking only requires a small net inward current to drive rhythmic firing in LC neurons.

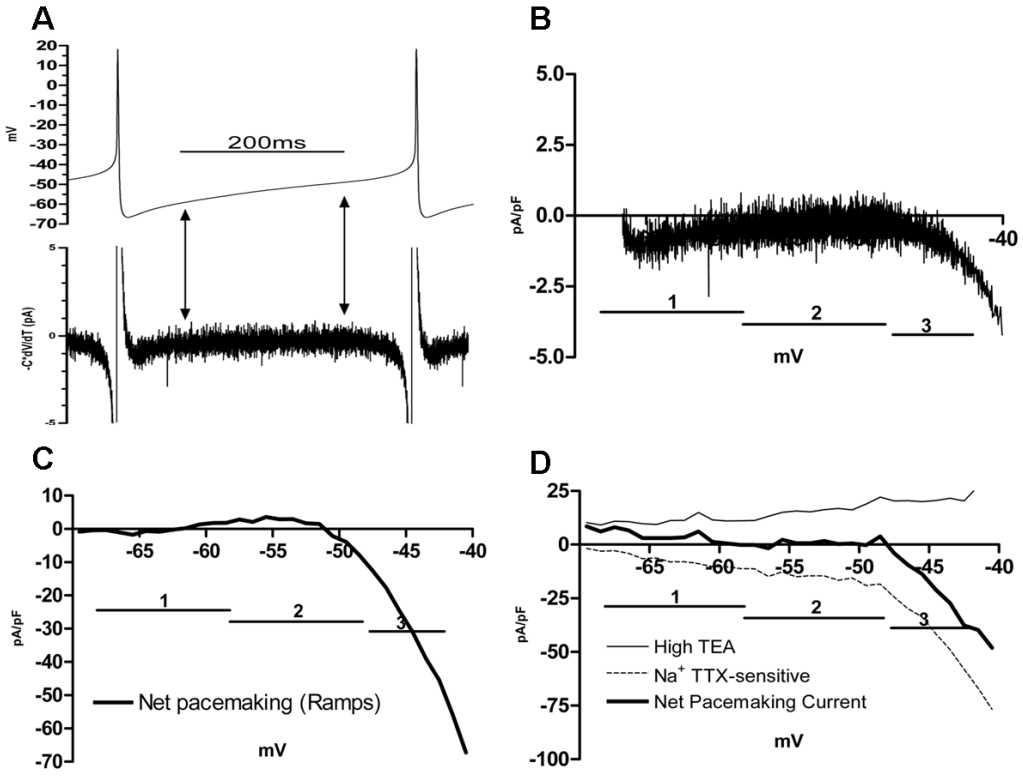

Figure 4.6. Net pacemaking current in mouse LC neurons. ***A***, Net pacemaking current calculated by differentiating the average of AP recordings (-C*dV/dt). ***B***, The current of ***A*** *filtered* and shown on a magnified scale. ***C***, The voltage ramp-evoked current obtained under control conditions (ACSF) shown for the interspike interval voltage range (zones 1-3). ***D***, The net voltage ramp-evoked current obtained by addition of the net inward current carried by TTX-sensitive Na^+ channels (current in ACSF – (ACSF + 1 μM TTX)) and the total outward current

4.5. Discussion

In the present study we have used depolarizing ramps to mimic the depolarization that occurs during the interspike interval voltage range (i.e. -68 to -42 mV) of

spontaneously firing mouse LC neurons. We also applied depolarizing pulses that altered membrane potential over a broader range so we could compare our electrophysiological data on LC neurons in the literature, as has primarily been presented for the rat.

The inhibition of APs by TTX (Figure 4.1 A), confirms the importance of TTX-sensitive voltage-dependent channels in AP generation and/or pacemaking. Direct evidence for a role of these channels in generation of the pacemaker current was provided by the presence of a TTX-sensitive inward current during the interspike interval. This current was activated during zone 1 (i.e. -68 to -58 mV) and increased approximately linearly during zone 2 (i.e. -58 to -48 mV) and then increased steeply during zone 3 (i.e. -48 to -42 mV; Figure 4.2). This behavior has been described for a range of neurons, where Na^+ channels are responsible for producing subthreshold and fast-activating currents [81, 181, 182]. In this respect mouse and rat are alike, as it has been known sometime that a TTX-sensitive Na^+ current, evoked over a similar voltage range, is present in rat LC neurons [94].

In some neurons, TTX did not completely block spiking activity (Figure 4.1 B). This TTX-resistant activity could suggest the involvement of other conductances within the interspike interval including TTX-insensitive Na^+ channels or voltage-dependent Ca^{2+} channels. The possible participation of a TTX-insensitive Na^+ current in the interspike interval seems unlikely, as experiments using low Na^+ solution together with TTX did not reveal a significant TTX-insensitive current (Figure 4.1 C, D). In rats, a Na^+-dependent TTX-insensitive current has been reported to be activated in the presence of opiates and during activation of orexin receptors [66, 183]. We therefore cannot rule out the presence of TTX-insensitive currents that modulate mouse LC pacemaking, as these

would require stimuli or circumstance other than the conditions used in our study. In contrast, voltage dependent Ca^{2+}conductances were demonstrated to be responsible for the TTX-resistant spiking activity, as they were reversibly inhibited by substitution of Ca^{2+} with Co^{2+} (Figure 4.1 E). However, our results in mice show that TTX-resistant spikes are not common in LC neurons (age 7 – 12 days), with less then 20% of neurons exhibiting this activity. Significantly, when TTX-resistant spikes were observed they were associated with membrane depolarization of ~ 9 mV. Such spiking behavior has been observed in other neuronal types where application of TTX caused depolarization and onset of neuronal firing not associated with normal pacemaking [174-176].

Studies on rat LC have also reported Ca^{2+} currents and suggested they contribute to pacemaking in LC neurons [22, 75, 94]. These currents were not observed in mouse LC neurons and this represents the greatest difference in electrophysiological properties between the two species (Figures 4.3, 4.4 A and B). Our results, however, show that Ca^{2+} currents were activated at more depolarized membrane potentials (> - 40 mV), as occur during the rising phase of the AP, but not during the pacemaker-depolarizing phase (i.e. -68 to -42 mV). Importantly, we found no evidence for T-type Ca^{2+} current even though we used a pulse voltage protocol designed specially to activate this channel subtype, which activates in more hyperpolarized membrane potentials and is a candidate pacemaker current (Figure 4.3). In contrast, we found evidence for such a current in rat LC neurons using the same pulse protocol and experimental conditions. In these experiments a Ca^{2+} inward current became active at ~ -55 mV, which is well within the interspike interval voltage range (see supplementary Figure 4.3). This result rules out methodological constraints and demonstrates that the membrane potential where Ca^{2+} conductances become active differs significantly in mouse and rat (~ -40 mV and ~ -55 mV respectively). A lack of a "persistent" Ca^{2+} current in mice may therefore affect

other Ca^{2+}-dependent pathways during normal pacemaking. Thus this Ca^{2+}-dependent mechanism could underlie the observation that rat LC exhibits relatively more frequent TTX-resistant spikes and subthreshold membrane oscillations than mice of the same age.

Due to the great variety of K^+ conductances and their specific activation kinetics and blockers, we studied K^+ conductances activated over the LC neuron pacemaker voltage range using broad-spectrum blockers that target certain classes of K^+ channels. Mouse LC neurons retain the same basic group of K^+ currents as reported for rat, having 4-AP and TEA-sensitive components. TEA at a high concentration (15 mM) is reported to block K_V1.1-5, K_V3.1-3 and some K_{Ca} (e.g. BK but not SK) channels [184]; these channels include key channels also blocked by 4-AP, including the A current (i.e. K_V1.4). Consistent with this, we found that TEA (15 mM) blocked the majority of outward currents activated by depolarizing ramps over the entire voltage range, including the pacemaker zones (Figure 4.5 C-E). Another important channel blocked by high TEA and Charybdotoxin (ChTx) is the BK channel. Involvement of BK, IK and SK channels were analyzed by applying depolarizing ramps and a combination of blockers (i.e. ChTx + apamin) (data not show). However, none of these currents were detected to function during the interspike interval voltage range. This result is consistent with reports in rat LC neurons, where the AHP exhibited two components (early and slow), with both being Ca^{2+}-dependent but insensitive to ChTx [168]. High TEA solution also had a strong effect on the falling phase of the action potential, increasing its width from ~6 ms to 13 ms (Figure 4.5 F). Thus K^+ channels activated during the AP are also likely to impact on pacemaking. When TEA was applied at low concentrations (10 μM), we found no evidence for a low TEA-sensitive current during the interspike

interval voltage range in mouse LC (Figure 4.5 A, B). In contrast, low TEA solution has been shown to block a persistent K^+ current ($K_V3.1$-3) in rat LC neurons [66]).

In the present paper, we found that application of square pulses from a negative holding potential (~ -100 mV) revealed a large 4-AP-senstive current (Figure 4.4 C, D). This result parallels findings in rat LC neurons, where 4-AP blocks a transient K^+ current (I_A), which is active in the interspike interval voltage range [185]. However, our method of inducing this current from a large negative holding potential would exaggerate the magnitude of the current, which is normally activated at more depolarized potentials by the much slower depolarizations that occur during pacemaking. Nevertheless, I_A will form part of the main 4-AP-sensitive current, as we demonstrated its presence using high TEA solution (Figure 4.5 C-F). A role for inward rectifier K^+ current (K_{IR}) was also investigated by using CsCl in the external solution (ACSF), providing no evidence for this current during application of voltage ramps (data not shown). In summary, the K^+ conductances that act in the interspike interval of mouse LC neurons are likely to be from $K_V1.1$-5 family.

An alternative method for measuring net pacemaker current is to differentiate the average of pairs of consecutive APs and obtain a profile of the net current that is activated during the interspike interval [150]. In our hands, the net current obtained by this procedure was similar to the currents revealed by voltage ramps, in either ACSF or by summing the pharmacologically isolated Na^+ and K^+ currents (Figure 4.6 A-D). Major differences between the currents obtained via the two methods emerge at membrane potentials positive to -48 mV (i.e. zone 3). The reason for this is that this region (zone 3) is highly sensitive to depolarization with some neurons showing significant activation of fast voltage dependent Na channels. Thus, the average of the

currents shows a much larger inward current in zone 3 than for the APs that are averaged based on aligning the AP rising phase. The result obtained over zones 1 & 2 indicates that the two methods produce similar outcomes.

In summary, we have found that a TTX-sensitive Na^+ current is the only inward conductance and a high TEA-sensitive K^+ conductance, probably composed of $K_V1.1$-5 channels, act to provide pacemaker depolarization and consequent threshold for AP generation. We also found that pacemaking in the neonatal mouse is similar but not identical to rat LC, with mice lacking a Ca^{2+} conductance during the pacemaker depolarization.

4.6. Supplementary material for this chapter:

4.6.1. Results

4.6.1.1. Identification of LC neurons in slices

To confirm identify and location of LC neurons we performed immunohistochemistry using an antibody against tyrosine hydroxylase (TH), a standard enzyme marker for noradrenergic neurons [20]. Supplementary Figures 4.1 A and B show the immuno-positive cells for TH, where the LC nucleus is clearly visible being a reasonably circumscribed and compact group of noradrenergic neurons. These observations parallel previous reports that identified LC morphology in rats and mice [1, 20, 186].

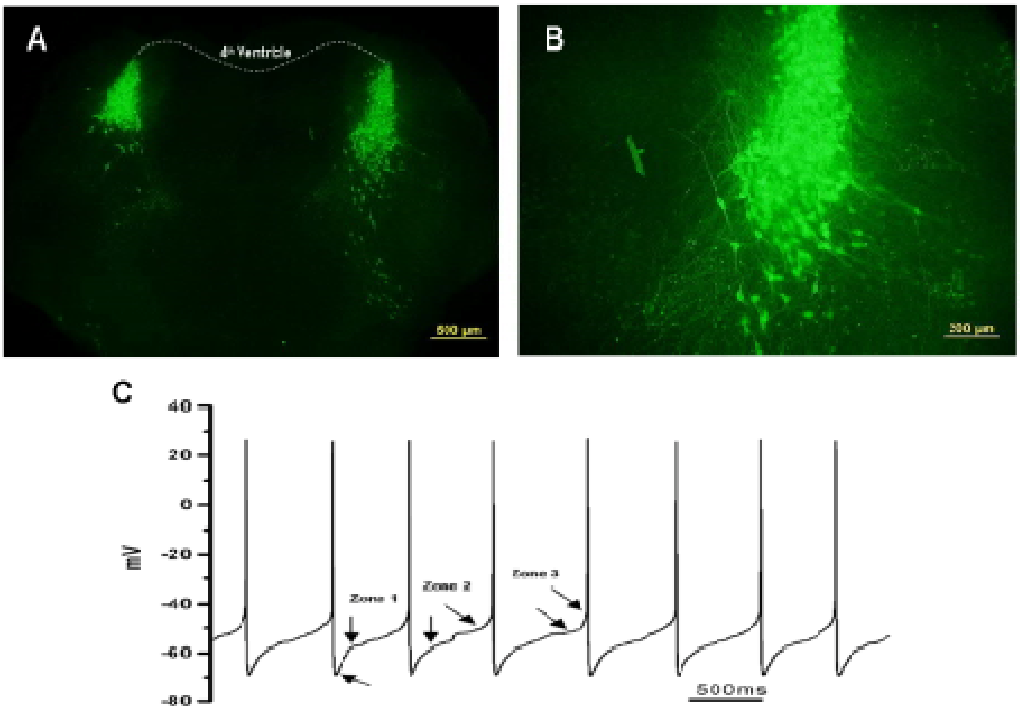

Supplementary Figure 4.1. TH-positive immunohistochemistry and neuronal action potentials (APs) recorded from the LC. **A**, Transverse section of the pons showing TH-positive LC neurons. Note the LC structure appears as two groups of neurons below the ventrolateral border of the 4th ventricle. **B**, Higher magnification of the left LC structure showing tightly packed multipolar neurons. **C**, Action potential recording showing the zones into which the interspike interval region has been divided: Zone 1) After hyperpolarizing zone (AHP) from -68 mV to -58 mV; Zone 2) Pacemaking zone from -58 mV to -48 mV; and Zone 3) Fast channel activation zone from -48 mV to -42 mV.

4.6.1.2. Voltage-dependent currents in isolated LC neurons

Characterization of the currents activated within the interspike interval depends on good voltage control of LC neurons. We further assessed the quality of our recordings using freshly isolated neurons. Due to their preparation, these cells have truncated processes and therefore simplified electrical properties, more like that of a spherical cell and hence are theoretically better for voltage clamping. Isolated neurons were still spontaneously active exhibiting activity that paralleled the behaviour of LC neurons in slices including the blocking action of 1μM TTX (supplementary Figure 4.2 A). Importantly, application of a ramp for voltages encompassed during the interspike interval (i.e. -68 - -42 mV) produced currents that were very similar, if not identical to neuronal recordings in slices with an inward TTX-sensitive Na^+ current (supplementary Figure 4.2 B), an outward K^+ current (supplementary Figure 4.2 C), and no evidence for a Ca^{2+} current (supplementary Figure 4.2 D). These data indicate that depolarizing voltage ramps applied within the interspike voltage range in mouse slice LC neurons were reliably voltage clamped. The findings are consistent with those reported for rat LC neurons with freshly dissociated rat LC neurons exhibiting the same basic properties as those recorded in slices [77, 187-189]

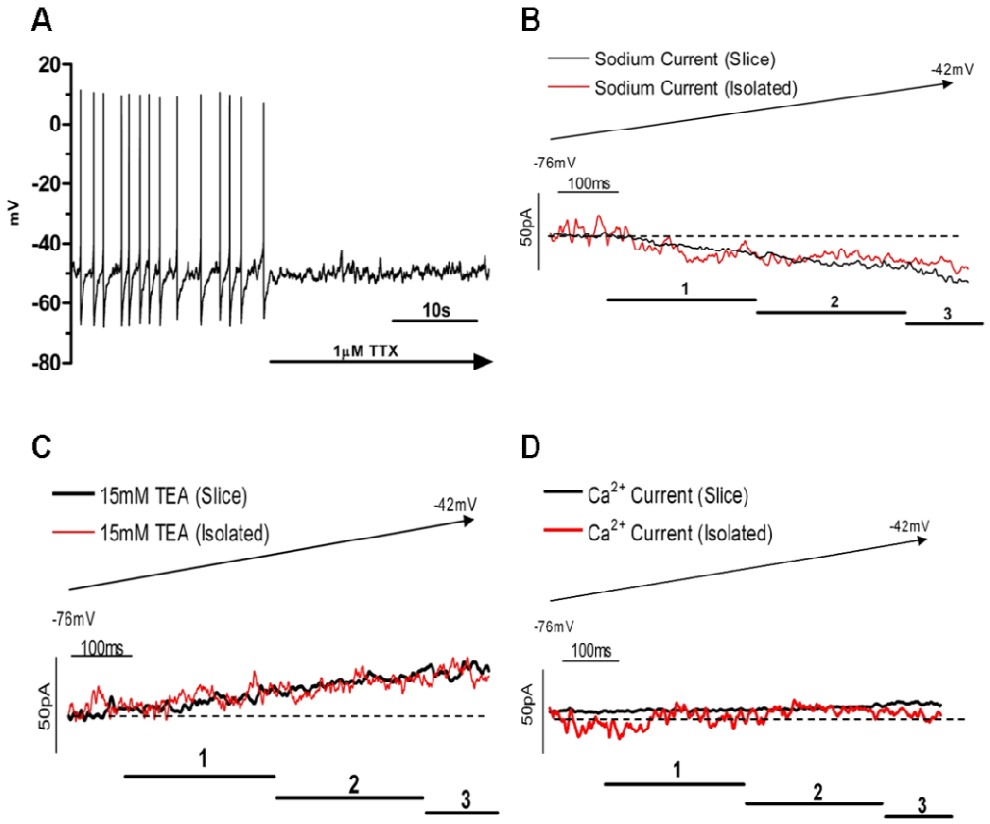

Supplementary Figure 4.2. Na^+, Ca^{2+} and K^+ currents in isolated LC neurons. ***A***, Effect of 1 µM TTX on pacemaking in an isolated neuron. Parts ***B-D*** provide a comparison between recordings from slices and isolated cells presenting plots of the average differential voltage ramp current (control – treatment) over the interspike interval voltage range zones. All experiments in isolated cells were made under the same conditions as for slice recordings. ***B,*** Average voltage ramp-evoked difference currents (in ACSF – (ACSF + 1 µM TTX)) for slice (black; n=9) and isolated (red; n=5) neurons. ***C,*** Voltage ramp-evoked difference currents in control solution (ACSF) – 15mM TEA solution (ACSF +15 mM TEA) for slice (black; n=8) and isolated (red; n=5) neurons. ***D,*** Average voltage ramp-evoked difference currents (in ACSF-Hepes solution + 1 µM TTX + 15 mM TEA + 150 nM Apamin) - Co^{2+} solution (same solution but with 2 mM Co^{2+} substituted for Ca^{2+}) for slice (black; n=11) and isolated (red; n=5) neurons

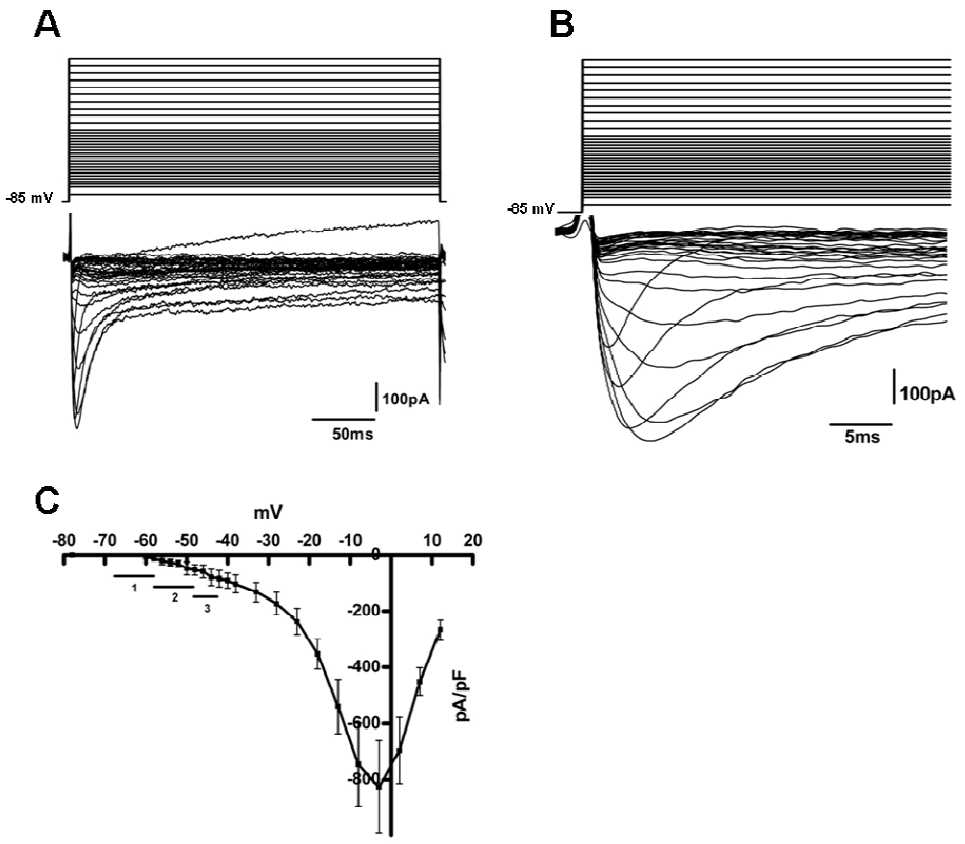

Supplementary Figure 4.3. Ca^{2+} currents evoked by depolarizing pulses in rats. The experiments shown here were performed exactly with the same protocol performed for mice. We used rats in the same age range used for mice. ***A,*** Representative differential Ca^{2+} current evoked by depolarizing pulses from a holding potential of -85mV using Cs^{+}-filled electrodes. The differential current was obtained by subtracting the currents recoded from pulses applied in Ca^{2+}-Hepes containing 1µM TTX – Co^{2+}-Hepes also containing 1µM TTX (n=6). ***B,*** Magnified view of the currents shown in ***A***. ***C***, I-V plots showing the differential current for the experiment presented in ***A*** (n=6). Plots show mean ± SEM. 1, 2 and 3 represent the interspike interval zones.

Chapter 5

Developmental changes in pacemaker currents in mouse locus coeruleus neurons

5.1. Abstract

The present study compares the electrophysiological properties and the currents that flow during the interspike interval in locus coeruleus (LC) neurons from infant (P7-12 day) and young adult (8-12 week) mice. The magnitude of the primary pacemaker currents, which flow during the interspike interval, increased in parallel during development. These pacemaker currents consist of an inhibitory voltage-dependent K^+ current and an excitatory TTX-sensitive Na^+ current. We found no evidence for the involvement of I_H or Ca^{2+} currents in pacemaking in infant or adult LC neurons. The incidence of TTX-resistant spikes, observed during current clamp recordings, was greater in adult neurons. Neurons from adult animals also showed an increase in voltage fluctuations, during the interspike interval, as revealed in the presence of 1 mM 4-AP. In summary, our results suggest that mouse LC neurons undergo changes in basic electrophysiological properties during development that influence pacemaking and hence spontaneous firing in LC neurons.

Key Words: pacemaker current; development; electrophysiology; sodium channel; potassium channel; calcium channel; voltage clamp; locus coeruleus.

5.2. Introduction

The locus coeruleus (LC) nucleus is located in the brainstem and contains spontaneously active noradrenergic neurons [1, 2]. This important nucleus is a major

site of noradrenaline production [190, 191] and controls several brain functions such as sleep regulation and vigilance [192, 193], monitoring of environmental stimuli [8, 10] and behaviour related to calm or stressful situations [13, 163-165]. We have recently characterized the currents responsible for driving pacemaking (spontaneous activity) in LC neurons in infant mice (P7-12) and found that depolarization, within the interspike interval, is driven by two major currents: a TTX-sensitive Na^+ current and a high TEA-sensitive K^+ current [194].

Even though the electrophysiological properties of LC neurons have been studied for decades there is no information on the development of pacemaker currents in this important neuron population. In contrast, such studies have been made on currents in other tyrosine hydroxylase-containing neurons, namely dopaminergic neurons in the mid brain and substantia nigra, which have been shown to change during development [138, 139]. LC neurons have been reported to exhibit developmental changes in electrical activity [144, 195], axonal branching [141], projections to other brain regions [142] and in low threshold responses in their terminals [140]. In addition, excitatory convergence on LC neurons is reduced in the aging brain [196], and LC neurons from aging brain exhibit a decrease in excitatory-related genes [197]. It has also been suggested that LC neuronal dysfunction increases the susceptibility of the aging brain to Parkinson's and Alzheimer's disease [24, 198, 199]. Thus, there is a significant body of evidence to suggest LC neurons undergo anatomical and electrical changes during development, which could impact on functions such as pacemaking and intercellular communication.

Here we compare the electrophysiological properties and pacemaker currents in LC neurons in brainstem slices from infant (7-12 days old) and adult (8-12 weeks old) mice.

Our results indicate that mouse LC neurons undergo changes in the two major currents that underlie pacemaking in these neurons (i.e. Na^+ and K^+ currents) over the ages tested.

5.3. Results

5.3.1. Electrophysiological properties of LC neurons from infant and adult mice

We first compared selected electrophysiological properties of LC neurons from infant (P7-12 day) and young adult (8-12 week) mice. Several of these properties changed over the developmental period examined. In particular, the proportion of neurons exhibiting spontaneous firing decreased (from ~90% to 50% of the sample; n = 96 and 33 for infant and adult mice, respectively) and the resting membrane potential was significantly different (from -54.1 ± 0.5 mV, n=26 to -60.7 ± 1.9 mV, n=33). The firing frequency of spontaneously active infant and adult LC neurons was not significantly different (infant: 2.0 ± 0.4 Hz, n=26; adult: 2.4 ± 0.4, n=18). The input resistance and membrane capacitance of 96 infant and 33 adult LC neurons were not significantly different (244 ± 10 and 283 ± 18 MΩ; 72.7 ±1.0 and 71.2 ± 1.9 pF, respectively). Electrode series resistance after achieving whole cell configuration was 4.6 ± 0.1 MΩ (infant, n=96) and 4.0 ± 0.1 MΩ (adult, n=33).

As thin slices (140 μm) were used to improve visualisation of neurons in adult slices, it is possible that the quiescent (not spontaneously firing) neurons present in slices were a consequence of damage and this could be consistent with the lower membrane

potential of -68 ± 2 mV (n=15) exhibited by this group compared to -55 ± 2 mV (n=18) for the spontaneously active group of neurons. However, if so this was not obviously evident by comparison the input resistance of quiescent compared to spontaneously active adult LC neurons, which were not significantly different (291 ± 26 MΩ, n=15 compared to 265 ± 18 MΩ, n=18 respectively). The quiescent cells also exhibited robust and persistent action potentials upon depolarization, activity that was indistinguishable to that of spontaneously active neurons.

Studies were also made on LC neurons in the presence of TTX. Input resistance and membrane capacitance of 33 infant and 22 adult LC neurons in 1 μM TTX were not significantly different (294 ± 22 and 248 ± 14 MΩ and 63 ± 2 and 70 ± 2 pF, respectively). The incidence of TTX-resistant spikes, observed during current clamp recordings, was greater in adult neurons (~17% vs. 65%; n = 14 and 12 for infant and adult mice, respectively).

Application of depolarizing voltage ramps showed the net current evoked in ACSF was larger in adult neurons (Figure 5.1 A-B). Previously we have characterized the currents flowing during the interspike interval (i.e., membrane potential range -68 mV to -42 mV) in spontaneously active LC neurons in infant animals [194]. We therefore compared these currents in infant and adult mice even though only 50% of adult neurons were spontaneously active (see above). These comparisons for net current are illustrated in Figure 5.1 C and show that the outward current flowing during the interspike interval is larger in adult neurons at membrane potentials greater than ~ -46 mV. Comparison of action potentials from neurons that were spontaneously active and fired at similar frequencies (~ 2 Hz) indicated the AHP was larger in neurons from adult mice (Fig. 5.1 D).

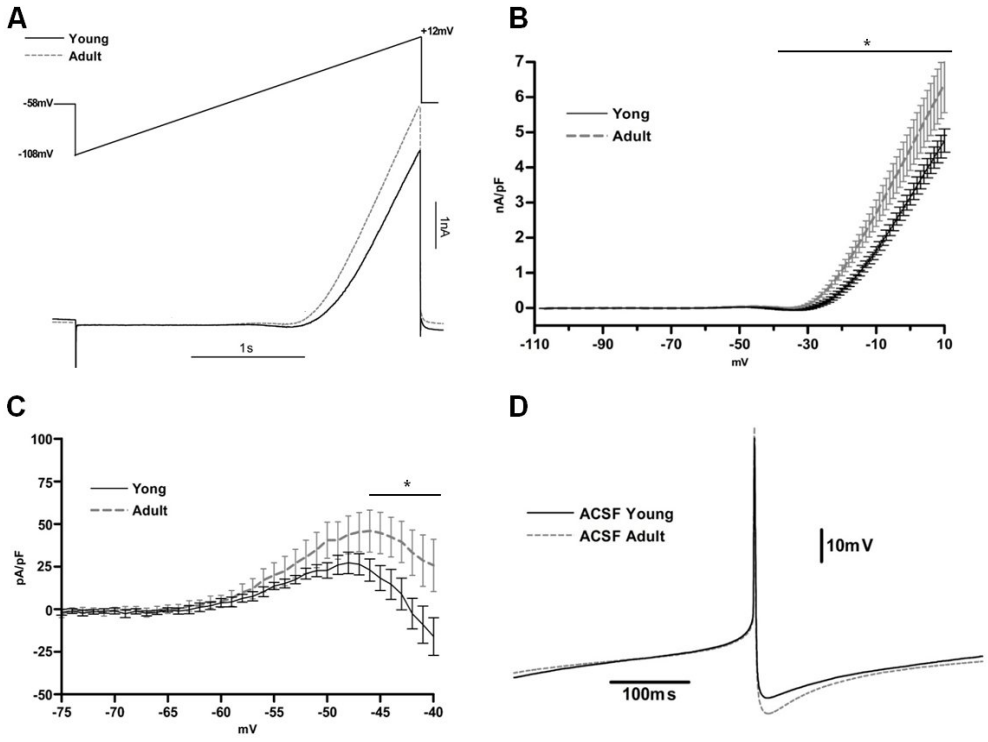

Figure 5.1: Age-related differences in current–voltage relationships and action potentials in LC neurons. *A,* Averaged voltage ramp-evoked currents (lower traces) recorded from LC neurons (holding potential -58 mV; n=10 for infant and adult mice) after application of the voltage protocol shown above. Slices were bathed in ACSF. *B,* Mean current–voltage relationships constructed from data in A after each individual current response was normalized to cell size (based on capacitance measurements and expressed in nA/pF). *C,* Magnified view of the current–voltage relationship of B over the membrane potential range corresponding to the interspike interval (-68 to -42 mV). Note, there are age-related differences between the current–voltage relationships at Vm more depolarized than ~ -46 mV. *D,* Overlay of representative action potentials from an infant and adult mouse showing larger after-hyperpolarization in adult neurons. Asterisks over horizontal bars in B and C indicate significant difference in data points ($p<0.05$). Data are shown as mean ± SEM.

5.3.2. Outward currents in infant and adult mice

The basis of the increase in outward current observed during development was further investigated by including various combinations of TTX (1 μM) and broad-spectrum K^+ channel blockers in the bath and rapid exchange-perfusion solutions (Figure 5.2). Under these conditions "total" K^+ current was greater in adult neurons (Figure 5.2 A, B), with the difference becoming significant when Vm was more positive than ~ -42 mV (Figure 5.2 C).

We next examined the effect of 4-AP on spontaneous firing (Figure 5.3). Application of 1 mM 4-AP increased firing rate in both infant and adult neurons (Figure 5.3 A, B). There was also a substantial increase in membrane voltage noise during the interspike interval in adult neurons which often appeared as discrete events such as might be caused by spontaneous transmitter release (Figure 5.3 C, D). When quantified (as events/s in ACSF vs. ACSF containing 1mM 4-AP) the increase in such activity was clearly greater in adult neurons (0.77 ± 0.28 to 3.02 ± 0.70 events/s for infant, and 1.13 ± 0.20 to 5.53 ± 0.45 events/s for adults; $n = 6$ both ages, $p < 0.05$).

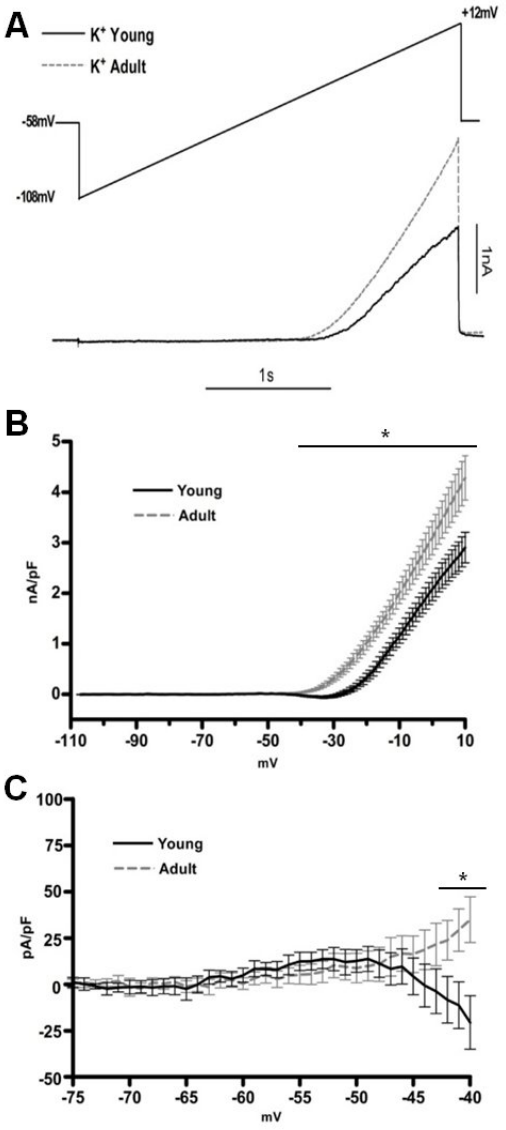

Figure 5.2: Age-related differences in "total" K^+ current evoked by depolarizing ramps in LC neurons. ***A,*** Averaged differential TEA/Apamin-sensitive currents determined by recording responses in the presence of 1 μM TTX and subtracting corresponding records obtained in the presence of 1 μM TTX + 15 mM TEA + 150 nM Apamin (n=11 and 9 neurons for infant and adult mice respectively). ***B,*** Mean current–voltage relationship constructed from the differential currents obtained in **A**. ***C,*** Magnified view over the interspike interval voltage range demonstrating that the differential currents became significantly different at Vm positive to ~ -42 mV. Graphs **B** and **C** show mean ± SEM; Asterisks over bars indicate regions where there are significant age-related differences between data points ($p<0.05$).

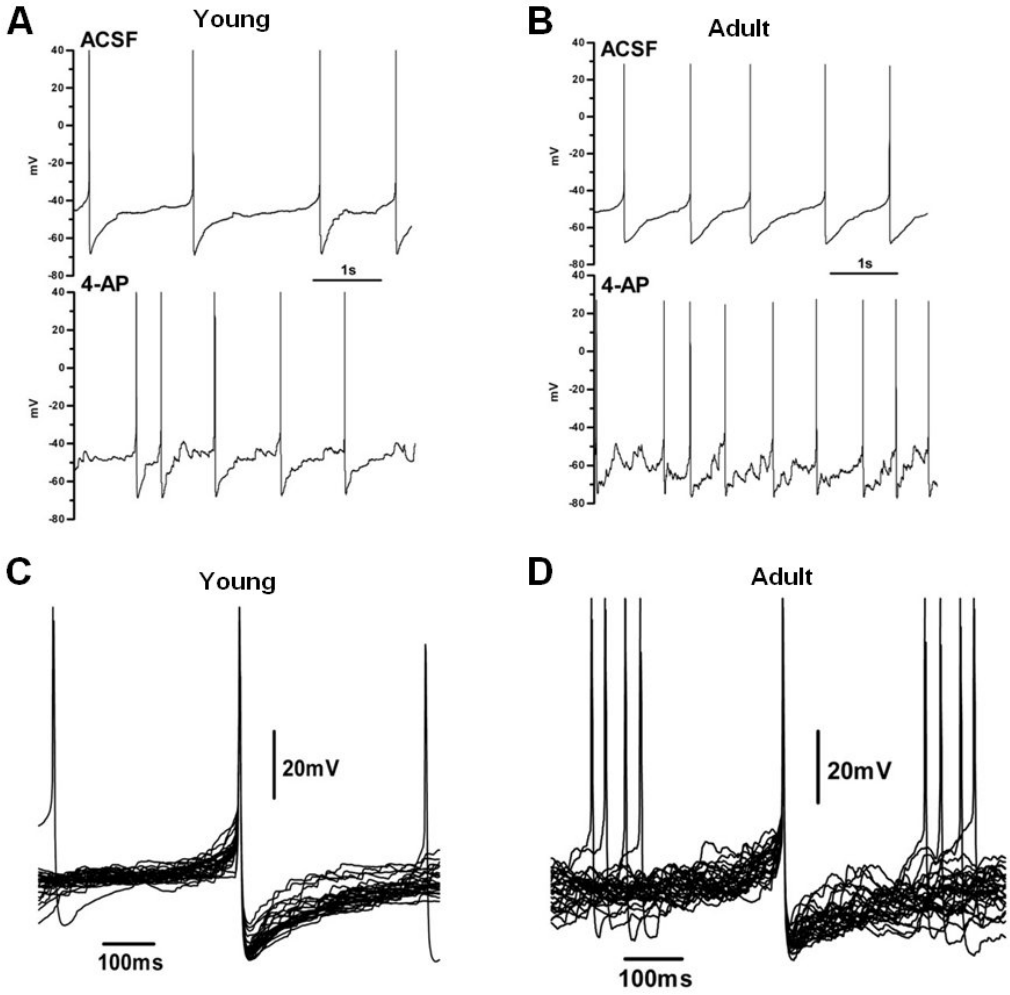

Figure 5.3: Age-dependent effects of 4-AP on spontaneous activity in LC neurons. ***A*** and ***B***, Representative recordings of Vm demonstrating that 4-AP (1 mM) caused an enhancement in the frequency of action potentials and baseline voltage noise in neurons from an infant (**A**) and an adult (**B**) mouse. ***C*** and ***D***, Action potentials recorded in the presence of 4-AP for the neurons of **A** and **B** presented as overlays aligned at the peak to facilitate comparison of the relative voltage noise during the interspike interval, which was larger in adult neurons.

The effect of 4-AP on voltage dependent currents was examined by applying depolarizing step pulses to voltage clamped neurons held at hyperpolarized Vm (Figure 5.4). This allowed a better comparison of 4-AP sensitive currents in infant and adult neurons. Neurons from infant mice (n=8) exhibited a transient differential outward current (Figure 5.4 A). In contrast, neurons from adult mice (n=7) exhibited currents comprised of an initial transient outward component followed by a later sustained "inward" component. This sustained inward component was not investigated further but being a differential current could reflect time-dependent 4-AP related effects on the outward current [180]. The current voltage relationship of the peak 4-AP sensitive outward current differed markedly in infant and adult neurons (Figure 5.4 C). In infant animals the relationship was linear and showed little voltage dependence. In contrast, the relationship for adult neurons exhibited strong voltage dependence. Furthermore, the currents were smaller for most of the interspike interval voltage range but increased sharply at Vm positive to -45 mV in adults.

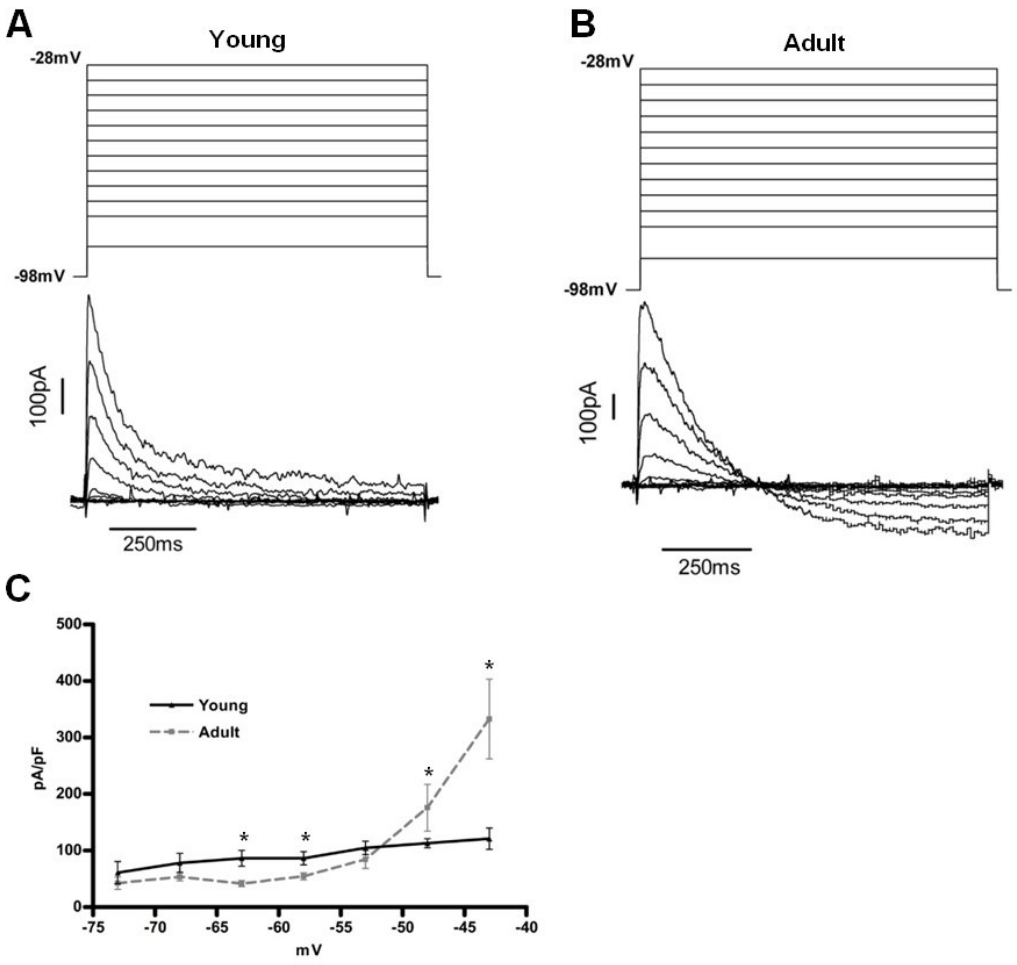

Figure 5.4: Age-related effects of 4-AP on currents evoked by depolarizing pulses. ***A*** and ***B***, Average differential 4-AP-sensitive currents obtained by recording currents from the first pulse protocol obtained in the presence of 1 μM TTX and subtracting the corresponding currents from the second pulse protocol obtained in the presence of 1 μM TTX + 1 mM 4-AP. ***C,*** Current–voltage relationships constructed from the differential currents of **A** and **B** plotted over the interspike interval voltage range (n=8 for young; n=7 for adult).. Graph in **C** shows mean ± SEM with * denoting significant age-related differences (p<0.05).

5.3.3. Differences in inward currents during development

We next compared inward currents in infant and adult mice. The Na^+ current, measured as a differential current obtained by applying depolarizing ramps in the absence and presence of 1 μM TTX is shown in Figure 5.5 A. Current voltage relationships obtained from these ramps showed that the differential inward current was larger in infant neurons at very depolarized potentials (> -30 mV) (Figure 5.5 B). In contrast, the differential current across membrane potentials, corresponding to the interspike interval voltage range, was larger in adult neurons (Figure 5.5 C).

The hyperpolarization-activated current (I_H) is another inward current that is known to change during development [200]. Accordingly, we tested for the presence of this current by applying a voltage protocol that consisted of six pre-conditioning pulses (3 s duration, in 10 mV steps from -58 mV to -118 mV) followed by a 1 s pulse to -118 mV. The latter pulse was designed to fully activate I_H currents. We failed to detect I_H in either infant or adult neurons using this protocol (n = 6 for both ages, Figure 5.6 A, B). This is consistent with our previous finding in infant mice [194], and suggests that I_H is not present in mouse LC neurons during postnatal development.

Ca^{2+} currents were investigated by applying depolarizing ramps to neurons firstly bathed in HEPES-ACSF based solution containing TTX, K^+ channel blockers followed by rapid perfusion of the same solution but with $CaCl_2$ substituted by equimolar $CoCl_2$ (see Methods). Under these conditions the differential inward current was larger in neurons from infant mice (Figure 5.7 A). However, close inspection of the current-voltage relationship showed this difference was only significant at very depolarized potentials (> -10 mV; Figure 5.7 B). There was no evidence that Ca^{2+} channels played a role during the interspike interval voltage range in either infant or adult neurons (Figure

5.7 C). The lack of a Ca^{2+} current during the interspike interval in mouse LC neurons contrasts with equivalent neurons in infant rats where a persistent Ca^{2+} current is clearly important (Figure 5.7 C; see also [94, 194]

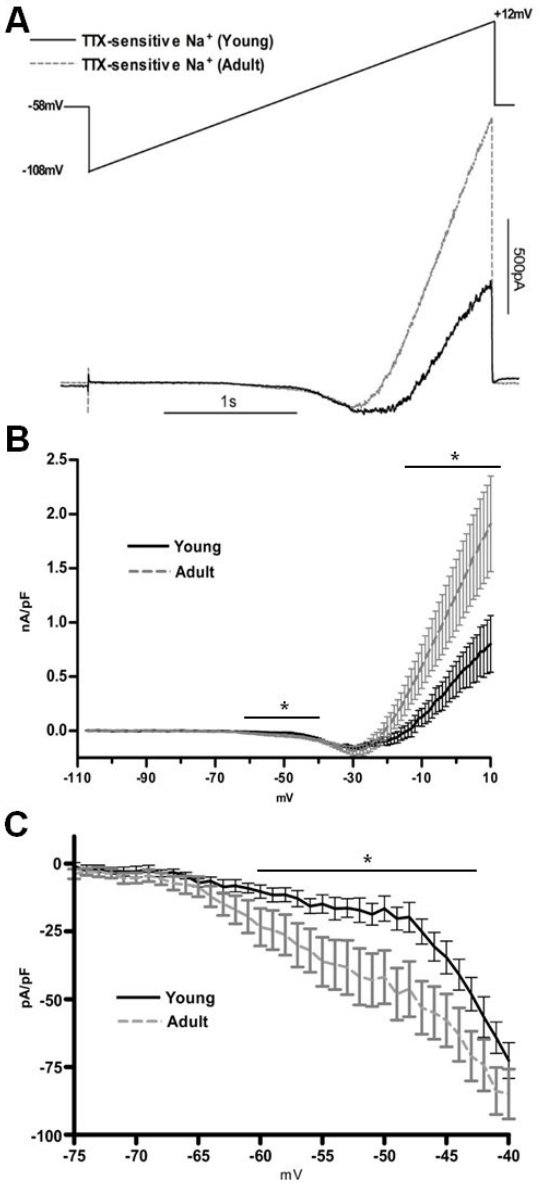

Figure 5.5: Age-related differences in voltage ramp-evoked TTX-sensitive Na^{+} currents. ***A,*** Averaged differential currents obtained by recording currents from the first ramp protocol obtained in ACSF and subtracting currents from the second ramp

protocol obtained in the presence of 1 μM TTX (n=8 and 9 LC neurons for infant and adult mice respectively). ***B,*** Mean current–voltage relationships constructed from the differential currents of (**A**) showing the two regions that exhibited significant age-related differences. ***C,*** Magnified view over the interspike interval voltage range demonstrating that the TTX-sensitive current was larger in this region in neurons from adults. Graphs **B** and **C** show the mean ± SEM (* significantly different, $p<0.05$).

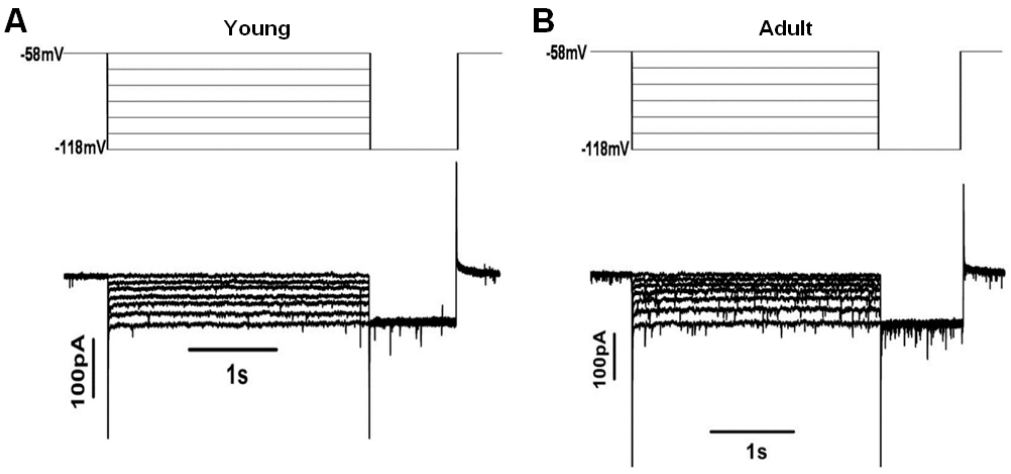

Figure 5.6: Lack of evidence for hyperpolarization-activated current (I_H) in LC neurons. ***A*** and ***B***, Representative pulse-evoked currents obtained in ACSF + 1 μM TTX showing that I_H currents were not active in LC neurons from infant (**A**) mice and adult (**B**) mice (n = 6 for both ages).

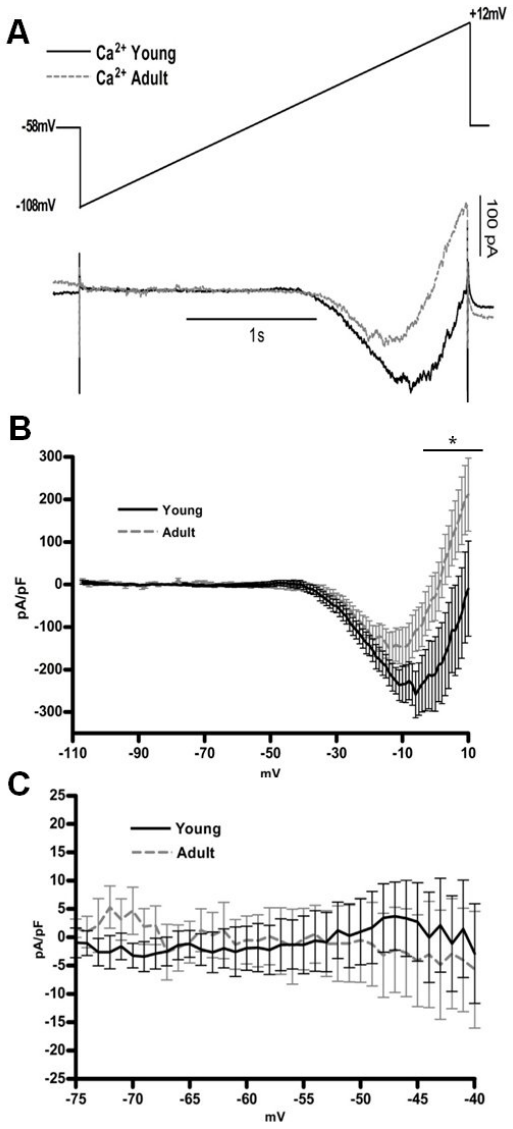

Figure 5.7: Age-related differences in LC neuronal Ca^{2+}-related currents. ***A,*** Averaged differential currents determined by recording currents from the first ramp protocol obtained in HEPES-ACSF containing 1 μM TTX + 15 mM TEA + 150 nM apamin and subtracting corresponding currents from the second ramp protocol obtained using the same solution with Ca^{2+} substituted by equimolar concentration of Co^{2+} (n=11 and 8 neurons from infant and adult mice respectively). ***B,*** Mean current–voltage relationships constructed from the differential currents of **A** showing that significant age-related differences were only achieved for Vm more depolarized than -10 mV. ***C,*** Magnified view over the interspike interval voltage range demonstrating that there was no evidence for pacemaker–associated Ca^{2+} currents in LC neurons from infant or adult mice. Graphs **B** and **C** show mean ± SEM (* significantly different, $p<0.05$).

5.4. Discussion

We have investigated the electrophysiological properties, especially the currents flowing during the interspike interval and associated with pacemaking, in infant (7-12 days old) and adult (8-12 weeks old) mice. The younger age range was selected because voltage clamp control from LC neurons in slices is best achieved over this age range and not at younger ages [194, 201]. The 8-12 week old group was chosen for two reasons. First, mice are considered adult at 8-12 weeks and second to ensure that any changes we observed would be associated with postnatal development rather than aging per se (see [202]). We found that the major ionic currents involved in pacemaking in mouse LC neurons change during postnatal development as has been shown for other tyrosine hydroxylase expressing neurons [138, 139].

Comparison of several electrophysiological properties showed spontaneous activity (AP firing) decreased from 90% to 50% in infant vs. adult neurons. The more hyperpolarized resting membrane potential, but similar input resistances we observed in adult LC neurons provide a likely explanation. Together, these two properties would combine to reduce spontaneous activity. The possibility remains that the enhanced numbers of quiescent cells was a consequence of damage through using thinner slices, though the input resistance of the quiescent cells was not significantly different. The average firing rate of active adult neurons was 2.4 compared to 2.0 for infant mice, but these were not significantly different. In this regard, the spontaneous firing rate of rat LC neurons has been reported to increase during postnatal development [144].

TTX-resistant spikes have been reported in rat LC neurons over a range of ages [21, 94, 167]. Such spikes were rarely observed in our recordings from infant LC neurons; however, they appeared to be more prevalent in adult neurons but this was not

quantified. Interestingly, application of the K^+ channel blocker 4-AP increased baseline voltage noise during the interspike interval (Figure 5.3). This was more pronounced in LC neurons from adult mice. It is also known that 4-AP can enhance synaptic activity in different neuronal types [203, 204]. This coupled with observations suggesting the number of synaptic connections on LC neurons changes during development as shown in rats [205] would increase spontaneous neurotransmitter release and baseline noise. Other factors such as the extent of electrotonic coupling and marked changes in dendritic architecture might also combine to increase baseline noise during development.

Comparison of action potential shape indicated the AHP was larger in adult neurons (Figure 5.1 D). Application of depolarizing ramps under control conditions demonstrated that LC neurons from adult mice exhibited larger outward currents, especially at depolarized membrane potentials (~ -45 mV). Experiments using K^+ channel blockers (i.e. 15 mM TEA + 150 nM apamin) showed this outward current was a K^+ current, and the differential outward current (i.e. ramp currents in ACSF + TTX minus ramp currents in ACSF + TTX + K^+ channel blocker solution) was larger in adult neurons near the same membrane potential. Thus K^+ conductances are more active in adult LC neurons and most likely underlie the larger AHP we observed in adult LC neurons.

There are numerous reports of the presence of large 4-AP sensitive currents, probably composed of a fast transient K^+ current (I_A) in rat LC neurons in culture or in freshly prepared slices [67, 185]. We tested for the presence of this current in infant and adult mice LC neurons by recording differential currents to depolarizing voltage pulses and found that similar transient outward currents were present at both ages (Figure 5.4).

The peak amplitude of the transient outward current was smaller in adult neurons over membrane potentials that corresponded to most of the interspike interval voltage range, however, its amplitude increased at membrane potentials positive to -45 mV (Figure 5.4 C). The 4-AP sensitive transient K^+ current exhibited a relatively slow inactivation time course compared to rat LC neurons [185], though slow inactivating 4-AP sensitive transient K^+ currents have been reported in other neurons [180]. Thus, these results suggest that 4-AP sensitive currents in mouse LC neurons undergo significant changes during development including a change in their sensitivity to 4-AP.

A TTX-sensitive Na^+ current is the major pacemaker current in mouse LC neurons and is also dominant in the generation of the action potential. A TTX-sensitive Na^+ current has been reported present in several neuronal types, where Na^+ channels are responsible for producing subthreshold and fast-activating currents [81, 181, 182]. The key finding in the present study is that this pacemaker current is enhanced during development. An increased TTX-sensitive Na^+ conductance within the interspike interval in adults would help secure pacemaking in neurons as they become more hyperpolarized during development. In contrast, the role of the larger TTX-sensitive Na^+ currents we observed at very depolarized potentials in infant mice is more difficult to explain. Some caution is needed here, however, as measurement of differential currents at very depolarized potentials, where large conductances are activated, raises questions about the extent to which the soma and dendrites of large LC neurons can be confidently voltage clamped. This will impinge on the resultant currents especially when there are significant changes in dendritic architecture during development. However, it remains an interesting point, and if true it suggests developmental differences exist between the Na^+ channels that underlie pacemaking and the action potential.

Two other inward currents that serve a role on pacemaking were also investigated in this study. The hyperpolarization-activated current (I_H) participates in pacemaking in a variety of neuron populations, that discharge repetitively/tonically [206-209]. As previously shown I_H does not subserve a role in pacemaking in LC neurons from infant mice [194]. The present study indicates that that this current is also not present in adult LC neurons, suggesting I_H does not have an obvious role in LC pacemaking at any stage during postnatal development. Voltage-dependent Ca^{2+} currents can also drive pacemaking, and we have shown that while Ca^{2+} currents are present in infant LC neurons in mice, they are not active during the interspike interval voltage range and thus do not play a role in pacemaking [194]. This finding differs with that in infant rat LC neurons where a Ca^{2+} current is reported to be active within the interspike interval [94]. Here we expand these observations and show that these species differences are not related to development, as LC neurons from adult mice also showed no evidence of a functional Ca^{2+} current over the pacemaker voltage range.

In summary, our results demonstrate that the electrophysiological properties of mouse LC neurons change during development. Careful examination of the currents flowing during the interspike interval voltage range showed there were parallel increases in a voltage-dependent TEA-sensitive K^+ conductance and the TTX-sensitive Na^+ current during development.

5.5. Ongoing and future studies

Studies will be undertaken to determine the involvement of specific ion channels known to be functional in LC neurons (e.g. inward rectifier K^+ channels, TASK-1 and 3 etc).

Investigations will also be made of membrane properties and particularly baseline noise in the presence of synaptic inputs blocked (e.g. glutamatergic, GABAergic, glycinergic, noradrenergic etc).

Experiments will be made to further investigate the possible role of TTX-resistant Na^+ current in adults compared to infant LC neurons.

We will also further investigate the role of I_h. This current was not obviously present but it remains possible that there is a small I_h current, that may be revealed by pharmacological comparison of control records with those obtained in the presence of an inhibitor of I_h (e.g. ZD 7288).

Chapter 6

Effects of mitochondrial disruption on ionic currents and pacemaking in neurons of the locus coeruleus

6.1. **Abstract**

This study evaluates the effects of challenging mitochondrial function on ionic currents in locus coeruleus (LC) neurons. Application of the protonophore carbonyl cyanide m-chlorophenylhydrazone (CCCP; 1 μM) to isolated LC neurons and neurons in slices respectively induced a small but measurable decrease in the mitochondrial membrane potential (Ψm) and a small depolarization that enhanced, followed by large hyperpolarization that inhibited, neuronal firing. The latter whole cell recording experiments, when repeated under voltage clamp applying ramp and depolarizing pulse protocols, demonstrated a CCCP-induced inward followed by a dominating outward current exhibiting a reversal potential near -82 mV. The outward current was dependent on Ca^{2+} entry being blocked by external Cd^{2+} (300 nM), Ca^{2+} free (EGTA) external solution and nifedipine (10 μM), the latter suggesting a role for L-type Ca^{2+} channels (Ca_{V-L}). This finding was unexpected given that the outward current could be generated at potentials well below the known threshold for activation of Ca_{V-L}. The outward current was likely to be in large part generated by SK type Ca^{2+}-activated K^+ channels, as the current was blocked by intracellularly applied CsF and was substantially inhibited by external application of apamin (1 μM). This current was not obviously activated by increases in cytosolic Ca^{2+} concentration ($[Ca^{2+}]_c$), as application of CCCP (1 μM), while causing similar increases in $[Ca^{2+}]_c$, only generated outward current when there was Ca^{2+} entry. The finding that relatively small changes in mitochondrial membrane potential (Ψm) correlate with marked changes in ionic conductances and hence neuronal firing suggests that mitochondria may serve as a fine tune regulator of pacemaking in LC neurons.

6.2. Introduction

Locus coeruleus (LC) neurons are known to play a fundamental role in brain function, impacting on many physiological processes such as regulation of sleep and vigilance [192, 193], learning and memory [210], behavioral flexibility [162], and a range of other functions (for review see [211]).

The pacemaker mechanism that generates spontaneous firing in LC neurons has been studied for long time [94, 167, 212]. It is also known that external agents can impact on pacemaking due to recruitment of additional ionic currents that modulate the normal pacemaker mechanisms [169-172]. The present work has focused on the role played by mitochondria on LC pacemaking, investigating the combination of mitochondria-associated ionic currents that may act as fine tune regulators of this process.

Mitochondria are intracellular organelles that appear to be involved in vast range of different pathways, including energy production [96], neuronal death [213], oxidative stress [214], neurodegenerative diseases [215] and their role in buffering intracellular Ca^{2+} and resultant impact on Ca^{2+}-dependent pathways [111, 216, 217]. Mitochondrial functions are in general dependent on mitochondrial membrane potential (Ψm), this being generated by the action of the mitochondrial electron transport chain, where the energy generated by the transport of electrons is used to drive H^+ against its gradient concentration across the mitochondrial inner membrane [96].

It is known that different ionic currents can be activated directly or indirectly by mitochondria-associated mechanisms. One of these is carried by ATP-dependent K^+

channels ($I_{K\text{-}ATP}$). ATP is the "energy currency" of every cell and a decrease in the ATP/ADP ratio can activate $I_{K\text{-}ATP}$ causing hyperpolarization [218]. This outcome has been proposed to be a protective mechanism in neurons, since hyperpolarization leads to decreased neuronal firing and hence less energy spent in this process giving time for the cells to recover from ATP depletion [219]. Other channels that can be activated by perturbing mitochondrial function are Ca^{2+}-activated K^+ channels (K_{Ca}). The activation of these channels has been suggested to participate in different processes in neurons, including controlling action potential duration, firing frequency and spike frequency adaptation [220-222]. Another important contribution of mitochondria to pacemaking involves the production of reactive species such as free radicals. It has been demonstrated that reactive species can interact with ionic channels modulating their activity [103]. Therefore, is possible that mitochondria exert a role acting as a multifocal regulator of the pacemaker process adjusting neuronal metabolism according to firing rate or vice versa.

The present study investigates ionic currents activated by perturbations in mitochondrial function induced through application of CCCP. It was found that the mitochondrial protonophore CCCP caused activation of a nifedipine-sensitive Ca^{2+} conductance that was present even at hyperpolarized potentials. Ca^{2+} entry through these channels in turn activated an outward current largely carried by SK-type Ca^{2+}-activated K^+ channels and one, which was not obviously activated by intracellular Ca^{2+} release.

6.3. Results

6.3.1. Effect of CCCP on spontaneous LC firing, Ψm and voltage-dependent currents

The effect of mitochondrial disruption on spontaneous firing and hence pacemaking of LC neurons was investigated by rapid application of 1 μM CCCP in ACSF. Application of this mitochondrial protonophore initially induced a small neuronal depolarization and increase in firing rate with maximal effect at ~ 1 min. This was followed by a large hyperpolarization that completely abolished spontaneous firing, achieving its peak after ~ 3 min exposure to CCCP (Figure 6.1 A). Hyperpolarization was likely to be the primary reason for this CCCP-associated inhibition as neuronal firing recommenced during injection of depolarizing current (Figure 6.1 A, black dash). Voltage clamp experiments made at a holding potential of -78 mV confirmed the effect observed in figure 6.1 A, with the response to 1 μM CCCP exhibiting a small inward current peaking at ~ 1 min, followed by an outward current reaching an asymptotic peak after ~ 5 min and achieving an amplitude of 46 ±1 pA after ~ 3 min of treatment (Figure 6.1 B, black arrow). Ψm measurement by JC-1 experiments on isolated LC neurons (see Methods) revealed that 1 μM CCCP treatment significantly decreased relative Ψm, with decreases in the red/green fluorescence to 86.3 ± 5% and 78.1 ± 6% after 60s and 180s of CCCP application respectively (Figure 6.1 C).

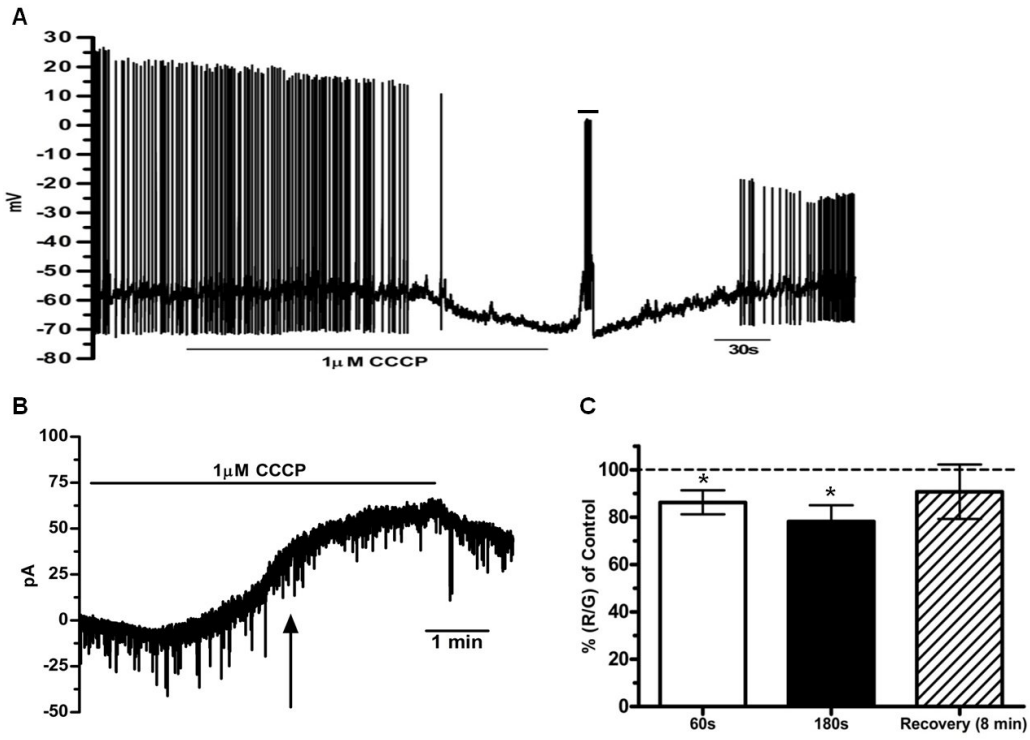

Figure 6.1: Effect of CCCP treatment on neuronal membrane potential and Ψm of LC neurons. ***A,*** Representative current clamp recording showing that application of 1 μM CCCP in ACSF caused hyperpolarization, which abolished spontaneous firing but which could be reinstated by depolarization and partially reversed (n=8). ***B,*** Representative voltage clamp continuous recording from a holding potential of -78 mV demonstrating that 1 μM CCCP induced a small inward followed by an outward current (n=5). ***C.*** Measurement using the fluophore JC-1 in isolated LC neurons indicating that 1 μM CCCP induced a small decrease in relative Ψm, as the red/green ratio was respectively reduced to 86.3 ± 5% and 78.1 ± 6% after 60s and 180s of CCCP application through the rapid perfusion system (n=10). Graph shows mean ± SEM, $p < 0.05$.

The voltage dependency of the CCCP-induced currents was investigated using two different voltage protocols. The first involved applying depolarizing ramps at 40 mV/s from a holding potential of -58 mV and the second, applying depolarizing pulses from a holding potential of -88 mV now in the presence of 1 μM TTX. Rapid application of 1 μM CCCP with voltage ramps applied 60s and 180s later induced two different effects on the evoked currents: first, the neurons exhibited increased conductance as was evident at hyperpolarized membrane potentials and with increasing depolarization there was an induction of an "outward inflection" in the I-V relationship (Figure 6.2 A, B). The differential current calculated by subtracting the current in ACSF from that in 1 μM CCCP (i.e. test-control) revealed that the induced leakage reversed at -82 ± 0.7 mV (Figure 6.2 C).

Application of depolarizing pulses from a holding potential of -88 mV revealed that the CCCP-induced "leakage" current was a "non-inactivating" current, at least for the duration of the applied pulses, as shown by the representative differential recordings (i.e. test-control) in figure 6.3 A (180 s, 1μM CCCP). I-V graphs constructed from the differential pulse-evoked currents exhibited a similar I-V relationship, as those elicited by depolarizing ramps (Figure 6.3 B) and a reversal potential of -83 ±1.2 mV (Figure 6.3 C).

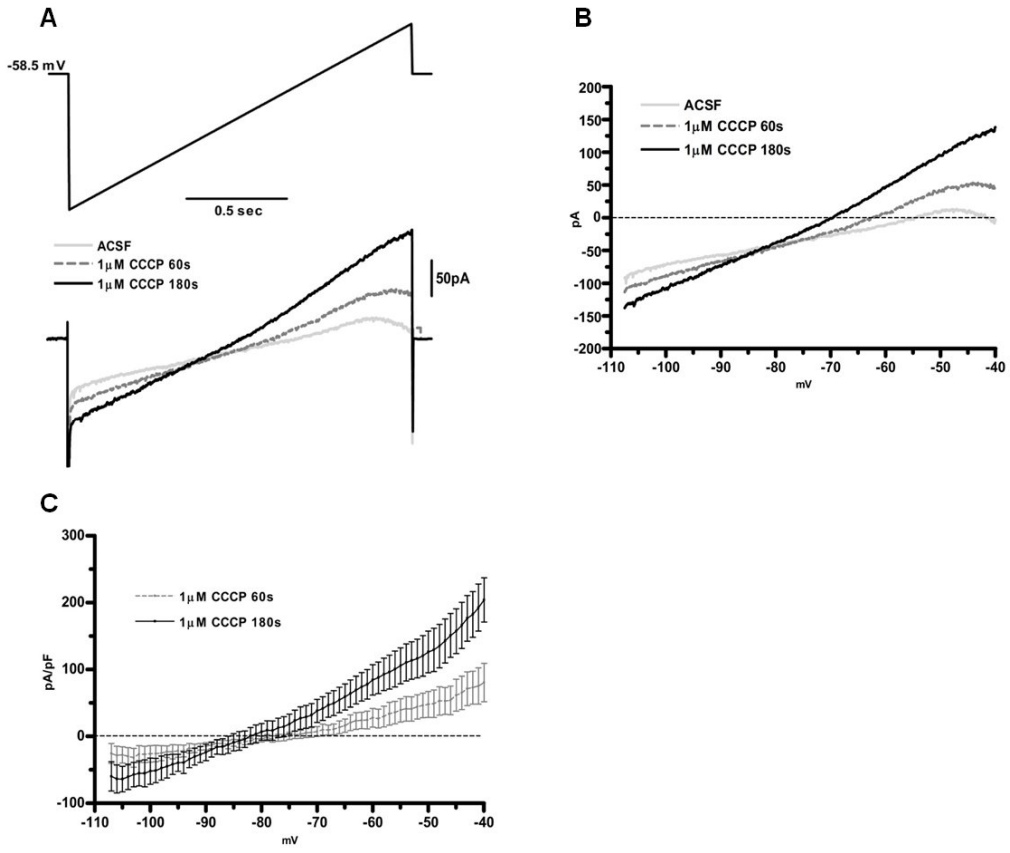

Figure 6.2: Effect of CCCP on voltage-dependent currents evoked by depolarizing ramps. *A*, Representative recording of the currents evoked by depolarizing ramps during application of 1 μM CCCP in ACSF (test solution), showing the current evoked in ACSF (control solution; light grey line) and 1 μM CCCP 60s (dashed grey line) and 180s (solid black line) after rapid application of this test solution (n=8). *B*, I-V plot for the currents presented in A. *C*, Mean differential currents (i.e. CCCP test – control) with records obtained 60s (light grey line) and 180s (black line) after rapid application of CCCP (n=8).

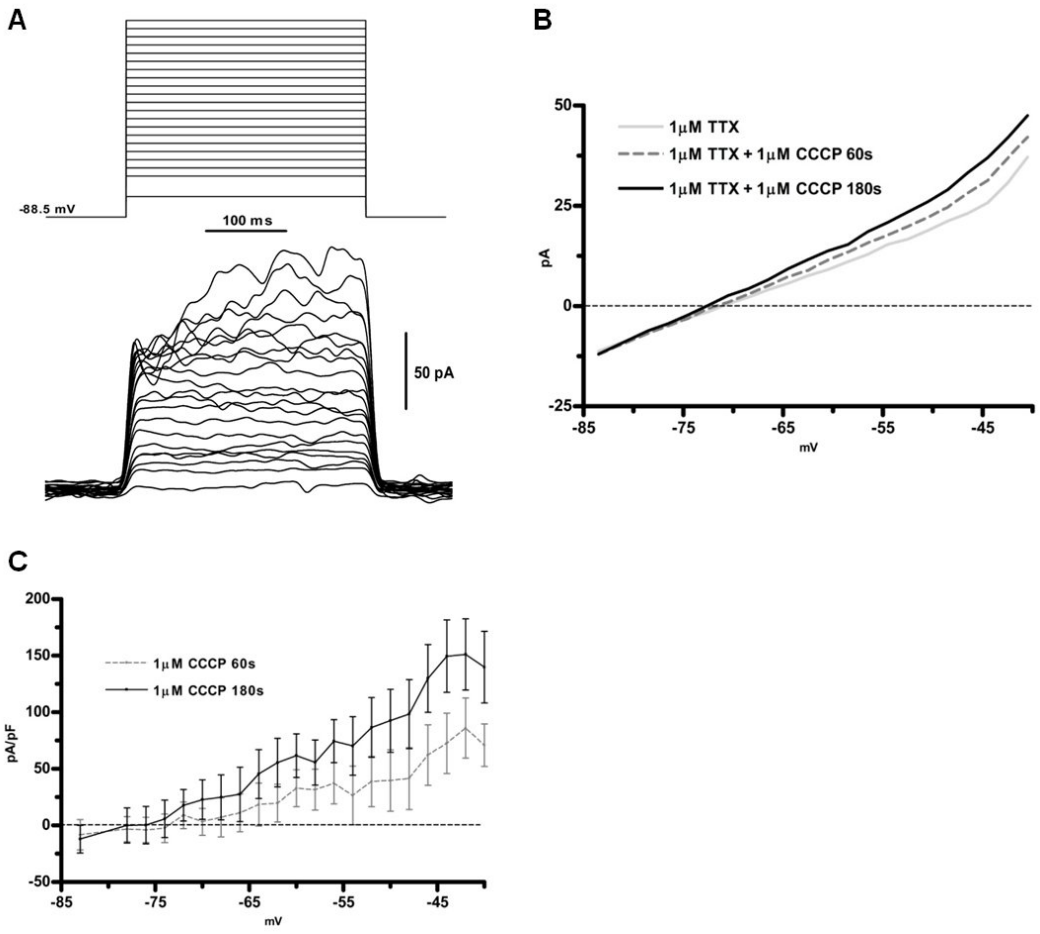

Figure 6.3: Effect of CCCP on voltage dependent currents evoked by depolarizing pulses. *A,* Representative depolarizing pulse-evoked differential currents obtained by taking the currents in test solution (i.e. 1 μM CCCP + 1 μM TTX ACSF) and subtracting the corresponding currents in control (i.e. 1 μM TTX ACSF). *B,* Averaged I-V plot showing the currents evoked by pulses for control (light grey line) and the test CCCP solution 60s (dashed grey line) and 180s (solid black line) after its application. *C,* Mean differential I-V plots (i.e. test-control) 60s (light grey dashed line) and 180s (black dashed line) after application of the CCCP solution. Graph shows mean ± SEM with n=9 for A, B and C.

6.3.2. CCCP-induced outward conductance is dependent on Ca^{2+} entry but independent on $[Ca^{2+}]_c$

It has been shown that depolarization of Ψm by application of CCCP increases cytosolic Ca^{2+} concentration ($[Ca^{2+}]_c$) [100]. This was also the case here, as 1 μM CCCP induced an increase in $[Ca^{2+}]_c$ in both standard ACSF and Ca^{2+}-free (500 μM EGTA) solutions (Figure 6.4 A).

The increase in $[Ca^{2+}]_c$ could activate Ca^{2+}-dependent K^+ channels (K_{Ca}) and result in neuronal hyperpolarization. Based on this, we examined the dependency of external and cytosolic Ca^{2+} on the CCCP-induced hyperpolarization. The outward current or hyperpolarization induced by 1 μM CCCP was abolished in ACSF containing 300 μM $CdCl_2$, as was observed for both voltage and current clamp recordings (Figure 6.4 B, C). The dependency on extracellular Ca^{2+} was further confirmed when the slice was perfused with Ca^{2+}-free (500 μM EGTA) ACSF solution, which abolished the CCCP-induced hyperpolarization (Figure 6.4 D). These results suggest that external Ca^{2+} entry and not an increase in $[Ca^{2+}]_c$ is the necessary step for activation of the CCCP-induced hyperpolarization.

Further support for this was provided by the finding that the CCCP-induced hyperpolarization or outward current persisted when 15mM EGTA was present in the internal pipette solution (Figure 6.5 A, B). Application of depolarizing ramps also supported this view, as CCCP induced a similar outward current independent on whether the internal pipette solution contained high or low EGTA (cf. Figure 6.5 C, D with Figure 6.2 B, C).

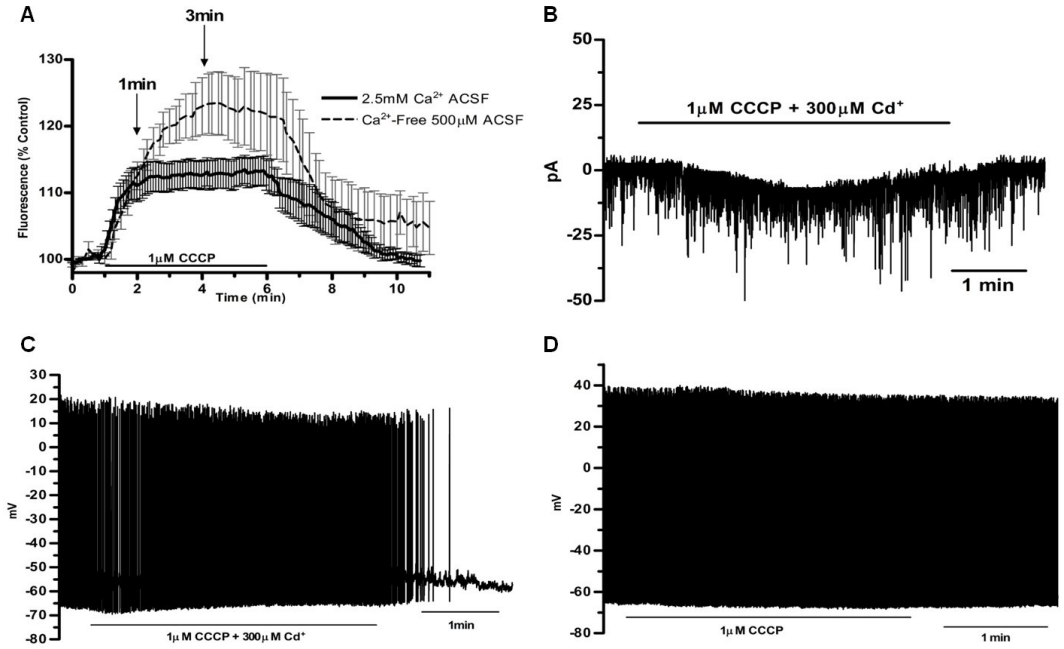

Figure 6.4: The CCCP-induced outward conductance is dependent on Ca^{2+} entry but independent on $[Ca^{2+}]_c$. ***A,*** Mean increases in cytosolic Ca^{2+} concentration ($[Ca^{2+}]_c$) induced by application of 1 μM CCCP measured by the fluophore Oregon Green in Ca^{2+}-free 500 μM EGTA (n=8) and normal 2.5 mM Ca^{2+} (n=7) ACSF solutions. Plots show mean ± SEM. ***B,*** Representative voltage clamp continuous recording from a holding potential of -78 mV demonstrating that the outward current induced by 1 μM CCCP was inhibited by addition of 300 μM $CdCl_2$ in the external solution (n=5). ***C*** and ***D***, Representative current clamp recordings showing that the CCCP-induced hyperpolarization was abolished in 300 μM $CdCl_2$ ACSF (**C**) and 500 μM EGTA Ca^{2+}-free ACSF (**D**) solutions (n=6 for **C** and n=5 for **D**).

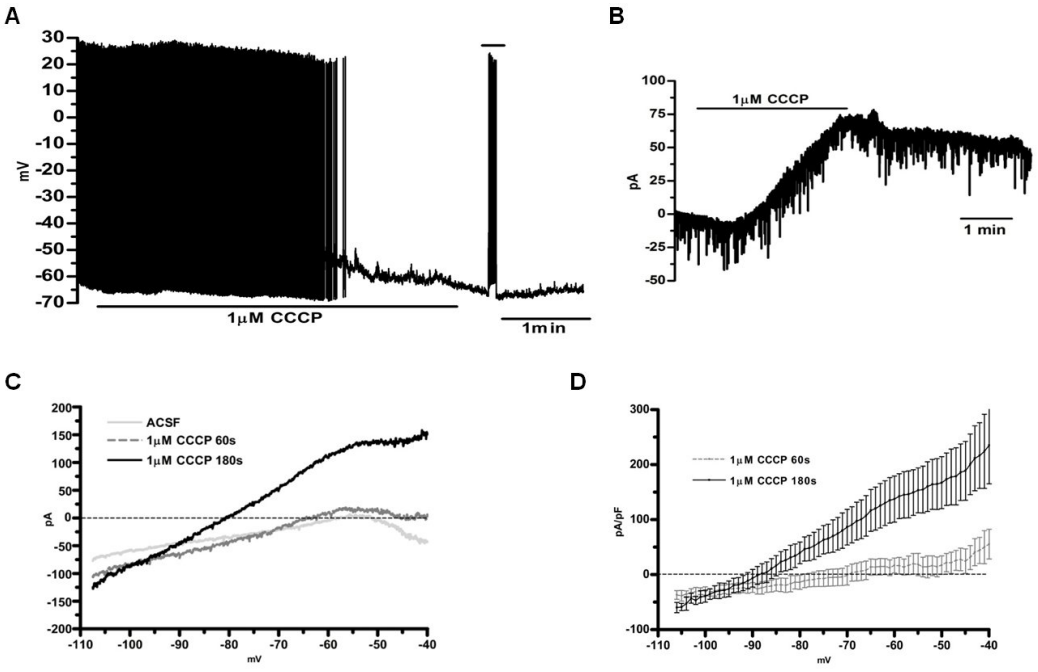

Figure 6.5: Lack of effect of high internal Ca^{2+} buffering on CCCP-induced responses. ***A,*** Representative current clamp recording demonstrating that dialysis of the neurons with 15 mM EGTA in the internal pipette solution did not impact on the 1 μM CCCP-induced hyperpolarization (n=7). ***B,*** Representative voltage clamp continuous recording at a holding potential of -78 mV showing a typical 1 μM CCCP-induced response despite using the 15 mM EGTA pipette solution (n=7). ***C,*** I-V plots obtained using the 15 mM EGTA pipette solution showing the averaged currents evoked by depolarizing ramps in control (light grey line) and 1 μM CCCP, the latter recorded 60s (dashed grey line) and 180s (solid black line) after application of the test (i.e. 1 μM CCCP ACSF) solution (n=7). ***D,*** Mean differential I-V plots (i.e. test-control) obtained using the 15 mM EGTA pipette solution 60s (light grey dashed line) and 180s (black dashed line) after application of the 1 μM CCCP solution (n=7).

6.3.3. Calcium channel modulation and Ψm

Our next aim was investigate whether there was a correlation between the CCCP-induced depolarization of Ψm and the activity of Ca^{2+} channels. Co-application of 1 μM CCCP + 10 μM nifedipine using the rapid perfusion system, inhibited the CCCP-induced hyperpolarization and outward current (Figure 6.6 A, B), suggesting that the hyperpolarization was triggered by Ca^{2+} entry through L-type Ca^{2+} channels. However, the small initial inward current induced by CCCP was not obviously inhibited by nifedipine (Figure 6.6 B), indicating that inward conductances other than nifedipine-sensitive Ca^{2+} channels were also activated. I/V plots constructed from the depolarizing pulse protocol of figure 6.6 C indicated that the differential outward current evoked by depolarizing pulses was largely inhibited over the voltage range shown (cf. Figure 6.6 E with Figure 6.3 C). This indicates that this outward current exhibits considerable dependence on nifedipine-sensitive Ca^{2+} entry suggesting a key involvement of L-type Ca^{2+} channels. However, if L-type Ca^{2+} channels are recruited by the mitochondrial protonophore then their dependence on a threshold voltage for activation is now lost.

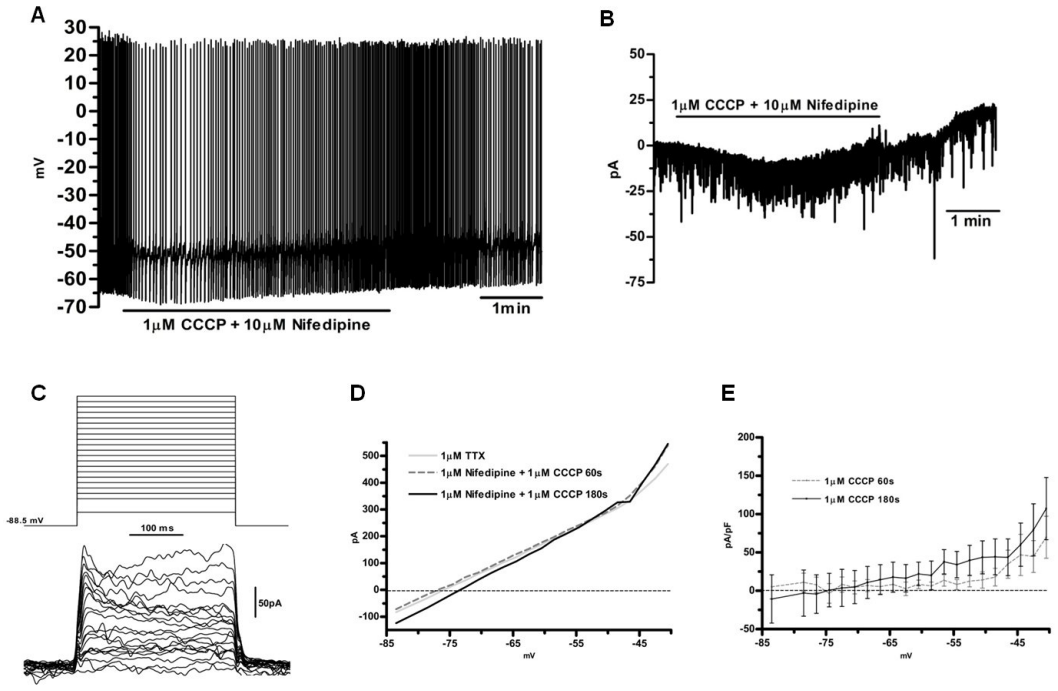

Figure 6.6: Nifedipine inhibits the CCCP-induced hyperpolarization and outward current. *A,* Representative current clamp recording demonstrating that rapid application of 10 μM nifedipine together with 1 μM CCCP ACSF prevented the hyperpolarization normally induced by 1 μM CCCP (n=5). *B,* Representative voltage clamp continuous recording from a holding potential of -78 mV showing this same test solution inhibited the CCCP-induced outward current (n=5). *C,* Representative differential depolarizing pulse-induced recordings constructed by taking the currents obtained in the test solution (i.e. 1 μM CCCP + 10 μM nifedipine + 1 μM TTX ACSF) and subtracting the corresponding currents in control solution (i.e. 1 μM TTX ACSF) in response to a sequence of depolarizing pulses. Collection of these records was commenced 180s after application of the test solution. *D,* I-V plots showing the averaged currents evoked by the depolarizing pulses in control (light grey line) and test solutions, the latter recorded 60s (dashed grey line) and 180s (solid black line) after application of the test solution. *E,* Mean differential I-V plots (i.e. test-control) shown 60s (light grey dashed line) and

180s (black dashed line) after application of the test solution. Graph shows mean ± SEM (n=10 for C, D and E).

6.3.4. The CCCP-induced outward current is partially inhibited by apamin

The nature of the CCCP-induced outward current was further investigated. As has been shown this current was dependent on external Ca^{2+} (Figure 6.4 D) indicating it was carried by either Ca^{2+}-activated K^+ or Cl^- channels. However, participation of $I_{K\text{-}Ca}$ and not $I_{Cl\text{-}Ca}$ was suggested, as the outward current was inhibited in experiments using CsF in the internal pipette solution, as measured under voltage clamp at a fixed potential or with a depolarizing step protocol (Figure 6.7 A-C). Rapid co-application of apamin test solution (i.e. 1 μM apamin + 1 μM CCCP in 1 μM TTX ACSF) inhibited the CCCP-induced outward current as measured after 180s of treatment (Figure 6.8 A). Application of depolarizing pulses further supported this observation as the low voltage threshold differential outward current, which was substantial under control conditions (Figure 6.3 C), was now markedly inhibited (Figure 6.8 B-D). Charybdotoxin was also tested (100 nM) but had no significant effect on the CCCP-induced current (data not shown). These results suggest that SK channels underlie the major component of the CCCP-induced outward current.

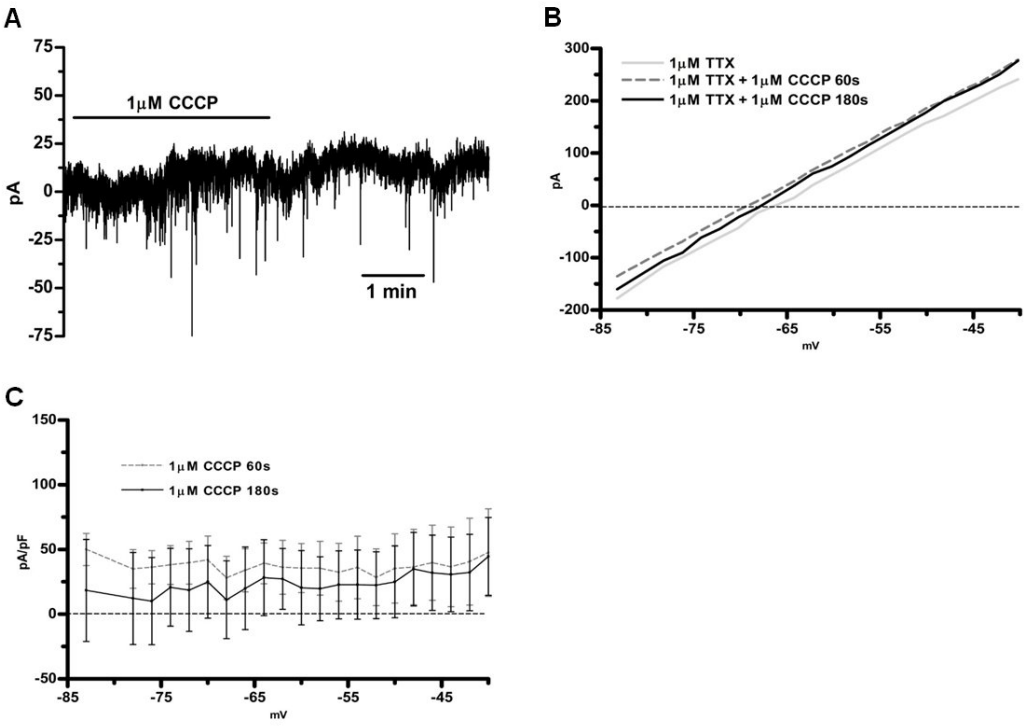

Figure 6.7: Effect of CsF-filled internal pipette solutions on the CCCP-induced outward current. ***A,*** Representative voltage clamp continuous recording from a holding potential of -78 mV demonstrating that no outward current was induced by 1 μM CCCP treatment when CsF was present in the internal pipette solution (n=3). ***B,*** I-V plots showing the averaged currents evoked by depolarizing pulses in control (i.e. 1 μM TTX ACSF; light grey line) and test (i.e. 1 μM CCCP + 1μM TTX ACSF) solutions, the latter recorded 60s (dashed grey line) and 180s (solid black line) after application of the test solution. ***C,*** Mean differential I-V plots (i.e. test-control) obtained 60s (light grey dashed line) and 180s (black dashed line) after application of the test solution. Graph shows mean ± SEM (n=6 for **B** and **C**).

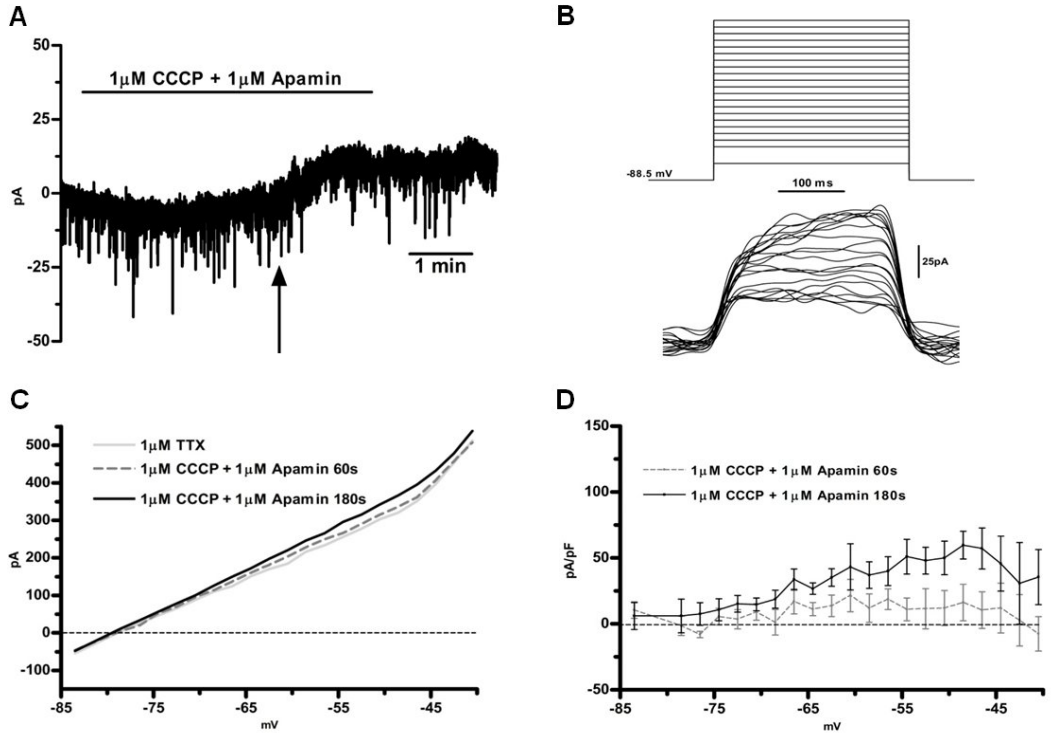

Figure 6.8: Effect of apamin on the CCCP-induced outward current. ***A,*** Representative voltage clamp continuous recording at holding potential of -78 mV demonstrating that the co-application of apamin (1 μM) and 1 μM CCCP inhibited the CCCP-induced outward current (n=4). ***B,*** Representative differential currents obtained by subtracting the depolarizing pulse-induced currents in control (i.e. 1 μM TTX ACSF) from the corresponding currents in test solution (i.e. 1 μM CCCP + 1 μM apamin + 1 μM TTX ACSF) with records shown obtained 180 s after application of the test solution. ***C,*** Averaged I-V plots showing the currents evoked by depolarizing pulses for control (light grey line) and test solutions, the latter obtained 60s (dashed grey line) and 180s (solid black line) after application of the test solution. ***D,*** Mean differential I-V plots (i.e. test-control) shown 60s (light grey dashed line) and 180s (black dashed line) after application of the test solution. Graph shows mean ± SEM, (n=7 for **B, C** and **D**).

6.4. Discussion

The present study investigates mechanisms associated with mitochondria that cause changes in ionic channel conductances and consequently modulate pacemaking in LC neurons. It is demonstrated that the hyperpolarization induced by CCCP and associated depolarization of Ψm, as previously reported in LC [70], is independent of intracellular Ca^{2+} released by stores but is dependent on Ca^{2+} entry through nifedipine-sensitive channels, suggesting an involvement of L-type Ca^{2+} channels.

Pacemaking in mouse LC neurons is mediated primarily for two conductances that activate during the interspike interval, a major TTX-sensitive Na^{+} current and a high TEA-sensitive K^{+} current, with little or no involvement of Ca^{2+} currents [194]. It is also known, that external stimuli can evoke other conductances that modulate the firing rate of LC neurons according to system needs [169-172]. The effect of interfering with mitochondrial function and associated depolarization of Ψm represents another means by which new currents are recruited that can modulate pacemaking.

Application of CCCP (1 μM) induced a small depolarization in Ψm and an initial neuronal depolarization that increased firing rate followed by a sustained hyperpolarization that abolished generation of action potentials (Figure 6.1). These results in part parallel previous reports showing that depolarization of Ψm correlates with generation of an outward current in various neurons [70, 223-225]. Significantly, the change induced by the protonophore CCCP when applied at 1 μM only caused a small change in Ψm (Figure 6.1 C), suggesting that relatively small perturbations in mitochondrial function can activate and/or modulate membrane currents that influence

pacemaking. In this regard, it has recently been demonstrated that small fluctuations in Ψm of similar magnitude, as that reported here can occur spontaneously in neurons [226], suggesting that mitochondria may modulate pacemaking under physiological conditions.

Depolarizing ramps demonstrated that CCCP treatment induced an outward current that reversed at potentials negative to ~ -82 mV. This is close to the reversal potential reported for K^+ ions in LC neurons. These results were supported by application of depolarizing pulses. Taken together, these findings indicate that application of CCCP leads to activation and/or modulation of K^+ channels resulting in membrane hyperpolarization and cessation of action potentials.

Studies on other neurons have indicated that CCCP induces Ca^{2+} release from mitochondria into the cytosol [102, 227], and that Ca^{2+} released into the cytosol causes activation of $I_{K\text{-}Ca}$ [100, 228]. It is possible that this also the case in rat LC neurons, as has been indicated from studies involving metabolic inhibition of mitochondria where charybdotoxin-sensitive $I_{K\text{-}Ca}$ channels were activated [70]. However, our mouse LC studies contrast with these findings in that we found that the CCCP-induced hyperpolarization was dependent on Ca^{2+} entry but not Ca^{2+} release from mitochondrial or other Ca^{2+} stores. Thus while CCCP induced a large increase in $[Ca^{2+}]_c$ independent of the presence of extracellular Ca^{2+} (Figure 6.4 A), a CCCP-induced hyperpolarization or outward current was only induced when extracellular Ca^{2+} was present or Ca^{2+} entry was impeded, as the response was abolished when neurons were bathed in 500 μM EGTA Ca^{2+} free ACSF or in 300 nM Cd^{2+} ACSF. A similar finding has also been reported in hippocampal neurons, where changes in mitochondrial metabolism increase the conductance of Ca^{2+} channels that in turn increased K^+ conductance, this modulating

membrane excitability [229]. Further support for a lack of involvement of $[Ca^{2+}]_c$ was provided by the finding that the CCCP-induced hyperpolarization or outward current was not obviously altered when the internal pipette solution was changed to contain a high concentration of the Ca^{2+} chelator EGTA (i.e. 15 mM). These results suggest that the CCCP-induced hyperpolarization is mediated by Ca^{2+} entry and not Ca^{2+} released from mitochondrial and/or other stores.

The pathway underlying Ca^{2+} entry was investigated using known blockers of Ca^{2+} channels. Surprisingly, we found that the hyperpolarization or outward current was inhibited by nifedipine (10 μM). This suggests an involvement of L-type Ca^{2+} channels. However, such channels should only be functional at potentials positive to about -45 mV, yet the outward current, which was activated even at very negative potentials (e.g. -78 mV) was blocked by application of nifedipine. Thus nifedipine either blocks Ca^{2+} entry through another channel or CCCP and the resultant perturbation of mitochondrial function activates L-type channels outside the normal activation range. Possible support for the latter is provided by recent findings of cross talk between L-type Ca^{2+} channels and mitochondria, as identified in heart cells [120].

We also aimed to identify the nature of the outward current induced by CCCP. Voltage ramp experiments showed a reversal potential of ~ -82 mV. This together with the finding that use of CsF in the internal pipette solution blocked the CCCP-induced outward current, suggest that the current is carried by K^+ channels. Further to this, application of 10 μM apamin partially inhibited the CCCP-induced outward current whereas charybdotoxin did not block this current (data not shown). Together, these data suggest that the CCCP-induced outward current is mediated by K^+ conductances with SK channels carrying most of the outward current.

In conclusion, we have demonstrated that application of 1 μM CCCP caused a small but significant change in Ψm and a small neuronal depolarization or inward current followed by a large hyperpolarization or outward current. The latter was likely to largely involve SK-type Ca^{2+}-activated K^+ channels, as it was blocked by removal of extracellular Ca^{2+}, Cd^{2+}, nifedipine, CsF and partially inhibited by apamin. The fact that nifedipine inhibited the response suggests that Ca^{2+} entry may be mediated by L-type Ca^{2+} channels. Should this be the case, it suggests that these channels have been induced to allow Ca^{2+} entry even at potentials well negative of their normal activation voltage range. Another surprising finding was that Ca^{2+} entry but not intracellular Ca^{2+} release was a prerequisite for generation of the outward conductance suggesting that the Ca^{2+} entry pathway and responding SK type Ca^{2+}-activated channels are in close proximity, this structure possibly constituting a microdomain [117, 230, 231]. Finally, we raise the hypothesis that mitochondria may provide a fine tune regulator of ionic currents and hence LC neuronal pacemaking through a dynamic feedback between LC firing and mitochondrial activity.

6.5. Ongoing and future studies

A considerable number of experiments have been made to analyse the influence of free radicals in the pacemaking process of LC neurons. They have not been included in the present thesis because they are incomplete and need further work.

I have carried out experiments analysing the role of free radicals in the pacemaker process in our animal model. Surprisingly, antioxidants (Trolox and DTT) were directly

applied in LC neurons producing small changes in the mitochondrial membrane potential (MMP) and activating ionic current. Interestingly, even though all neurons changed their MMP and activated ionic currents, part of the neurons activated only outward currents and the remaining ones activated outward and inward currents. These findings were independent of intracellular Ca^{2+} release, since none of the treatments increase intracellular Ca^{2+} concentration.

When combined with CCCP, the antioxidants impacted profoundly on the MMP generating a drastic reduction in the red/green ratio in JC-1 experiments. Both antioxidants activated outward and inward currents, but combination of CCCP+Trolox seemed to slightly increase the inward current. Combination of CCCP+DTT had a similar effect but the inward current seemed to be even more pronounced. Both antioxidants were able to reverse the CCCP-induced hyperpolarization in 40% of the neurons tested.

These results suggest two possibilities: 1) there are two different populations of LC neurons as judged by the sensitivity to the antioxidants; 2) there is a necessary basal level of free radicals in the intracellular space that seems to be part of the regulation of ionic channels in mice LC neurons.

This work needs further studies and will constitute part of my postdoctoral research.

6.6. Supplementary Results

6.6.1. Effect of High BAPTA on the CCCP-induced hyperpolarization

To further confirm that the CCCP-induced hyperpolarization was independent of intracellular Ca^{2+}, high BAPTA (10mM) was added to the internal pipette solution producing no differences in the CCCP-induced hyperpolarization (Supplementary Figure 6.1).

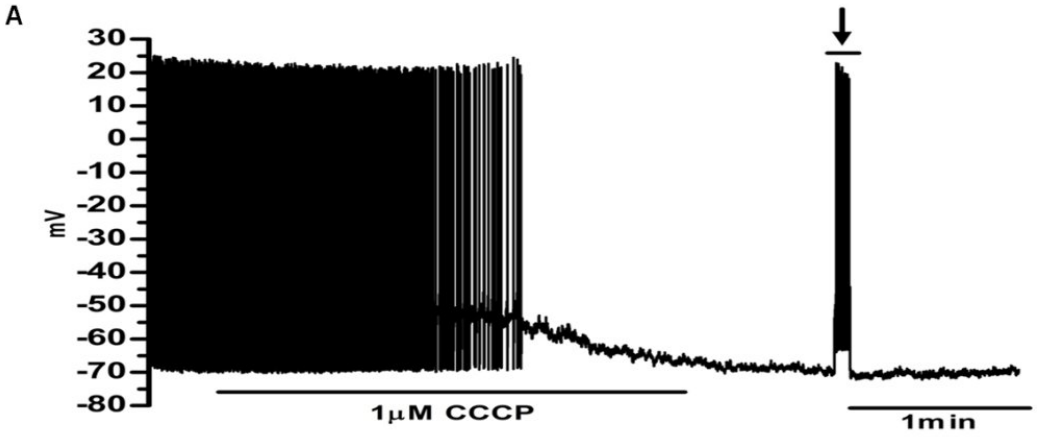

Supplementary Figure 6.1: Effect of High (10mM) BAPTA internal pipette solution on the CCCP-induced outward current. ***A,*** Representative current clamp recording demonstrating that High BAPTA did not alter the CCCP-induced hyperpolarization.

Chapter 7

General Discussion

The research of this thesis was generated in a 3.5-year period and comprises 4 individual research chapters, studying a different aspect of the pacemaker process occurring in mice LC neurons. As has been stated, my specific interest in LC neurons came from their fundamental participation in modulating many brain activities and their possible role in neuropathologies such as PD. The LC provides the largest pool of noradrenergic neurons in the brain that project to virtually all cerebral regions. As such they have a fundamental role in brain homeostasis, one that is so important that deletion of the LC causes irreversible clinical coma. LC neurons are spontaneously active due to an intrinsic pacemaker process and it is this mechanism, which holds the key for most functions exerted by these neurons. Importantly, these neurons tend to entrain their pacemaker cycles such that LC firing leads to synchronised neurotransmitter release over large brain regions. The understanding of the pacemaker process and all related mechanisms such as neuronal synchronisation represent a step further to understanding of fundamental brain functions such as mood states and specific neuropathologies.

Chapter 3 presents methodological findings that improve the quality of electrophysiological experiments, an outcome that is of general relevance. During the experiments it was observed that voltage control during voltage clamp experiments could be more easily achieved when mice were anesthetized with Ketamine prior to being euthanized by decapitation compared to animals that did not receive any anaesthesia. Ketamine has protective effects against damage caused by ischemia; as the slice preparation procedure could lead to ischemia, ketamine was chosen as the standard anaesthetic for all studies in this thesis. The protective effect probably arose from the combination of NMDA inhibition along with blockage of Na^+ and K^+ channels exerted by Ketamine, decreasing metabolic demands and other processes that could damage the

cells during the slicing procedure. Electrophysiologically, it was reflected as an increase in input resistance in the ketamine group compared to control groups, indicating better neuronal viability. This improvement in neuronal electrical properties increased the rate of success in voltage clamp experiments.

Chapter 4 presents a detailed characterization of the basic pacemaker currents responsible for driving membrane depolarization to reach threshold and initiate an action potential in mice LC neurons. A TTX-sensitive Na^+ current was identified as the unique inward current present within the interspike interval having as a counterpart a high TEA-sensitive K^+ current, probably composed of $K_V1.1$-5 channels. Ca^{2+} currents were also present in LC neurons but did not subserve in pacemaking, being activated at membrane potentials positive to the interspike interval voltage range. This finding suggested an important difference between the pacemaker currents in mouse and rat LC neurons, as it has been previously demonstrated that rat LC neurons exhibit a persistent Ca^{2+} current active within the interspike interval. This lack of a persistent Ca^{2+} current probably has a significant impact on the rest state of mouse and rat LC neurons, as Ca^{2+}-dependent pathways would probably have a different state of activation for both species. Moreover, the net pacemaker current determined by differentiating the average of interspike interval voltage recordings compared closely to pharmacologically isolated currents measured under voltage clamp. Overall, this third chapter is of special importance in providing insight into the currents responsible for driving pacemaking in mouse LC neurons. It not only provides the background necessary to further studies involving mouse LC neurons but it also paves the way for the use of transgenic mice.

Chapter 5 presents a study comparing ionic currents of mouse LC neurons during development. This is of fundamental importance, as the majority of electrophysiological

studies reported in the literature have been performed on neurons from very young animals. The use of LC from infant animal models is justified due the difficulty and poorer quality of slice (also cell isolation) preparations when adult animals are used; however the resultant findings may not necessarily apply to adults. Comparison of electrophysiological properties of infant and adult mice LC neurons in slices demonstrated a decrease in spontaneous firing from 90 to 50%, respectively. This reduction in firing of adult LC neurons correlated with a more negative resting membrane potential and changes in the magnitude of ionic currents. It was found that the depolarization-induced K^+ current was increased in adult neurons. The magnitude of the TTX-sensitive Na^+ current was also changed, being larger within the interspike interval. Such an increase could compensate for the more negative resting membrane potential of adult neurons. In comparison, Ca^{2+} currents were almost unchanged at the two ages. The sensitivity to the K^+ blocker 4-AP was changed, with this agent also causing substantial increase in voltage noise. TTX-resistant spikes that were not common in infant mice were more frequently observed in adult LC neurons. These results indicate that a range of electrophysiological properties change during development.

The finding that mitochondria can have a role in pacemaking in various tissues led to the studies of Chapter 6, which presents an examination of the effects of perturbation of mitochondrial function on the electrophysiological properties of LC neurons induced by application of the protonophore CCCP (1 μM). This caused a depolarization of the mitochondrial membrane potential and induced a small depolarization followed by a sustained membrane hyperpolarization, the latter leading to abolition of spontaneous action potentials. It was demonstrated that the membrane hyperpolarization was caused by a non-inactivating K^+ current mainly carried by Ca^{2+}-activated K^+ channels of the SK

type (i.e. apamin-sensitive). External Ca^{2+} entry was a mandatory step for generation of the outward current and not release from intracellular Ca^{2+} sources, suggesting that this process occurs in cellular microdomains. The CCCP-induced outward current was dependent on the activity of nifedipine-sensitive channels, suggesting that L-type Ca^{2+} channels are involved in this process. This was a surprising finding given that these channels were activated at membrane potentials more hyperpolarized than their usual range of activation. However, the findings fit with recent findings on other cells where disturbances in mitochondrial function led to direct modulation of the activity of L-type channels. The fact that this also happens in LC neurons in a case where there was only a small depolarization in mitochondrial membrane potential highlights the potential significance of this mechanism in the brain. While these mechanisms are of fundamental relevance to LC pacemaking they are also of considerable importance to understanding the consequences on neuronal function that stroke-associated ischemia/reperfusion and other neuropathologies such as PD where mitochondrial dysfunction has been implicated. The possibility that mitochondrial insult can lead to enhanced persistent Ca^{2+} influx by targeting L-type Ca^{2+} channels could represent a major challenge to neuronal survival.

Taken together the results presented here demonstrated that the pacemaker process of mice LC neurons is a complex process driven by a combination of currents that balance each other to generate spontaneous activity. The pacemaker currents driving this process show differences between infant and adult animals, suggesting that postnatal developmental adaptations happen in this system. In addition, this thesis suggests a direct involvement of a new component (mitochondria) in modulation of LC pacemaking. Our study suggested that such mitochondrial modulation, as reflected by a decrease in the proton gradient (viz. mitochondrial membrane potential) resulted in

direct and/or indirect activation of ionic channels changing factors such as membrane potential and by this means impacting on spontaneous LC neuronal firing. These findings led to the suggestion that mitochondria act as a multi point regulator of pacemaking in LC neurons.

Perspectives

- Analysis of the noradrenergic signalling provided by LC neurons in the development and progression of Parkinson's diseases.

The solid base constructed in the present thesis will allow me to undergo studies analysing the influence of LC neurons in the progression of PD. Animal models where LC neurons will be deleted along with transgenic models where specific ionic channels present in LC neurons will be deleted, will allow me to analyse the impact of noradrenergic signalling on the viability/death of Substantia Nigra (SN) neurons. Comparisons will also be made between the effects and relative sensitivities to mitochondrial challenge of SN compared to LC neurons and the protective effects of noradrenaline. This project aim is to identify the very early symptoms of PD developed when LC neurons start to inefficiently deliver noradrenaline to the brain and SN. Hopefully, all these studies will contribute to the finding of an early intervention for PD, preventing the development and progression of this pathology.

References

1. Swanson, L.W., *The locus coeruleus: a cytoarchitectonic, Golgi and immunohistochemical study in the albino rat.* Brain Res, 1976. **110**(1): p. 39-56.
2. Foote, S.L., F.E. Bloom, and G. Aston-Jones, *Nucleus locus ceruleus: new evidence of anatomical and physiological specificity.* Physiol Rev, 1983. **63**(3): p. 844-914.
3. Olson, L. and K. Fuxe, *On the projections from the locus coeruleus noradrealine neurons: the cerebellar innervation.* Brain Res, 1971. **28**(1): p. 165-71.
4. Ennis, M. and G. Aston-Jones, *GABA-mediated inhibition of locus coeruleus from the dorsomedial rostral medulla.* J Neurosci, 1989. **9**(8): p. 2973-81.
5. Ennis, M. and G. Aston-Jones, *Activation of locus coeruleus from nucleus paragigantocellularis: a new excitatory amino acid pathway in brain.* J Neurosci, 1988. **8**(10): p. 3644-57.
6. Jouvet, M., *The role of monoamines and acetylcholine-containing neurons in the regulation of the sleep-waking cycle.* Ergeb Physiol, 1972. **64**: p. 166-307.
7. Aston-Jones, G., C. Chiang, and T. Alexinsky, *Discharge of noradrenergic locus coeruleus neurons in behaving rats and monkeys suggests a role in vigilance.* Prog Brain Res, 1991. **88**: p. 501-20.
8. Aston-Jones, G., et al., *Locus coeruleus neurons in monkey are selectively activated by attended cues in a vigilance task.* J Neurosci, 1994. **14**(7): p. 4467-80.
9. Arnsten, A.F. and P.S. Goldman-Rakic, *Selective prefrontal cortical projections to the region of the locus coeruleus and raphe nuclei in the rhesus monkey.* Brain Res, 1984. **306**(1-2): p. 9-18.
10. Vankov, A., A. Herve-Minvielle, and S.J. Sara, *Response to novelty and its rapid habituation in locus coeruleus neurons of the freely exploring rat.* Eur J Neurosci, 1995. **7**(6): p. 1180-7.
11. Usher, M., et al., *The role of locus coeruleus in the regulation of cognitive performance.* Science, 1999. **283**(5401): p. 549-54.
12. Ward, D.G. and C.G. Gunn, *Locus coeruleus complex: elicitation of a pressor response and a brain stem region necessary for its occurrence.* Brain Res, 1976. **107**(2): p. 401-6.

13. Foote, S.L., G. Aston-Jones, and F.E. Bloom, *Impulse activity of locus coeruleus neurons in awake rats and monkeys is a function of sensory stimulation and arousal.* Proc Natl Acad Sci U S A, 1980. **77**(5): p. 3033-7.
14. Graham, A.W. and G.K. Aghajanian, *Effects of amphetamine on single cell activity in a catecholamine nucleus, the locus coeruleus.* Nature, 1971. **234**(5324): p. 100-2.
15. Rasmussen, K. and G.K. Aghajanian, *Effect of hallucinogens on spontaneous and sensory-evoked locus coeruleus unit activity in the rat: reversal by selective 5-HT2 antagonists.* Brain Res, 1986. **385**(2): p. 395-400.
16. Williams, J.T. and R.A. North, *Opiate-receptor interactions on single locus coeruleus neurones.* Mol Pharmacol, 1984. **26**(3): p. 489-97.
17. Andrade, R., C.P. Vandermaelen, and G.K. Aghajanian, *Morphine tolerance and dependence in the locus coeruleus: single cell studies in brain slices.* Eur J Pharmacol, 1983. **91**(2-3): p. 161-9.
18. Masuko, S., et al., *Noradrenergic neurons from the locus ceruleus in dissociated cell culture: culture methods, morphology, and electrophysiology.* J Neurosci, 1986. **6**(11): p. 3229-41.
19. Miyake, M., M.J. Christie, and R.A. North, *Single potassium channels opened by opioids in rat locus ceruleus neurons.* Proc Natl Acad Sci U S A, 1989. **86**(9): p. 3419-22.
20. Ballantyne, D., et al., *Rhythms, synchrony and electrical coupling in the Locus coeruleus.* Respir Physiol Neurobiol, 2004. **143**(2-3): p. 199-214.
21. Christie, M.J., J.T. Williams, and R.A. North, *Electrical coupling synchronizes subthreshold activity in locus coeruleus neurons in vitro from neonatal rats.* J Neurosci, 1989. **9**(10): p. 3584-9.
22. Ishimatsu, M. and J.T. Williams, *Synchronous activity in locus coeruleus results from dendritic interactions in pericoerulear regions.* J Neurosci, 1996. **16**(16): p. 5196-204.
23. Rash, J.E., et al., *Identification of connexin36 in gap junctions between neurons in rodent locus coeruleus.* Neuroscience, 2007. **147**(4): p. 938-56.
24. Gesi, M., et al., *The role of the locus coeruleus in the development of Parkinson's disease.* Neurosci Biobehav Rev, 2000. **24**(6): p. 655-68.

25. Wichmann, T. and M.R. DeLong, *Pathophysiology of parkinsonian motor abnormalities.* Adv Neurol, 1993. **60**: p. 53-61.
26. Brotchie, P., R. Iansek, and M. Horne, *A neural network model of neural activity in the monkey globus pallidus.* Neurosci Lett, 1991. **131**(1): p. 33-6.
27. Whitton, P.S., *Inflammation as a causative factor in the aetiology of Parkinson's disease.* Br J Pharmacol, 2007. **150**(8): p. 963-76.
28. Parker, W.D., Jr., J.K. Parks, and R.H. Swerdlow, *Complex I deficiency in Parkinson's disease frontal cortex.* Brain Res, 2008. **1189**: p. 215-8.
29. Forno, L.S., *Neuropathology of Parkinson's disease.* J Neuropathol Exp Neurol, 1996. **55**(3): p. 259-72.
30. Bing, G., et al., *Locus coeruleus lesions potentiate neurotoxic effects of MPTP in dopaminergic neurons of the substantia nigra.* Brain Res, 1994. **668**(1-2): p. 261-5.
31. Fornai, F., et al., *Noradrenergic modulation of methamphetamine-induced striatal dopamine depletion.* Ann N Y Acad Sci, 1998. **844**: p. 166-77.
32. Kilbourn, M.R., P. Sherman, and L.C. Abbott, *Reduced MPTP neurotoxicity in striatum of the mutant mouse tottering.* Synapse, 1998. **30**(2): p. 205-10.
33. Aghajanian, G.K., *Tolerance of locus coeruleus neurones to morphine and suppression of withdrawal response by clonidine.* Nature, 1978. **276**(5684): p. 186-8.
34. Koob, G.F., R. Maldonado, and L. Stinus, *Neural substrates of opiate withdrawal.* Trends Neurosci, 1992. **15**(5): p. 186-91.
35. Valentino, R.J., et al., *Activation of the locus ceruleus brain noradrenergic system during stress: circuitry, consequences, and regulation.* Adv Pharmacol, 1998. **42**: p. 781-4.
36. Bunney, B.S. and G.K. Aghajanian, *d-Amphetamine-induced depression of central dopamine neurons: evidence for mediation by both autoreceptors and a striato-nigral feedback pathway.* Naunyn Schmiedebergs Arch Pharmacol, 1978. **304**(3): p. 255-61.
37. Nestler, E.J., M. Alreja, and G.K. Aghajanian, *Molecular control of locus coeruleus neurotransmission.* Biol Psychiatry, 1999. **46**(9): p. 1131-9.

38. Alreja, M. and G.K. Aghajanian, *Activation of locus coeruleus (LC) neurones by cholera toxin: mediation by cAMP-dependent protein kinase.* Neurosci Lett, 1991. **134**(1): p. 113-7.
39. Alreja, M. and G.K. Aghajanian, *Pacemaker activity of locus coeruleus neurons: whole-cell recordings in brain slices show dependence on cAMP and protein kinase A.* Brain Res, 1991. **556**(2): p. 339-43.
40. Pineda, J., J.H. Kogan, and G.K. Aghajanian, *Nitric oxide and carbon monoxide activate locus coeruleus neurons through a cGMP-dependent protein kinase: involvement of a nonselective cationic channel.* J Neurosci, 1996. **16**(4): p. 1389-99.
41. Nestler, E.J. and G.K. Aghajanian, *Molecular and cellular basis of addiction.* Science, 1997. **278**(5335): p. 58-63.
42. Vander, A.J., J.H. Sherman, and D.S. Luciano, *Human physiology : the mechanisms of body function*. 7th ed. McGraw-Hill's college custom series. 1998, Boston: McGraw Hill. xxviii, 818 p.
43. Ballard, C., *The heart and blood*. 2003, Chicago, Ill.: Heinemann Library. 48 p.
44. DiFrancesco, D., *The contribution of the 'pacemaker' current (if) to generation of spontaneous activity in rabbit sino-atrial node myocytes.* J Physiol, 1991. **434**: p. 23-40.
45. Irisawa, H., H.F. Brown, and W. Giles, *Cardiac pacemaking in the sinoatrial node.* Physiol Rev, 1993. **73**(1): p. 197-227.
46. Van Helden, D.F., *Pacemaker potentials in lymphatic smooth muscle of the guinea-pig mesentery.* J Physiol, 1993. **471**: p. 465-79.
47. Hashitani, H., D.F. Van Helden, and H. Suzuki, *Properties of spontaneous depolarizations in circular smooth muscle cells of rabbit urethra.* Br J Pharmacol, 1996. **118**(7): p. 1627-32.
48. van Helden, D.F., et al., *Role of calcium stores and membrane voltage in the generation of slow wave action potentials in guinea-pig gastric pylorus.* J Physiol, 2000. **524 Pt 1**: p. 245-65.
49. van Helden, D.F. and M.S. Imtiaz, *Ca2+ phase waves: a basis for cellular pacemaking and long-range synchronicity in the guinea-pig gastric pylorus.* J Physiol, 2003. **548**(Pt 1): p. 271-96.

50. Imtiaz, M.S., et al., *SR Ca2+ store refill--a key factor in cardiac pacemaking.* J Mol Cell Cardiol, 2010. **49**(3): p. 412-26.
51. Lakatta, E.G. and D. DiFrancesco, *What keeps us ticking: a funny current, a calcium clock, or both?* J Mol Cell Cardiol, 2009. **47**(2): p. 157-70.
52. Strogatz, S.H. and I. Stewart, *Coupled oscillators and biological synchronization.* Sci Am, 1993. **269**(6): p. 102-9.
53. Imtiaz, M.S., D.W. Smith, and D.F. van Helden, *A theoretical model of slow wave regulation using voltage-dependent synthesis of inositol 1,4,5-trisphosphate.* Biophys J, 2002. **83**(4): p. 1877-90.
54. Imtiaz, M.S., et al., *Pacemaking through Ca2+ stores interacting as coupled oscillators via membrane depolarization.* Biophys J, 2007. **92**(11): p. 3843-61.
55. Bird, S.J. and M.J. Kuhar, *Iontophoretic application of opiates to the locus coeruleus.* Brain Res, 1977. **122**(3): p. 523-33.
56. Cedarbaum, J.M. and G.K. Aghajanian, *Noradrenergic neurons of the locus coeruleus: inhibition by epinephrine and activation by the alpha-antagonist piperoxane.* Brain Res, 1976. **112**(2): p. 413-9.
57. Guyenet, P.G. and G.K. Aghajanian, *Excitation of neurons in the nucleus locus coeruleus by substance P and related peptides.* Brain Res, 1977. **136**(1): p. 178-84.
58. Wang, Y.Y. and G.K. Aghajanian, *Excitation of locus coeruleus neurons by an adenosine 3',5'-cyclic monophosphate-activated inward current: extracellular and intracellular studies in rat brain slices.* Synapse, 1987. **1**(5): p. 481-7.
59. Aghajanian, G.K. and Y.Y. Wang, *Common alpha 2- and opiate effector mechanisms in the locus coeruleus: intracellular studies in brain slices.* Neuropharmacology, 1987. **26**(7B): p. 793-9.
60. North, R.A. and J.T. Williams, *On the potassium conductance increased by opioids in rat locus coeruleus neurones.* J Physiol, 1985. **364**: p. 265-80.
61. Williams, J.T., R.A. North, and T. Tokimasa, *Inward rectification of resting and opiate-activated potassium currents in rat locus coeruleus neurons.* J Neurosci, 1988. **8**(11): p. 4299-306.
62. Aghajanian, G.K. and Y.Y. Wang, *Pertussis toxin blocks the outward currents evoked by opiate and alpha 2-agonists in locus coeruleus neurons.* Brain Res, 1986. **371**(2): p. 390-4.

63. Oyamada, Y., et al., *Respiration-modulated membrane potential and chemosensitivity of locus coeruleus neurones in the in vitro brainstem-spinal cord of the neonatal rat.* J Physiol, 1998. **513 (Pt 2)**: p. 381-98.
64. Alvarez, V.A., et al., *Frequency-dependent synchrony in locus ceruleus: role of electrotonic coupling.* Proc Natl Acad Sci U S A, 2002. **99**(6): p. 4032-6.
65. Torrecilla, M., et al., *G-protein-gated potassium channels containing Kir3.2 and Kir3.3 subunits mediate the acute inhibitory effects of opioids on locus ceruleus neurons.* J Neurosci, 2002. **22**(11): p. 4328-34.
66. Murai, Y. and T. Akaike, *Orexins cause depolarization via nonselective cationic and K+ channels in isolated locus coeruleus neurons.* Neurosci Res, 2005. **51**(1): p. 55-65.
67. Forsythe, I.D., P. Linsdell, and P.R. Stanfield, *Unitary A-currents of rat locus coeruleus neurones grown in cell culture: rectification caused by internal Mg2+ and Na+.* J Physiol, 1992. **451**: p. 553-83.
68. Sausbier, U., et al., *Ca2+ -activated K+ channels of the BK-type in the mouse brain.* Histochem Cell Biol, 2006. **125**(6): p. 725-41.
69. Stocker, M. and P. Pedarzani, *Differential distribution of three Ca(2+)-activated K(+) channel subunits, SK1, SK2, and SK3, in the adult rat central nervous system.* Mol Cell Neurosci, 2000. **15**(5): p. 476-93.
70. Murai, Y., et al., *Ca2+-activated K+ currents in rat locus coeruleus neurons induced by experimental ischemia, anoxia, and hypoglycemia.* J Neurophysiol, 1997. **78**(5): p. 2674-81.
71. Bayliss, D.A., et al., *TASK-1 is a highly modulated pH-sensitive 'leak' K(+) channel expressed in brainstem respiratory neurons.* Respir Physiol, 2001. **129**(1-2): p. 159-74.
72. Nieber, K., J. Sevcik, and P. Illes, *Hypoxic changes in rat locus coeruleus neurons in vitro.* J Physiol, 1995. **486 (Pt 1)**: p. 33-46.
73. Shen, K.Z. and R.A. North, *Substance P opens cation channels and closes potassium channels in rat locus coeruleus neurons.* Neuroscience, 1992. **50**(2): p. 345-53.
74. van den Pol, A.N., et al., *Hypocretin (orexin) enhances neuron activity and cell synchrony in developing mouse GFP-expressing locus coeruleus.* J Physiol, 2002. **541**(Pt 1): p. 169-85.

75. Filosa, J.A. and R.W. Putnam, *Multiple targets of chemosensitive signaling in locus coeruleus neurons: role of K+ and Ca2+ channels.* Am J Physiol Cell Physiol, 2003. **284**(1): p. C145-55.
76. Alreja, M. and G.K. Aghajanian, *Opiates suppress a resting sodium-dependent inward current and activate an outward potassium current in locus coeruleus neurons.* J Neurosci, 1993. **13**(8): p. 3525-32.
77. Chieng, B. and J.M. Bekkers, *GABA(B), opioid and alpha2 receptor inhibition of calcium channels in acutely-dissociated locus coeruleus neurones.* Br J Pharmacol, 1999. **127**(7): p. 1533-8.
78. Bennett, B.D., J.C. Callaway, and C.J. Wilson, *Intrinsic membrane properties underlying spontaneous tonic firing in neostriatal cholinergic interneurons.* J Neurosci, 2000. **20**(22): p. 8493-503.
79. Forti, L., et al., *Ionic mechanisms of autorhythmic firing in rat cerebellar Golgi cells.* J Physiol, 2006. **574**(Pt 3): p. 711-29.
80. Chan, C.S., et al., *HCN2 and HCN1 channels govern the regularity of autonomous pacemaking and synaptic resetting in globus pallidus neurons.* J Neurosci, 2004. **24**(44): p. 9921-32.
81. Bevan, M.D. and C.J. Wilson, *Mechanisms underlying spontaneous oscillation and rhythmic firing in rat subthalamic neurons.* J Neurosci, 1999. **19**(17): p. 7617-28.
82. Do, M.T. and B.P. Bean, *Subthreshold sodium currents and pacemaking of subthalamic neurons: modulation by slow inactivation.* Neuron, 2003. **39**(1): p. 109-20.
83. Magistretti, J., et al., *Kinetic and functional analysis of transient, persistent and resurgent sodium currents in rat cerebellar granule cells in situ: an electrophysiological and modelling study.* J Physiol, 2006. **573**(Pt 1): p. 83-106.
84. Taddese, A. and B.P. Bean, *Subthreshold sodium current from rapidly inactivating sodium channels drives spontaneous firing of tuberomammillary neurons.* Neuron, 2002. **33**(4): p. 587-600.
85. Magistretti, J. and A. Alonso, *Fine gating properties of channels responsible for persistent sodium current generation in entorhinal cortex neurons.* J Gen Physiol, 2002. **120**(6): p. 855-73.

86. Raman, I.M., et al., *Altered subthreshold sodium currents and disrupted firing patterns in Purkinje neurons of Scn8a mutant mice.* Neuron, 1997. **19**(4): p. 881-91.
87. Magistretti, J. and A. Alonso, *Multiple conductance substates in pharmacologically untreated Na(+) channels generating persistent openings in rat entorhinal cortex neurons.* J Membr Biol, 2006. **214**(3): p. 165-80.
88. Enomoto, A., et al., *Participation of sodium currents in burst generation and control of membrane excitability in mesencephalic trigeminal neurons.* J Neurosci, 2006. **26**(13): p. 3412-22.
89. Golomb, D., C. Yue, and Y. Yaari, *Contribution of persistent Na+ current and M-type K+ current to somatic bursting in CA1 pyramidal cells: combined experimental and modeling study.* J Neurophysiol, 2006. **96**(4): p. 1912-26.
90. Crill, W.E., *Persistent sodium current in mammalian central neurons.* Annu Rev Physiol, 1996. **58**: p. 349-62.
91. Vervaeke, K., et al., *Contrasting effects of the persistent Na+ current on neuronal excitability and spike timing.* Neuron, 2006. **49**(2): p. 257-70.
92. Wilson, C.J. and J.C. Callaway, *Coupled oscillator model of the dopaminergic neuron of the substantia nigra.* J Neurophysiol, 2000. **83**(5): p. 3084-100.
93. Puopolo, M., E. Raviola, and B.P. Bean, *Roles of subthreshold calcium current and sodium current in spontaneous firing of mouse midbrain dopamine neurons.* J Neurosci, 2007. **27**(3): p. 645-56.
94. Williams, J.T., et al., *Membrane properties of rat locus coeruleus neurones.* Neuroscience, 1984. **13**(1): p. 137-56.
95. Michel, P.P., et al., *Role of activity-dependent mechanisms in the control of dopaminergic neuron survival.* J Neurochem, 2007. **101**(2): p. 289-97.
96. Lehninger, A.L., D.L. Nelson, and M.M. Cox, *Lehninger principles of biochemistry*. 5th ed. 2008, New York: W.H. Freeman. 1 v. (various pagings).
97. Hajnoczky, G., et al., *Mitochondrial calcium signalling and cell death: approaches for assessing the role of mitochondrial Ca2+ uptake in apoptosis.* Cell Calcium, 2006. **40**(5-6): p. 553-60.
98. de Oliveira, M.R. and J.C. Moreira, *Acute and chronic vitamin A supplementation at therapeutic doses induces oxidative stress in*

submitochondrial particles isolated from cerebral cortex and cerebellum of adult rats. Toxicol Lett, 2007. **173**(3): p. 145-50.

99. Klamt, F., et al., *Vitamin A treatment induces apoptosis through an oxidant-dependent activation of the mitochondrial pathway.* Cell Biol Int, 2008. **32**(1): p. 100-6.
100. Babcock, D.F., et al., *Mitochondrial participation in the intracellular Ca2+ network.* J Cell Biol, 1997. **136**(4): p. 833-44.
101. de Oliveira, R.B., et al., *Can electrons travel through actin microfilaments and generate oxidative stress in retinol treated Sertoli cell?* Mol Cell Biochem, 2007. **301**(1-2): p. 33-45.
102. Barstow, K.L., et al., *The modulation of action potential generation by calcium-induced calcium release is enhanced by mitochondrial inhibitors in mudpuppy parasympathetic neurons.* Neuroscience, 2004. **124**(2): p. 327-39.
103. Ferranti, R., M.M. da Silva, and A.J. Kowaltowski, *Mitochondrial ATP-sensitive K+ channel opening decreases reactive oxygen species generation.* FEBS Lett, 2003. **536**(1-3): p. 51-5.
104. Bergmann, F. and B.U. Keller, *Impact of mitochondrial inhibition on excitability and cytosolic Ca2+ levels in brainstem motoneurones from mouse.* J Physiol, 2004. **555**(Pt 1): p. 45-59.
105. Lehninger, A.L., *Energy coupling in electron transport.* Fed Proc, 1967. **26**(5): p. 1333-4.
106. Lehninger, A.L., E. Carafoli, and C.S. Rossi, *Energy-linked ion movements in mitochondrial systems.* Adv Enzymol Relat Areas Mol Biol, 1967. **29**: p. 259-320.
107. Rossi, C.S., et al., *Proton movements across the mitochondrial membrane supported by hydrolysis of adenosine triphosphate.* Eur J Biochem, 1967. **2**(3): p. 332-40.
108. Kirichok, Y., G. Krapivinsky, and D.E. Clapham, *The mitochondrial calcium uniporter is a highly selective ion channel.* Nature, 2004. **427**(6972): p. 360-4.
109. Babcock, D.F. and B. Hille, *Mitochondrial oversight of cellular Ca2+ signaling.* Curr Opin Neurobiol, 1998. **8**(3): p. 398-404.

110. Kovacs, R., et al., *Mitochondrial calcium ion and membrane potential transients follow the pattern of epileptiform discharges in hippocampal slice cultures.* J Neurosci, 2005. **25**(17): p. 4260-9.
111. Ishii, K., K. Hirose, and M. Iino, *Ca2+ shuttling between endoplasmic reticulum and mitochondria underlying Ca2+ oscillations.* EMBO Rep, 2006. **7**(4): p. 390-6.
112. Gutteridge, J.M. and B. Halliwell, *Comments on review of Free Radicals in Biology and Medicine, second edition, by Barry Halliwell and John M. C. Gutteridge.* Free radical biology & medicine, 1992. **12**(1): p. 93-5.
113. Halliwell, B. and J.M. Gutteridge, *Oxygen free radicals and iron in relation to biology and medicine: some problems and concepts.* Archives of biochemistry and biophysics, 1986. **246**(2): p. 501-14.
114. Zima, A.V. and L.A. Blatter, *Redox regulation of cardiac calcium channels and transporters.* Cardiovasc Res, 2006. **71**(2): p. 310-21.
115. Choi, Y.B. and S.A. Lipton, *Redox modulation of the NMDA receptor.* Cellular and molecular life sciences : CMLS, 2000. **57**(11): p. 1535-41.
116. Davidson, S.M. and M.R. Duchen, *Calcium microdomains and oxidative stress.* Cell Calcium, 2006. **40**(5-6): p. 561-74.
117. Rizzuto, R. and T. Pozzan, *Microdomains of intracellular Ca2+: molecular determinants and functional consequences.* Physiol Rev, 2006. **86**(1): p. 369-408.
118. Collins, A. and M. Larson, *Differential sensitivity of inward rectifier K+ channels to metabolic inhibitors.* J Biol Chem, 2002. **277**(39): p. 35815-8.
119. Collins, A., H. Wang, and M.K. Larson, *Differential sensitivity of Kir2 inward-rectifier potassium channels to a mitochondrial uncoupler: identification of a regulatory site.* Mol Pharmacol, 2005. **67**(4): p. 1214-20.
120. Viola, H.M. and L.C. Hool, *Cross-talk between L-type Ca2+ channels and mitochondria.* Clin Exp Pharmacol Physiol, 2010. **37**(2): p. 229-35.
121. Campbell, D.L., J.S. Stamler, and H.C. Strauss, *Redox modulation of L-type calcium channels in ferret ventricular myocytes. Dual mechanism regulation by nitric oxide and S-nitrosothiols.* J Gen Physiol, 1996. **108**(4): p. 277-93.

122. Akaishi, T., et al., *Hydrogen peroxide modulates whole cell Ca2+ currents through L-type channels in cultured rat dentate granule cells.* Neurosci Lett, 2004. **356**(1): p. 25-8.

123. Thatcher, R.W., *Cyclic cortical reorganization during early childhood.* Brain Cogn, 1992. **20**(1): p. 24-50.

124. Thatcher, R.W., R.A. Walker, and S. Giudice, *Human cerebral hemispheres develop at different rates and ages.* Science, 1987. **236**(4805): p. 1110-3.

125. Johnson, M.H., *Functional brain development in humans.* Nat Rev Neurosci, 2001. **2**(7): p. 475-83.

126. Rogoff, B., *Apprenticeship in Thinking: Cognitive Development in Social Context*

Vol. 1. 1990: Oxford University Press.

127. Bandtlow, C.E. and D.R. Zimmermann, *Proteoglycans in the developing brain: new conceptual insights for old proteins.* Physiol Rev, 2000. **80**(4): p. 1267-90.

128. Chang, S., F.G. Rathjen, and J.A. Raper, *Extension of neurites on axons is impaired by antibodies against specific neural cell surface glycoproteins.* J Cell Biol, 1987. **104**(2): p. 355-62.

129. Murakami, F., W.J. Song, and H. Katsumaru, *Plasticity of neuronal connections in developing brains of mammals.* Neurosci Res, 1992. **15**(4): p. 235-53.

130. Katz, L.C. and C.J. Shatz, *Synaptic activity and the construction of cortical circuits.* Science, 1996. **274**(5290): p. 1133-8.

131. Calabrese, B., M.S. Wilson, and S. Halpain, *Development and regulation of dendritic spine synapses.* Physiology (Bethesda), 2006. **21**: p. 38-47.

132. Adams, I. and D.G. Jones, *Synaptic remodelling and astrocytic hypertrophy in rat cerebral cortex from early to late adulthood.* Neurobiol Aging, 1982. **3**(3): p. 179-86.

133. Adams, I. and D.G. Jones, *Quantitative ultrastructural changes in rat cortical synapses during early-, mid- and late-adulthood.* Brain Res, 1982. **239**(2): p. 349-63.

134. Foster, R.E., B.W. Connors, and S.G. Waxman, *Rat optic nerve: electrophysiological, pharmacological and anatomical studies during development.* Brain Res, 1982. **255**(3): p. 371-86.

135. Guido, W., E. Gunhan-Agar, and R.S. Erzurumlu, *Developmental changes in the electrophysiological properties of brain stem trigeminal neurons during pattern (barrelette) formation.* J Neurophysiol, 1998. **79**(3): p. 1295-306.
136. Gogtay, N., et al., *Dynamic mapping of human cortical development during childhood through early adulthood.* Proc Natl Acad Sci U S A, 2004. **101**(21): p. 8174-9.
137. Burke, S.N. and C.A. Barnes, *Neural plasticity in the ageing brain.* Nat Rev Neurosci, 2006. **7**(1): p. 30-40.
138. Di Mascio, M., et al., *Reduced chaos of interspike interval of midbrain dopaminergic neurons in aged rats.* Neuroscience, 1999. **89**(4): p. 1003-8.
139. Ishida, Y., et al., *Age-Dependent Changes in Dopaminergic Neuron Firing Patterns in Substantia Nigra Pars Compacta.* Journal of Neural Transmission. Supplementa, 2009. **73** (G. Di Giovanni et al. (eds.), Birth, Life and Death of Dopaminergic Neurons in the Substantia Nigra).
140. Shirokawa, T., Y. Ishida, and K. Isobe, *Changes in electrophysiological properties of axon terminals of locus coeruleus neurons with age in F344 rat.* Neurosci Lett, 2000. **289**(1): p. 69-71.
141. Shirokawa, T., Y. Ishida, and K.I. Isobe, *Age-dependent changes in axonal branching of single locus coeruleus neurons projecting to two different terminal fields.* J Neurophysiol, 2000. **84**(2): p. 1120-2.
142. Ishida, Y., et al., *Age-dependent changes in projections from locus coeruleus to hippocampus dentate gyrus and frontal cortex.* Eur J Neurosci, 2000. **12**(4): p. 1263-70.
143. Klapstein, G.J., et al., *Electrophysiological and morphological changes in striatal spiny neurons in R6/2 Huntington's disease transgenic mice.* J Neurophysiol, 2001. **86**(6): p. 2667-77.
144. Nakamura, S., F. Kimura, and T. Sakaguchi, *Postnatal development of electrical activity in the locus ceruleus.* J Neurophysiol, 1987. **58**(3): p. 510-24.
145. Graham, B.A., A.M. Brichta, and R.J. Callister, *Pinch-current injection defines two discharge profiles in mouse superficial dorsal horn neurones, in vitro.* J Physiol, 2007. **578**(Pt 3): p. 787-98.

146. Graham, B.A., et al., *Distinct physiological mechanisms underlie altered glycinergic synaptic transmission in the murine mutants spastic, spasmodic, and oscillator.* J Neurosci, 2006. **26**(18): p. 4880-90.
147. Akaike, N. and A.J. Moorhouse, *Techniques: applications of the nerve-bouton preparation in neuropharmacology.* Trends Pharmacol Sci, 2003. **24**(1): p. 44-7.
148. Barry, P.H., *JPCalc, a software package for calculating liquid junction potential corrections in patch-clamp, intracellular, epithelial and bilayer measurements and for correcting junction potential measurements.* J Neurosci Methods, 1994. **51**(1): p. 107-16.
149. Smiley, S.T., et al., *Intracellular heterogeneity in mitochondrial membrane potentials revealed by a J-aggregate-forming lipophilic cation JC-1.* Proc Natl Acad Sci U S A, 1991. **88**(9): p. 3671-5.
150. Khaliq, Z.M. and B.P. Bean, *Dynamic, nonlinear feedback regulation of slow pacemaking by A-type potassium current in ventral tegmental area neurons.* J Neurosci, 2008. **28**(43): p. 10905-17.
151. Collins, V.J., C.A. Gorospe, and E.A. Rovenstine, *Intravenous nonbarbiturate, nonnarcotic analgesics: preliminary studies. 1. Cyclohexylamines.* Anesth Analg, 1960. **39**: p. 302-6.
152. Bergman, S.A., *Ketamine: review of its pharmacology and its use in pediatric anesthesia.* Anesth Prog, 1999. **46**(1): p. 10-20.
153. Mathisen, L.C., et al., *Effect of ketamine, an NMDA receptor inhibitor, in acute and chronic orofacial pain.* Pain, 1995. **61**(2): p. 215-20.
154. Newcomer, J.W., et al., *Ketamine-induced NMDA receptor hypofunction as a model of memory impairment and psychosis.* Neuropsychopharmacology, 1999. **20**(2): p. 106-18.
155. Reeker, W., et al., *High-dose S(+)-ketamine improves neurological outcome following incomplete cerebral ischemia in rats.* Can J Anaesth, 2000. **47**(6): p. 572-8.
156. Berman, R.M., et al., *Antidepressant effects of ketamine in depressed patients.* Biol Psychiatry, 2000. **47**(4): p. 351-4.
157. Stefanovic, A., et al., *Acute and chronic effects of ketamine on semantic priming: modeling schizophrenia?* J Clin Psychopharmacol, 2009. **29**(2): p. 124-33.

158. Himmelseher, S. and M.E. Durieux, *Revising a dogma: ketamine for patients with neurological injury?* Anesth Analg, 2005. **101**(2): p. 524-34, table of contents.
159. Morgan, C.J. and H.V. Curran, *Acute and chronic effects of ketamine upon human memory: a review.* Psychopharmacology (Berl), 2006. **188**(4): p. 408-24.
160. Schnoebel, R., et al., *Ketamine impairs excitability in superficial dorsal horn neurones by blocking sodium and voltage-gated potassium currents.* Br J Pharmacol, 2005. **146**(6): p. 826-33.
161. Leong, D., E. Puil, and D. Schwarz, *Ketamine blocks non-N-methyl-D-aspartate receptor channels attenuating glutamatergic transmission in the auditory cortex.* Acta Otolaryngol, 2004. **124**(4): p. 454-8.
162. Aston-Jones, G., J. Rajkowski, and J. Cohen, *Role of locus coeruleus in attention and behavioral flexibility.* Biol Psychiatry, 1999. **46**(9): p. 1309-20.
163. Swaab, D.F., A.M. Bao, and P.J. Lucassen, *The stress system in the human brain in depression and neurodegeneration.* Ageing Res Rev, 2005. **4**(2): p. 141-94.
164. Sodero, A.O., et al., *Locus coeruleus activity in perinatally protein-deprived rats: effects of fluoxetine administration.* Eur J Pharmacol, 2004. **503**(1-3): p. 35-42.
165. Charney, D.S., G.R. Heninger, and A. Breier, *Noradrenergic function in panic anxiety. Effects of yohimbine in healthy subjects and patients with agoraphobia and panic disorder.* Arch Gen Psychiatry, 1984. **41**(8): p. 751-63.
166. Aston-Jones, G. and F.E. Bloom, *Activity of norepinephrine-containing locus coeruleus neurons in behaving rats anticipates fluctuations in the sleep-waking cycle.* J Neurosci, 1981. **1**(8): p. 876-86.
167. Williams, J.T. and K.C. Marshall, *Membrane properties and adrenergic responses in locus coeruleus neurons of young rats.* J Neurosci, 1987. **7**(11): p. 3687-94.
168. Osmanovic, S.S. and S.A. Shefner, *Calcium-activated hyperpolarizations in rat locus coeruleus neurons in vitro.* J Physiol, 1993. **469**: p. 89-109.
169. Christie, M.J., J.T. Williams, and R.A. North, *Mechanisms of tolerance to opiates in locus coeruleus neurons.* NIDA Res Monogr, 1987. **78**: p. 158-68.

170. Rasmussen, K. and G.K. Aghajanian, *Withdrawal-induced activation of locus coeruleus neurons in opiate-dependent rats: attenuation by lesions of the nucleus paragigantocellularis.* Brain Res, 1989. **505**(2): p. 346-50.

171. Harris, G.C., Z.E. Hausken, and J.T. Williams, *Cocaine induced synchronous oscillations in central noradrenergic neurons in vitro.* Neuroscience, 1992. **50**(2): p. 253-7.

172. Christie, M.J., et al., *Where is the locus in opioid withdrawal?* Trends Pharmacol Sci, 1997. **18**(4): p. 134-40.

173. Callister, R.J., J.R. Keast, and P. Sah, *Ca(2+)-activated K+ channels in rat otic ganglion cells: role of Ca2+ entry via Ca2+ channels and nicotinic receptors.* J Physiol, 1997. **500 (Pt 3)**: p. 571-82.

174. Avery, R.B. and D. Johnston, *Multiple channel types contribute to the low-voltage-activated calcium current in hippocampal CA3 pyramidal neurons.* J Neurosci, 1996. **16**(18): p. 5567-82.

175. Koschak, A., et al., *alpha 1D (Cav1.3) subunits can form l-type Ca2+ channels activating at negative voltages.* J Biol Chem, 2001. **276**(25): p. 22100-6.

176. Jackson, A.C., G.L. Yao, and B.P. Bean, *Mechanism of spontaneous firing in dorsomedial suprachiasmatic nucleus neurons.* J Neurosci, 2004. **24**(37): p. 7985-98.

177. Bean, B.P., *The action potential in mammalian central neurons.* Nat Rev Neurosci, 2007. **8**(6): p. 451-65.

178. Williams, J.T., G. Henderson, and R.A. North, *Characterization of alpha 2-adrenoceptors which increase potassium conductance in rat locus coeruleus neurones.* Neuroscience, 1985. **14**(1): p. 95-101.

179. Hetzenauer, A., et al., *Brain activation pattern induced by stimulation of L-type Ca2+-channels: contribution of Ca(V)1.3 and Ca(V)1.2 isoforms.* Neuroscience, 2006. **139**(3): p. 1005-15.

180. Jackson, A.C. and B.P. Bean, *State-dependent enhancement of subthreshold A-type potassium current by 4-aminopyridine in tuberomammillary nucleus neurons.* J Neurosci, 2007. **27**(40): p. 10785-96.

181. Martina, M. and P. Jonas, *Functional differences in Na+ channel gating between fast-spiking interneurones and principal neurones of rat hippocampus.* J Physiol, 1997. **505 (Pt 3)**: p. 593-603.

182. Naundorf, B., F. Wolf, and M. Volgushev, *Unique features of action potential initiation in cortical neurons.* Nature, 2006. **440**(7087): p. 1060-3.
183. Wang, Y.Y. and G.K. Aghajanian, *Intracellular GTP gamma S restores the ability of morphine to hyperpolarize rat locus coeruleus neurons after blockade by pertussis toxin.* Brain Res, 1987. **436**(2): p. 396-401.
184. Liebau, S., et al., *Selective blockage of Kv1.3 and Kv3.1 channels increases neural progenitor cell proliferation.* J Neurochem, 2006. **99**(2): p. 426-37.
185. Pan, W.J., S.S. Osmanovic, and S.A. Shefner, *Adenosine decreases action potential duration by modulation of A-current in rat locus coeruleus neurons.* J Neurosci, 1994. **14**(3 Pt 1): p. 1114-22.
186. Shipley, M.T., et al., *Dendrites of locus coeruleus neurons extend preferentially into two pericoerulear zones.* J Comp Neurol, 1996. **365**(1): p. 56-68.
187. Ingram, S., et al., *Efficacy and kinetics of opioid action on acutely dissociated neurons.* Mol Pharmacol, 1997. **52**(1): p. 136-43.
188. Arima, J., et al., *alpha2-Adrenoceptor-mediated potassium currents in acutely dissociated rat locus coeruleus neurones.* J Physiol, 1998. **508 (Pt 1)**: p. 57-66.
189. Connor, M., S.L. Borgland, and M.J. Christie, *Continued morphine modulation of calcium channel currents in acutely isolated locus coeruleus neurons from morphine-dependent rats.* Br J Pharmacol, 1999. **128**(7): p. 1561-9.
190. Samuels, E.R. and E. Szabadi, *Functional neuroanatomy of the noradrenergic locus coeruleus: its roles in the regulation of arousal and autonomic function part I: principles of functional organisation.* Curr Neuropharmacol, 2008. **6**(3): p. 235-53.
191. Samuels, E.R. and E. Szabadi, *Functional neuroanatomy of the noradrenergic locus coeruleus: its roles in the regulation of arousal and autonomic function part II: physiological and pharmacological manipulations and pathological alterations of locus coeruleus activity in humans.* Curr Neuropharmacol, 2008. **6**(3): p. 254-85.
192. Roussel, B., et al., *[Locus ceruleus, paradoxal sleep, and cerebral noradrenaline].* C R Seances Soc Biol Fil, 1967. **161**(12): p. 2537-41.
193. Hobson, J.A., R.W. McCarley, and P.W. Wyzinski, *Sleep cycle oscillation: reciprocal discharge by two brainstem neuronal groups.* Science, 1975. **189**(4196): p. 55-8.

194. de Oliveira, R.B., et al., *Pacemaker currents in mouse locus coeruleus neurons.* Neuroscience, 2010.

195. Fujii, Y., S. Nakamura, and H. Ito, *Developmental changes in the electrical activity of locus coeruleus neurons during cortical spreading depression.* Brain Res Dev Brain Res, 1997. **104**(1-2): p. 91-100.

196. Downs, J.L., et al., *Orexin neuronal changes in the locus coeruleus of the aging rhesus macaque.* Neurobiol Aging, 2007. **28**(8): p. 1286-95.

197. Porkka-Heiskanen, T., et al., *The effect of age on prepro-orexin gene expression and contents of orexin A and B in the rat brain.* Neurobiol Aging, 2004. **25**(2): p. 231-8.

198. Rommelfanger, K.S. and D. Weinshenker, *Norepinephrine: The redheaded stepchild of Parkinson's disease.* Biochem Pharmacol, 2007. **74**(2): p. 177-90.

199. Grudzien, A., et al., *Locus coeruleus neurofibrillary degeneration in aging, mild cognitive impairment and early Alzheimer's disease.* Neurobiol Aging, 2007. **28**(3): p. 327-35.

200. Vasilyev, D.V. and M.E. Barish, *Postnatal development of the hyperpolarization-activated excitatory current Ih in mouse hippocampal pyramidal neurons.* J Neurosci, 2002. **22**(20): p. 8992-9004.

201. de Oliveira, R.B., et al., *Ketamine anesthesia helps preserve neuronal viability.* J Neurosci Methods, 2010.

202. Mora, F., G. Segovia, and A. del Arco, *Aging, plasticity and environmental enrichment: structural changes and neurotransmitter dynamics in several areas of the brain.* Brain Res Rev, 2007. **55**(1): p. 78-88.

203. Perreault, P. and M. Avoli, *Physiology and pharmacology of epileptiform activity induced by 4-aminopyridine in rat hippocampal slices.* J Neurophysiol, 1991. **65**(4): p. 771-85.

204. Martin, E.D. and M.A. Pozo, *Valproate reduced synaptic activity increase induced by 4-aminopyridine at the hippocampal CA3-CA1 synapse.* Epilepsia, 2004. **45**(5): p. 436-40.

205. Bondareff, W. and Y. Geinisman, *Loss of synapses in the dentate gyrus of the senescent rat.* Am J Anat, 1976. **145**(1): p. 129-36.

206. Halliwell, J.V. and P.R. Adams, *Voltage-clamp analysis of muscarinic excitation in hippocampal neurons.* Brain Res, 1982. **250**(1): p. 71-92.

207. Maccaferri, G. and C.J. McBain, *The hyperpolarization-activated current (Ih) and its contribution to pacemaker activity in rat CA1 hippocampal stratum oriens-alveus interneurones.* J Physiol, 1996. **497 (Pt 1)**: p. 119-30.

208. Momin, A., et al., *Role of the hyperpolarization-activated current Ih in somatosensory neurons.* J Physiol, 2008. **586**(Pt 24): p. 5911-29.

209. Thoby-Brisson, M., P. Telgkamp, and J.M. Ramirez, *The role of the hyperpolarization-activated current in modulating rhythmic activity in the isolated respiratory network of mice.* J Neurosci, 2000. **20**(8): p. 2994-3005.

210. Kety, S.S., *The possible role of the adrenergic systems of the cortex in learning.* Res Publ Assoc Res Nerv Ment Dis, 1972. **50**: p. 376-89.

211. Sara, S.J., *The locus coeruleus and noradrenergic modulation of cognition.* Nat Rev Neurosci, 2009. **10**(3): p. 211-23.

212. Aghajanian, G.K. and C.P. VanderMaelen, *alpha 2-adrenoceptor-mediated hyperpolarization of locus coeruleus neurons: intracellular studies in vivo.* Science, 1982. **215**(4538): p. 1394-6.

213. Randall, R.D. and S.A. Thayer, *Glutamate-induced calcium transient triggers delayed calcium overload and neurotoxicity in rat hippocampal neurons.* J Neurosci, 1992. **12**(5): p. 1882-95.

214. Andreyev, A.Y., Y.E. Kushnareva, and A.A. Starkov, *Mitochondrial metabolism of reactive oxygen species.* Biochemistry (Mosc), 2005. **70**(2): p. 200-14.

215. Vanitallie, T.B., *Parkinson disease: primacy of age as a risk factor for mitochondrial dysfunction.* Metabolism, 2008. **57 Suppl 2**: p. S50-5.

216. Gunter, T.E., et al., *Calcium and mitochondria.* FEBS Lett, 2004. **567**(1): p. 96-102.

217. Gunter, T.E., et al., *Mitochondrial calcium transport: mechanisms and functions.* Cell Calcium, 2000. **28**(5-6): p. 285-96.

218. Liu, Y., et al., *Mitochondrial ATP-dependent potassium channels: novel effectors of cardioprotection?* Circulation, 1998. **97**(24): p. 2463-9.

219. Yamada, K., et al., *Protective role of ATP-sensitive potassium channels in hypoxia-induced generalized seizure.* Science, 2001. **292**(5521): p. 1543-6.

220. Storm, J.F., *Potassium currents in hippocampal pyramidal cells.* Prog Brain Res, 1990. **83**: p. 161-87.

221. Faber, E.S. and P. Sah, *Ca2+-activated K+ (BK) channel inactivation contributes to spike broadening during repetitive firing in the rat lateral amygdala.* J Physiol, 2003. **552**(Pt 2): p. 483-97.
222. Faber, E.S. and P. Sah, *Calcium-activated potassium channels: multiple contributions to neuronal function.* Neuroscientist, 2003. **9**(3): p. 181-94.
223. Inoue, M., et al., *An ATP-driven Cl- pump regulates Cl- concentrations in rat hippocampal neurons.* Neurosci Lett, 1991. **134**(1): p. 75-8.
224. Pisani, A., et al., *Enhanced sensitivity of DJ-1-deficient dopaminergic neurons to energy metabolism impairment: role of Na+/K+ ATPase.* Neurobiol Dis, 2006. **23**(1): p. 54-60.
225. Song, X., et al., *Functional expression of BK channels in lateral globus pallidus neurons.* Neuroscience, 2010.
226. Buckman, J.F. and I.J. Reynolds, *Spontaneous changes in mitochondrial membrane potential in cultured neurons.* J Neurosci, 2001. **21**(14): p. 5054-65.
227. Marrion, N.V. and P.R. Adams, *Release of intracellular calcium and modulation of membrane currents by caffeine in bull-frog sympathetic neurones.* J Physiol, 1992. **445**: p. 515-35.
228. Cheranov, S.Y. and J.H. Jaggar, *Mitochondrial modulation of Ca2+ sparks and transient KCa currents in smooth muscle cells of rat cerebral arteries.* J Physiol, 2004. **556**(Pt 3): p. 755-71.
229. Nowicky, A.V. and M.R. Duchen, *Changes in [Ca2+]i and membrane currents during impaired mitochondrial metabolism in dissociated rat hippocampal neurons.* J Physiol, 1998. **507 (Pt 1)**: p. 131-45.
230. Garcia, M., et al., *GPI-anchored proteins associate to form microdomains during their intracellular transport in Caco-2 cells.* J Cell Sci, 1993. **104 (Pt 4)**: p. 1281-90.
231. Holthuis, J.C., G. van Meer, and K. Huitema, *Lipid microdomains, lipid translocation and the organization of intracellular membrane transport (Review).* Mol Membr Biol, 2003. **20**(3): p. 231-41.